

Team FEA

Frame Engineering Associates
Cal Poly SAE Formula Electric Chassis



Final Report

Brandon Stitt
Rachel Brooks
Christopher Pell

5 June, 2015

Table of Contents

| | |
|---|----|
| Executive Summary..... | 8 |
| Chapter 1: Introduction | 9 |
| <i>Project Definition and Justification</i> | 9 |
| <i>Suspension</i> | 9 |
| <i>Drivetrain</i> | 10 |
| <i>Areas to Improve</i> | 11 |
| <i>Shape and Packaging</i> | 11 |
| <i>Manufacturing</i> | 12 |
| <i>Attention to Detail</i> | 12 |
| <i>The Senior Project</i> | 13 |
| Chapter 2: Background | 16 |
| <i>Current Frames and Designs</i> | 16 |
| <i>Design Requirements and Specifications</i> | 19 |
| <i>Design Options</i> | 22 |
| <i>Concept Selection</i> | 25 |
| <i>Formula Electric Subsystem Placement</i> | 28 |
| <i>Space Usage</i> | 28 |
| <i>Lateral</i> | 28 |
| <i>Longitudinal</i> | 29 |
| <i>New Car Layout Concepts</i> | 29 |
| <i>Sidepod Configuration</i> | 29 |
| <i>Rear Motor Configuration</i> | 30 |
| <i>Layout Verification</i> | 31 |
| <i>Adhesive Testing and Results</i> | 34 |
| <i>Cockpit Mockup</i> | 37 |
| <i>FEA-Based Evolutionary Design in MATLAB</i> | 42 |
| <i>Zodiac Aerospace and Composite Sandwich Panels</i> | 53 |
| <i>Sandwich Panel Testing</i> | 55 |
| <i>Testing Setups</i> | 56 |

| | |
|---|-----|
| <i>Testing Fixtures</i> | 58 |
| <i>Panel Failure Observations</i> | 63 |
| <i>Results</i> | 67 |
| <i>2015-16 Rule Changes and Rules Clarifications</i> | 74 |
| <i>Cut-and-Fold Monocoque Design Evolution</i> | 75 |
| Chapter 4: Description of the Final Design | 79 |
| <i>Detailed Design Description</i> | 79 |
| <i>Analysis Results</i> | 92 |
| <i>Cost and Weight Analysis</i> | 96 |
| Chapter 5: Manufacturing..... | 98 |
| <i>Fiberglass Chassis</i> | 98 |
| <i>Carbon Chassis</i> | 100 |
| Chapter 6: Design Verification | 114 |
| <i>Rules Required Tests: Descriptions and Results</i> | 114 |
| <i>Senior Project Requirement Results</i> | 117 |
| Chapter 7: Conclusions and Recommendations | 120 |
| Appendix A: QFD | 122 |
| Appendix B: Drawing Packet..... | 123 |
| Appendix C: Vendor List..... | 132 |
| Appendix D: Supporting Analysis | 133 |
| Appendix E: Gantt Chart | 136 |
| Appendix F: FMEA..... | 138 |

List of Figures

- Figure 1.1: CAD of suspension
Figure 1.2: CAD of drivetrain mounts only
Figure 1.3: CAD of full drivetrain package
Figure 1.4: SAE Car Coordinates Which Will Be Used Throughout This Report
Figure 2.1: 2013-14 Cal Poly Formula Electric steel tube chassis.
Figure 2.2: Carbon monocoque chassis.
Figure 2.3: Cal Poly hybrid chassis.
Figure 2.4: Aluminum monocoque formula chassis.
Figure 2.5: Definition of the dimensions of the 95th percentile man.
Figure 2.6: Broomstick test diagram.
Figure 3.1: Matlab generated frame
Figure 3.2: Full cut and fold monocoque design
Figure 3.3: Formula shared tub design with cut and fold back
Figure 3.4: CAD of Two Future Formula Electric Concepts.
Figure 3.5: Samples from the Three Adhesive Testing Groups.
Figure 3.6: Force-Displacement Curves of the First Two Adhesive Groups
Figure 3.7: Force-Displacement Curves of the First Three Adhesive Groups
Figure 3.8: Illustration of the Peeling Deformation Caused by a Rivet in Test Group 4
Figure 3.9: Force-Displacement Curves of All Four Adhesive Groups
Figure 3.10: Front View of Entire Cockpit Mockup
Figure 3.11: View of Cockpit Mockup Showing Seat Mounting, Top Tube Mounting, and Steering Wheel
Figure 3.12: Double Bracket System to Allow Rotation of Vertical Mockup Components
Figure 3.13: Pedals in Cockpit Mockup
Figure 3.13a: Top Side Impact Tube in Cockpit Mockup
Figure 3.14: Dimensioned Sketch of Final Cockpit Mockup
Figure 3.15: Deformed FEA Result in MATLAB
Figure 3.16: SolidWorks and MATLAB FEA on a Sample Tube Structure
Figure 3.17: MATLAB Program Scoring Method Flowchart
Figure 3.18: Overall MATLAB Program Map
Figure 3.19: Weight and Score Change Across 80 Generations
Figure 3.20: Maximum Deflection Change Across 80 Generations for 7 Loading Cases
Figure 3.21: Maximum Rotation Change Across 80 Generations
Figure 3.22: Maximum Deflection of Rear Side Impact Test Across 80 Generations
Figure 3.23: Maximum Deflection of Front Hoop and Side Impact Tests Across 80 Generations
Figure 3.24: Long Beam Fixtures
Figure 3.25: Short Beam Fixtures
Figure 3.26: Plane Bending Fixtures
Figure 3.27: Core Crushing Fixtures
Figure 3.28: Concept Sketch of the Externally-Rifled Cylinder Torsion Test Concept
Figure 3.29: Concept Sketch of the 2-Bar Linkage Torsion Test Concept
Figure 3.30: Torsion Fixture
Figure 3.31: Thin Panel During Torsion Test
Figure 3.32: Thick Panel During Torsion Test
Figure 3.33: Long Beam Testing Before (Top) and After (Bottom) Failure

Figure 3.34: Thinner (Top) and Thicker (Bottom) Panel Failure Modes For Long Beam Test
Figure 3.35: Crushing Failure Of Thinner Sample Using Bottom Plate and Thicker Sample Using Bottom Peg
Figure 3.36: Thinner (Top) and Thicker (Bottom) Panels Showing Different Failure Modes in Plane Bending Test
Figure 3.37: The Four Major Failure Modes of the Short Beam Test
Figure 3.38: Long Beam Bending Results
Figure 3.38: Short Beam Shear Results: Transverse Paper Ribbon
Figure 3.39: Short Beam Shear Results: Parallel Paper Ribbon
Figure 3.40: Plane Bending Results
Figure 3.41: Core Crushing Results: 1.25" Round Against 1.25" Round
Figure 3.42: Core Crushing Results: 1.25" Round Against Flat Plate
Figure 3.43: Torsion Results
Figure 3.44: Rule 3.6.2 describing the weld test for SES.
Figure 3.45: Original steel tube frame.
Figure 3.46: Fiberglass composite floor frame design.
Figure 3.47: Cut and fold rear end frame design
Figure 3.48: Cut and Fold side and back frame design.
Figure 3.49: Full monocoque cut and fold frame design.
Figure 4.1: Cut-and-Fold Panel Geometry
Figure 4.2: The Main Bottom Panel
Figure 4.3: Front Top Panel (Left), Side Panels (Middle), and Rear Section (Right)
Figure 4.4: Exploded View of Impact Attenuator, Anti-Intrusion Plate, and Front Bulkhead, Shown in Order Left to Right
Figure 4.5: Assembled View of Impact Attenuator, Anti-Intrusion Plate, and Front Bulkhead
Figure 4.6: Roll Hoops and Mounting
Figure 4.7: Chassis With Roll Hoops
Figure 4.8: Structural Firewall and Mounting
Figure 4.9: Structural Firewall Placement Between Driver and Battery Box
Figure 4.10: Drivetrain Support Plate Mounts
Figure 4.11: Drivetrain and Support Plate Shown in Place in Rear of Car
Figure 4.12: Front Machined Plate
Figure 4.13: Front Machined Plate, Front View (Left) and Rear View (Right)
Figure 4.14: Front Machined Plates in Position in the Car
Figure 4.15: Jacking Point Configuration
Figure 4.15a: Redesigned Jacking Point
Figure 4.16: Middle Bulkhead with Tabs
Figure 4.17: Middle Bulkhead in Position in the Car
Figure 4.18: Sleeved Butt Joints for Removable Main Roll Hoop Braces
Figure 4.19: Rear Shock and Rocker Assembly Showing Suspension Bridge Function
Figure 4.20: Rear Bridge Mounting Tab
Figure 4.21: Front Suspension Mounting Tabs
Figure 4.22: Rear Suspension Mounting
Figure 4.23: Removing the Back Half of the Car to Remove the Batteries
Figure 4.24: Abaqus model assembly with interactions shown in yellow and green.
Figure 4.25: Von Mises Stress Contour Plot for the Torsional Loading Case
Figure 5.1: Fiberglass Panel in CNC Router

Figure 5.2: Fiberglass Panels After CNC Routing

Figure 5.3: Carbon Panel Clamped To Work Table. Insert holes are drilled through both panel and table.

Figure 5.4: Finished carbon panel after removal from the router

Figure 5.5: Application of resin and microballoons to groove in panel

Figure 5.6: Resin being spread onto carbon tape to wet entire surface

Figure 5.7: Completed pseudo-prepreg strip

Figure 5.8: Locating panel in jig

Figure 5.9: Smoothing wrinkles out of carbon tape. Tape has been laid up onto bend.

Figure 5.10: Peel ply completely covers wet carbon layup. Also visible is yellow masking tape marker for jig location.

Figure 5.11: Bend layup with tape, peel ply, and breather applied

Figure 5.12: Vacuum bag sealed around panel

Figure 5.13: Bag under full vacuum for resin cure

Figure 5.14: Close-up of a good vacuum on bend reinforcement

Figure 5.15: Carbon chassis with completed bend reinforcements and lap joints

Figure 6.1: Testing rig diagram for 3-point bend

Figure 6.2: Perimeter shear test data

Figure 6.3: Cal Poly Formula harness testing rig

List of Tables

Table 1.1: Engineering Design Requirements

Table 2.1: AF Rules Loading Cases

Table 3.1: AF Test Results of 2013-14 Chassis

Table 3.2: Trade study on weight for the two frames.

Table 3.3: Trade study on cost for the two frames.

Table 3.4: Trade study on time for the two frames.

Table 3.5: Suspension Forces

Table 3.6: Measured Panel Mass Properties

Table 3.7: Average Core Volumetric Density

Table 3.8: Measured Panel Mass Properties

Table 3.9: Tabulated Results

Table 3.10: Un-weighted Decision Matrix

Table 3.11: Weighted Decision Matrix

Table 3.12: Alternative tube calculations

Table 4.1: Composite Material Properties used in Abaqus

Table 4.2: Analysis Results for the AF Loading Cases and Cornell Torsion Loading Case

Table 4.3: Weight Analysis of the Final Design

Table 4.4: Bill of Materials and Cost Analysis for Final Design

Table 6.1: Composite material properties derived from 3 point bend test

Table 6.2: Chassis Initial Performance Goals and Results

Table 6.3: Weight Breakdown of Chassis Components

Executive Summary

The Cal Poly Formula Electric team has been in need of a chassis redesign, making that a logical choice for a senior project. The original goal of the project was to build the lightest possible frame while still maintaining adequate strength and stiffness.

The existing frame made a good starting point. The steel tube spaceframe weighed a colossal 105 lb. There was ample room for improvement, even with a similar spaceframe design. The greatest potential to reduce weight lay in submitting designs under the Alternative Frame (AF) rule set. This could avoid the added weight of many required tubes. The new 2014-15 rules introduced more strict requirements for tube sizes used in alternative frames. These new requirements effectively eliminated any advantage in building a steel tube frame under AF rules, making the developing chassis design no longer viable.

In response to the rule changes, possibilities were reevaluated and a cut-and-fold carbon composite monocoque was chosen as a good alternative to the steel tube design. This new design direction promised significant weight savings while maintaining the strength required to pass the tests set out in the AF rules. The primary body of the frame began as flat panels of 3/4" 3-ply carbon composite that was then cut to the desired outline and folded into shape. These folds were reinforced with a wet layup using carbon tape and the resin, and filled with glass micro-spheres in order to reduce the weight of the resin used. This folded panel was bolted to the front and main roll hoops. The roll hoops were still steel tubes, as this was required by any rule set.

Various properties were tested along the way in order to properly document chassis construction and justify FEA analysis to the FSAE officials. Most of these tests were destructive material tests on the composite panels themselves.

All major subsystems except the battery box were carried over from the existing car to the new one. The suspension, drivetrain, and space for the new battery box were all part of the design from the beginning for a seamless transition from one chassis to the next. Once the monocoque was completed, the other systems were simply assembled into it.

Once the entire car was assembled, the final tests for the chassis were to be passing technical inspection and performance at competition. Since the team was unable to get into the competition from the waitlist, this was not possible. Final design validation, instead, came from a technical inspection performed by Professor Fabijanac before the car was driven and from driver feedback.

Chapter 1: Introduction

Project Definition and Justification

The Cal Poly SAE Formula Electric team plans to compete in the Formula SAE Electric competition in Lincoln, Nebraska in June 2015. This is an international collegiate competition hosted annually by SAE International and the Sports Car Club of America. It tests the speed, agility, reliability, and design quality of student-built race cars. The concept of the competition is that a run of 1000 small open-wheel, open-cockpit cars will be produced and marketed to the weekend autocross market.

Much attention was given to the design and manufacturing of the suspension, drivetrain, and electrical system for the 2013-14 car, as will be discussed in the following paragraphs. The SAE team preferred to keep those systems largely unchanged for the next year.

Suspension

The 2013-14 suspension, shown in Figure 2, was designed and built as a senior project. The design was well thought out and the parts were made well, resulting in a high-quality system. Any major changes to the suspension this year would have been likely to degrade, rather than improve, the overall quality of the car.

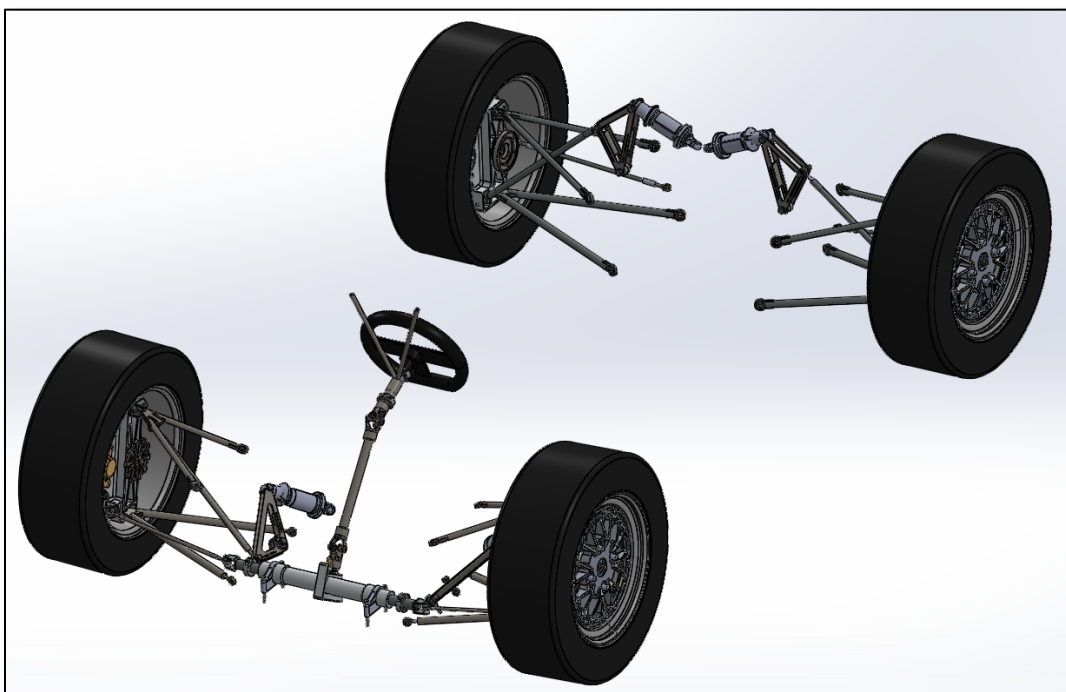


Figure 1.1: CAD of suspension

Drivetrain

The drivetrain interfaces with the chassis via a single vertical plate, shown in Figure 1.2. This plate is mounted by four bolts at the four corners. The motor and differential mount on either side of this vertical plate by means of smaller aluminum plates, or arms. The motor's casing bolts to the horseshoe-shaped piece on the left side of the frame in Figure 1.2, while its output shaft rests on a bearing in the other left-side arm. The differential rests on bearings in the right-side arms, with the sprocket between the arms and the CV joints and drive axles coming out the sides, as shown in Figure 4. The arms bolt to aluminum tabs which, in turn, bolt to the vertical main support plate.

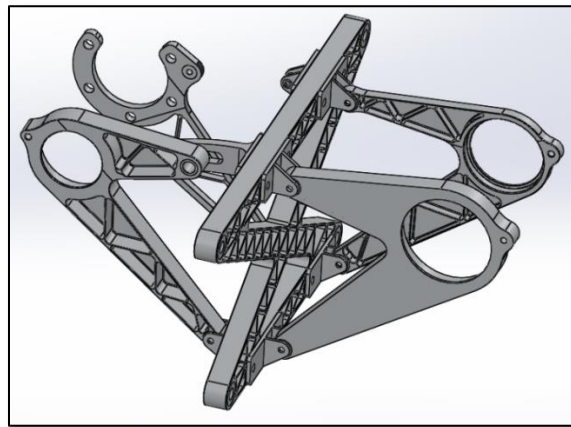


Figure 1.2: CAD of drivetrain mounts only

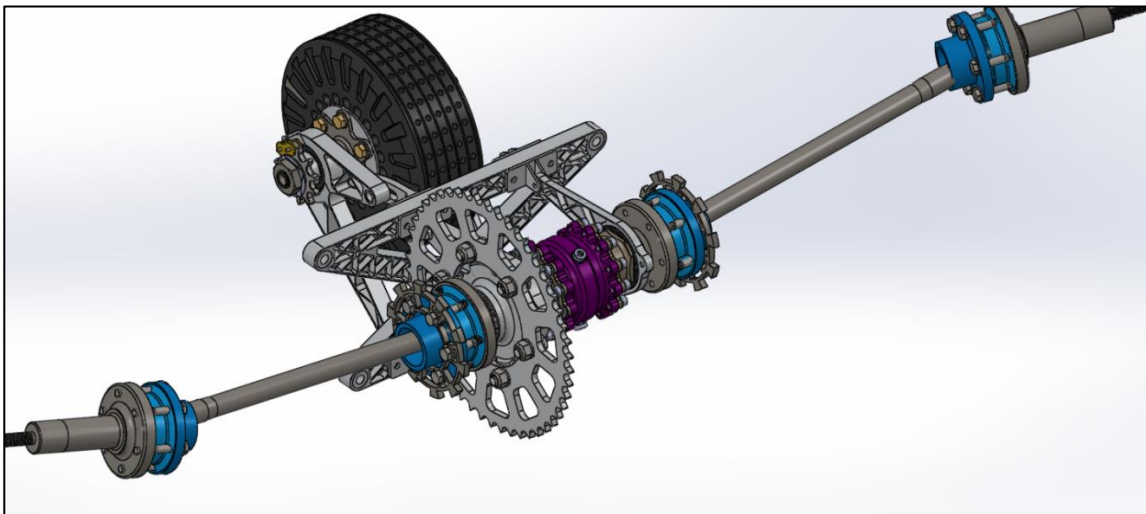


Figure 1.3: CAD of full drivetrain package

Because this drivetrain package is nicely self-contained and interfaces cleanly with the chassis (four bolts) and suspension (two spindles) the SAE team preferred to preserve it mostly intact.

Areas to Improve

Due to the overall quality of most of the car's internal subsystems, the areas left with the most room for improvement were the chassis and the battery box. Both of these components needed full-subsystem improvement best suited to the in-depth attention of a senior project. The car could also be further improved by small updates on a part-to-part basis. Candidates for this level of improvement included uprights, rotating drivetrain components, and the steering rack. The steering rack was already in progress as a collaborative senior project shared among the three Cal Poly SAE teams.

To decide whether the chassis or the battery box should be overhauled first, the impact of each system on the other was examined, along with overall effects of timing and whole-car design. The structure and form of the frame could contribute to improving the battery box. By rules, the battery box structure must support a 10g horizontal (front-rear and/or lateral) load and a 20g vertical load. By designing more frame structure in the area of the battery box, the chassis could help to support this load. The 2013-14 battery box was configured in a way that made frame design and packaging a nightmare. A senior project on the box would require changes in the frame to accommodate it, but better placement and orientation of the box over the course of a chassis project could improve accessibility and removability of the battery box. Another potential difficulty with beginning a battery box project in the spring was that the SAE team hoped to test the car extensively in the coming months. Data collected from this testing might well have prompted a change in battery pack size. With this possibility in mind, a battery box project would have needed to either delay the design phase until after a decision had been made, thus pushing back the project's timeline by an entire quarter or more, or the project team would have needed to be prepared to drastically change their design to accommodate the new pack. This potential for setback was clearly high enough to make the value of a spring battery box project dubious. A chassis senior project, on the other hand, could start quite easily in the spring. Most of the major subsystems were already well defined. This provided a clear picture of what components must be packaged where and what loads must be supported where. A new battery pack could be developed in parallel with a new space and support structure for the pack, leaving the way clear for a battery box design to begin in the fall.

Many areas for improvement on the 2013-14 chassis existed, under any rule set.

Shape and Packaging

The past year's battery box was very long, and oriented transverse to the car. To accommodate it, the chassis had to be very wide just behind the driver, quickly narrowing to only 11" at the rear suspension. In addition to this, the box had to slide out the side of the car for charging and maintenance, which

required packaging inside the box to be almost impossibly tight. This situation could be helped by reorienting the battery pack to make a shape that would fit into the available space better. A related packaging issue was that the motor sat extremely close to the battery box, yet no space was used behind the differential. By placing the motor in the unused space behind the differential, some more space could be bought for the batteries.

Manufacturing

The past year's chassis comprised roughly 75 tubes, with 10 supernodes of 6-8 tubes each, and weld angles as tight as 10 degrees, with extreme thickness differences. The tubes were outsourced for CNC bending and laser notching, costing the team \$1000 and a month of lead time in addition to countless hours of painstaking detailed notch modeling. The chassis jig was almost as expensive and time-consuming as the chassis itself. It did significantly decrease welding time and improve the finished product, at a cost of \$800 worth of 80/20 extrusion, 2 weeks of modeling, and 2 weeks of construction for the jig itself. The concept was good and the product was valuable, but a more efficient system was desperately needed.

Attention to Detail

The past year's chassis had several areas forgotten, procrastinated, and garage-engineered at the last minute. The list of these areas includes, but is not limited to:

- Front rocker/shock mounts
- Harness attachments
- Seat mounts
- Head rest
- Firewall
- Dashboard
- TSAL (Tractive System Active Light) mounting
- Radiator mounting
- Electrical box mounting/positioning
- Chain guard

By far the biggest fiasco, however, was the battery box and floor interface. By Structural Equivalency Spreadsheet (SES) guidelines, the box must have a stiffness equivalent to 2 steel tubes. Since the Garolite fiberglass box was mounted to 2 steel tubes in the floor, this should have been no problem. However, the SES as submitted appeared to the rules committee as though the box was a simply supported beam: its two ends sitting on solid structure, but no other steel underneath the middle. An attempt to clarify and resubmit the SES failed. Having submitted it once, if the team wanted to change the rules committee's evaluation of the box they would have had to submit the analysis required by the

Structural Requirement Certification Form (SRCF). Being a determined group, the team proceeded to do just that. They submitted an analysis of the box, together with the 2 tubes supporting it. This too was unacceptable. The 2 tubes were part of the chassis, not of the box itself, meaning that, to include those tubes in the analysis, an SRCF would need to be submitted for the entire frame. The rules committee required an analysis of the entire frame, so the team ran an analysis of the entire frame. The 2013-14 frame failed every test.

This situation obviously must not happen again. It can be avoided in several ways. By building to alternative frame rules, that final blow will never fall. To avoid ever reaching that point, empirical testing is needed. Any material used for battery support other than steel tubes should be tested to failure to ensure sufficient strength. If documents are submitted early and under the correct format, the rules committee is very willing to provide feedback on the submitted documents until they pass.

The Senior Project

The mission of Frame Engineering Associates (the senior project group) was to design, build, and test a chassis for the use of Formula Electric at the FSAE Lincoln 2015 competition. The project was sponsored and funded by the SAE team and operated on the spring senior project timeline. The final design review for the chassis was held in fall 2014, and the goal was to have a completed chassis by mid-January 2015. This would allow time to test and tune the chassis extensively over winter quarter 2015 so that the SAE team had a top-notch frame ready to put components into when they had components ready to put into it. This would allow both the senior project team and the SAE team time to test and tune the entire car over spring quarter 2015 in preparation for the competition in June. The senior project team intended to stay on track with this plan by strictly adhering to a Gantt chart schedule, seen in Appendix E.

As previously discussed, the suspension, wheels and tires, drivetrain, and brakes were to be carried over from the past year's car (the 2014 car) with minimal changes. Seat mounting and driver positioning would be re-evaluated, and the battery box would be reconfigured in collaboration with the electrical subsystem lead, as discussed in the preceding paragraphs.

The 2015 frame set out to make use of FSAE's Alternative Frame (AF) rules. For a more in-depth discussion of this decision, see Design Requirements and Specifications. This would be the first time a Cal Poly SAE team had entered a competition under the AF rule set. These rules required submission of the SRCF as a part of technical inspection. The SRCF is similar to the Structural Equivalency Spreadsheet (SES), but supersedes it, requiring analysis and testing data to validate every aspect of the design, proving that it meets requirements.

The primary goal of this project was to build a working chassis for Cal Poly's SAE Formula Electric team to use in the 2015 FSAE competition. This required that it pass all technical inspections, including the SRCF. Secondly, the chassis needed to be light and torsionally stiff. The goal for fully operational

weight of the chassis was 65lb. This was to include all tabs and permanent mounting for other systems. Adherence to this standard would be measured by building the car and driving it, then stripping all subsystems away until the bare chassis was left and weighing that chassis. The goal for torsional stiffness was 1800 foot pounds per degree, as defined by the Cornell paper (Design, Analysis and Testing of a Formula SAE Car Chassis). Cornell cites torsional stiffness as the primary determinant of chassis performance and handling characteristics. This was a parameter that would be tested by finite element analysis of the chassis under strictly defined loading cases. All coordinate directions used here and throughout this report are SAE standard coordinates, as shown in Figure 1. The Cornell loading case is defined with the rear right wheel constrained in the x, y, and z directions and the rear left wheel constrained in x and z but free to move in the y direction. The front right wheel is constrained in the z direction but free to move in x and y, and the front left wheel is loaded in the z direction. The effective torque on the chassis (in foot pounds) is the applied force times the distance between the applied force and the chassis centerline ($y=0$). The frame's torsional stiffness (ftlb/deg) is the effective torque divided by the frame's rotational deflection (in degrees) at the front track.

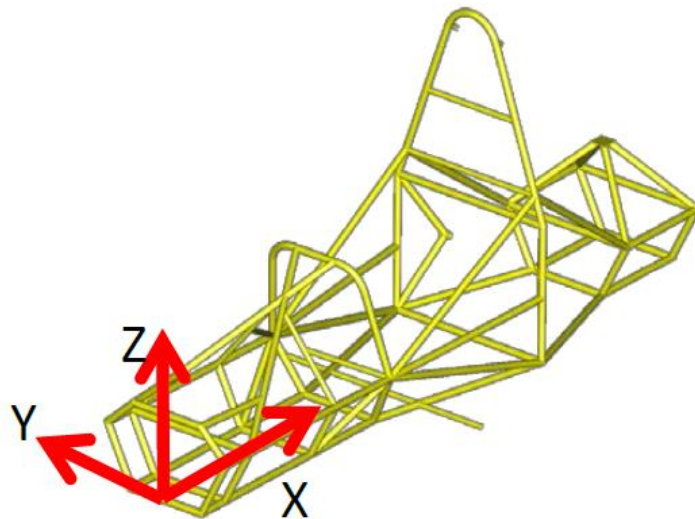


Figure 1.4: SAE Car Coordinates Which Will Be Used Throughout This Report

The following table contains a numerical breakdown of the design requirements for this project. These requirements were taken directly from the QFD in Appendix C, developed earlier in the quarter. For details of the Alternative Frame rules (AF 4.1-4.7), see Table 1.1.

Table 1.1: Engineering Design Requirements

| Category, with units | Target Value | Tolerance | Risk | Compliance |
|---|--------------|-----------|------|------------|
| weight (lb) | 65 | Min | H | A,T |
| torsional stiffness (ft-lb/deg) | 1800 | Min | M | A,T |
| time to get in (sec) | 5 | Max | H | T |
| time to get out (sec) | 5 | Min | M | T |
| number of steps to get in (n) | 5 | Max | H | T |
| number of steps to get out (n) | 5 | Med | M | T |
| total cost on cost report (\$) | 3000 | Med | M | A,I |
| Total cost of entire project (\$) | 10000 | Max | M | A,I |
| man hours to build frame (hours) | 200 | Max | H | A,T |
| manufacturing processes (n) | 5 | Max | H | A |
| AF 4.1-4.7 (avg safety factor) | 1.25 | Min | H | A |
| places that can cut paper (n) | 0 | Med | M | I |
| time to assemble car (min) | 30 | Max | H | T |
| people that think it's comfortable (%) | 75 | Med | L | A,T |
| line of sight (deg) | 160 | Med | L | A,T |
| people that think it looks good (%) | 75 | Max | M | A,T |
| number of rocks in chassis after 10 mins of driving | 0 | Min | L | T |
| time to disassemble car (min) | 20 | Med | H | T |

Chapter 2: Background

Current Frames and Designs

The Formula SAE competition is filled with many variations on similar frames. The current frames tend to follow one of two patterns: an all steel tube welded frame or a carbon monocoque. The frames rarely deviate from these two designs or some combination of the two. There are other types of frames that can be used, and they generally fall under the alternative frame rules. These rules allow teams to take a different approach to designing an FSAE chassis. These different design approaches could improve cost, ease of manufacture, performance, and more. The alternative frame rules have strict safety requirements to prevent teams from pushing the limits dangerously far. These requirements are difficult to design for, so most teams opt for the traditional steel tube frame or monocoque design.

The current steel tube frames tend to be very heavy and bulky. They are also the most common frame seen at competition because they require the least amount of previous knowledge and less design time in order to get a functional frame that passes technical inspection. They are required to pass a long list of required tube placement rules in order to keep the drivers safe. Most steel tube frames weigh over 65 pounds because of all the tubes required by the rules. These steel frames are rarely strong enough to meet the large loading standards of the alternative frame rules. The 2013-14 Cal Poly Formula Electric car seen in Figure 2.1 is a steel tube frame car that weighs 100 pounds. Even so, it is no longer acceptable by the newest 2015 Formula SAE rules. This weight disadvantage makes the fabrication of a steel tube frame less desirable, but the ease of manufacture tends to be chosen, despite the disadvantage of the added weight.

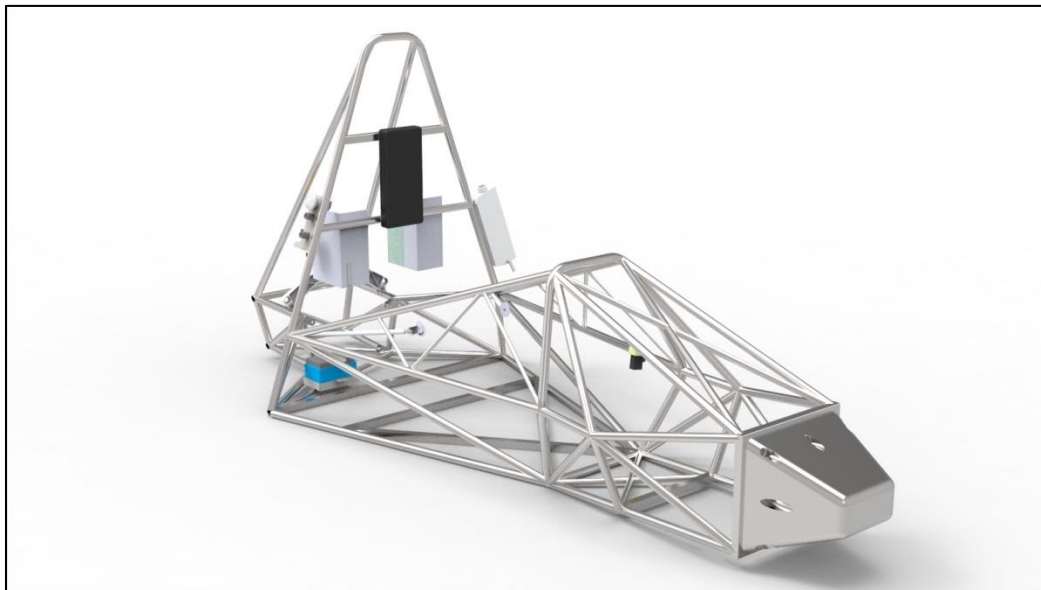


Figure 2.1: 2013-14 Cal Poly Formula Electric steel tube chassis.

The other common chassis design is a carbon monocoque. An example of this design is shown in Figure 2.2. These are less widespread than steel tube frames because they can be significantly more expensive and are more demanding to design and manufacture. Carbon monocoques, however, are usually lighter and stiffer than steel tube frames. Instead of 65 pounds or more, monocoques weigh an average of 50-60 pounds. The added stiffness of carbon sandwich construction allows for less frame deformation under driving conditions and allows the driver to more easily feel what the car is doing, contributing to better performance overall. Carbon monocoque development is normally a process of refinement over several design cycles. Each team must find the best manufacturing processes and layup schedule details that work the best for their own circumstances and requirements, which requires time and testing.



Figure 2.2: Carbon monocoque chassis.

One way to achieve the benefits of both the tube frame and the monocoque is to build a hybrid of the two designs. The front end of the car, usually the cockpit and everything in front of it, is contained in a composite half-tube while the rear end is supported by a tube subframe. Cal Poly's Formula combustion team currently uses this concept, shown in Figure 2.3. The hybrid frame can alleviate issues of monocoque design complexity and the heat and vibrations from a combustion engine. A major problem that arises is how to join the two halves in a way that maintains a stiff chassis and avoids adding too much weight.



Figure 2.3: Cal Poly hybrid chassis.

Other types of frames exist, but are rarely seen. One such example is the aluminum monocoque, seen in Figure 2.4. This concept, inspired by the aircraft industry and borrowed from Indy car racing, consists of steel bulkheads at high-load points and an aluminum stress skin holding them together. The bulkheads are lightened with as many holes as possible, and bonded and riveted to the aluminum skin. While they do not require the composites knowledge necessary for a good composite monocoque, these aluminum monocoques necessitate special skills of their own and have difficulty competing with the light weight of carbon.



Figure 2.4: Aluminum monocoque formula chassis.

Design Requirements and Specifications

The Formula SAE rules set out specific requirements for a competition-ready car. Under the standard spaceframe rules, many required tubes are listed, along with minimum diameters and wall thicknesses. Alternative frame (AF) rules stipulate only a few required tubes, but detail exacting tests that frames must pass in FEA models. A Structural Requirements Certification Form (SRCF) is required to defend design choices and verify adherence to AF rules standards. Since the competition rules are highly detailed, they will be the primary source of design and testing standards. When designing to the AF rules, many requirements in either the standard spaceframe or standard monocoque rules no longer apply. Whenever this causes a requirement to be ambiguous, a rules clarification is submitted to the FSAE rules committee for further explanation. This helps to ensure compliance with competition standards.

Any team submitting a chassis under the alternative frame rules is required to submit an SRCF. This entails a detailed description of the final design, a table of material properties used in analysis, and a table of safety factor and deflection results from FEA. This information serves to prove that the design meets the requirements for each of the seven loading cases defined by the alternative frame rules in Table 2.1.

Roll hoop requirements are well-defined and strict regardless of rule set. The main hoop must be a single piece of bent steel tubing that extends from the lowest chassis member on one, side up over the driver, and back down to the lowest member on the opposite side. The front hoop must also be steel tube, but is not required to be a solid piece. Both hoops must have a diameter of 1" and a wall thickness of 0.095". Alternatively, the wall thickness can be decreased to as little as 0.065", but the diameter must be increased to maintain the same cross-sectional area (A) and area moment of inertia ($E*I$).

Rule T3.10 outlines the required geometry of the two roll hoops. The main hoop and any bracing must be at least 2" from the helmet of a 95th percentile male driver. Dimensions for this driver, known as Percy, are given by the rules and shown in Figure 2.5. The tallest driver, not Percy, is the standard for the broomstick test. A straight line between the top of the main hoop and the top of the front hoop, as would be formed by a broomstick laid across the two, must be at least 2" from his helmet at any point. A diagram of the broomstick test appears in Figure 2.6

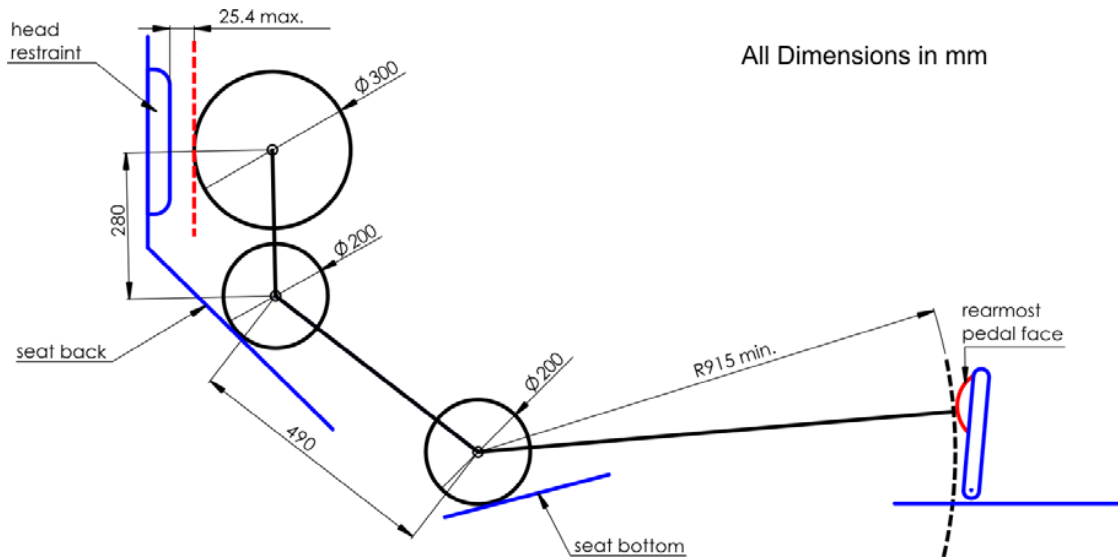


Figure 2.5: Definition of the dimensions of the 95th percentile man.

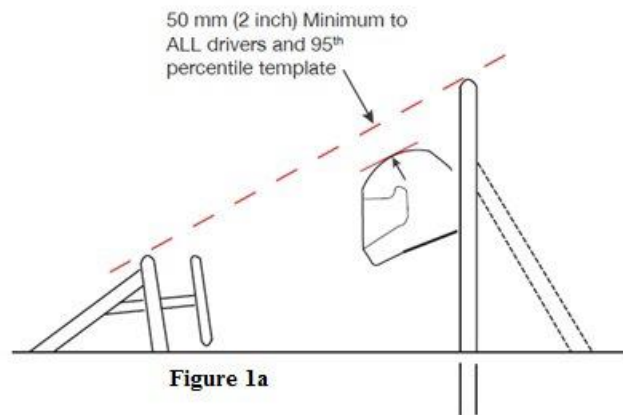


Figure 2.6: Broomstick test diagram.

In a monocoque concept, the front and main hoops can be joined to the composite structure with brackets. These brackets are to support a 30kN load in all directions, as stated in rule T3.40, in the monocoque section of the frame rules. While the hoops must each be a single piece, this is not required for the main hoop braces. They can be made removable through use of a double-lug joint or a sleeved butt joint, as defined in rule T3.17.

The alternative frame rules define a set of loading cases and boundary conditions that the chassis must meet, rather than dictating sizes of tubes and where they must be placed. This leaves design and construction largely up to individual teams to decide upon and justify, potentially allowing for lighter

and stiffer structures than are possible under traditional frame rules. AF rules are still under development, leaving much ambiguity about which standard frame rules still apply and which can be ignored. As such, individual teams must use their best engineering judgment, along with justifying all deviations from standard rules through proper analysis as outlined in Table 2.1. The fixtures, or boundary conditions, for these load tests are specified in AF 4.1-4.7 as “1. Fixed displacement (x,y,z) but not rotation of the bottom nodes of both sides of the front and main roll hoops,” and “2. Fixed displacement (x,y,z) but not rotation of the bottom nodes of the main hoop and both nodes where the main hoop and shoulder harness tube connect.” The frame must support these given loads and fixtures without any sort of failure and without any deflection more than 25mm at any point.

Among the few standard frame rules that do still apply are the requirement that the front and main roll hoops must be 1” diameter x .095” wall thickness tube and that a broomstick placed from the top of the main hoop to the top of the front hoop must clear the top of the driver’s helmet by at least 2”. However, the main hoop braces may be changed. Since the only function of these tubes is to support the main roll hoop, they can be configured in any number of ways. The only requirement by rules is that they pass the given loading cases, with emphasis on the rollover case, to demonstrate that they still sufficiently brace the main hoop. In addition to the specified loading cases, all subsystem interfaces must be verified through FEA and empirical testing. For details on this verification, see the Subsystem Interfaces heading in the Design Development section.

Table 2.1: AF Rules Loading Cases

| Rule | Test Name | Location | Force | Boundary Condition |
|--------|--------------------------------|---|--|--------------------|
| AF 4.1 | Main Roll Hoop | Top of Main Roll Hoop | $F_x = 6.0 \text{ kN}$, $F_y = 5.0 \text{ kN}$, $F_z = -9.0 \text{ kN}$ | 1 |
| AF 4.2 | Front Roll Hoop | Top of Front Roll Hoop | $F_x = 6.0 \text{ kN}$, $F_y = 5.0 \text{ kN}$, $F_z = -9.0 \text{ kN}$ | 1 |
| AF 4.3 | Side Impact | All structural locations between front roll hoop and main roll hoop from ground to 350mm above ground | $F_x = 0 \text{ kN}$, $F_y = 7.0 \text{ kN}$, $F_z = 0 \text{ kN}$ | 1 |
| AF 4.4 | Front Bulkhead | Actual attachment points between the impact attenuator and the front bulkhead | $F_x = 120 \text{ kN}$, $F_y = 0 \text{ kN}$, $F_z = 0 \text{ kN}$ | 2 |
| AF 4.5 | Shoulder Harness | Both shoulder harness attachment points simultaneously | 13.2 kN at seat belt attachment angle per attachment point | 1 |
| AF 4.6 | Lap and Anti-Submarine Harness | All harness attachment points simultaneously | 13 kN at lap belt attachment angle per attachment point. 6.5 kN at anti-submarine attachment angle per attachment point. | 1 |
| AF 4.7 | Front Bulkhead Off-Axis | Actual attachment points between the impact attenuator and the front bulkhead | $F_x = 120 \text{ kN}$, $F_y = 17.25 \text{ kN}$, $F_z = 0 \text{ kN}$ | 2 |

Chapter 3: Design Development

Design Options

Several options existed for the 2014-15 chassis. Beyond the standard options of space frame or monocoque, variations on each one can be many and complex. Each concept has its associated benefits and costs, ranging from difficult analysis of design to expense to uninspiring performance.

Option 1: Re-use the 2013-14 Formula Electric tube frame. This frame did not initially meet the revised competition rules, but it could be made competition ready by adding more support structure. Since it was not used for the '13-14 competition it could still be used in the 2015 competition. On the other hand, this would add even more weight to its already hulking 98 pounds.

Option 2: Build an entirely new tube frame under the current standard rule set. It would be a fully triangulated structure, roughly the same as every other year's frame. This method is fairly reliable but is also fairly restrictive to innovation and improvement.

Option 3: Use Matlab to design a steel tube frame under the alternative frame rules. The artificial intelligence program developed for this purpose is described in detail in the "FEA-Based Evolutionary Design in MATLAB" section later in this chapter. An example of the frames it produces can be seen in Figure 3.1, below. The greatest benefit has tended to come from the use of many small-diameter thin-wall tubes, creating a birdcage effect. Since this year's rules revision disallowed these small tubes, a computer-designed chassis has proven to be far less beneficial than it originally seemed.

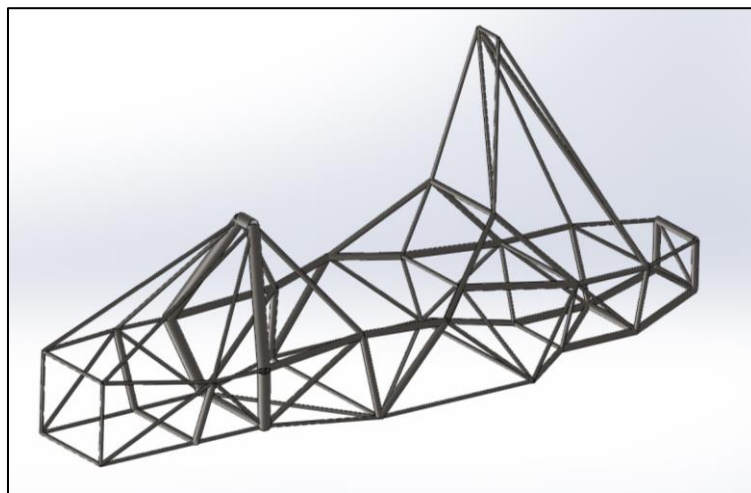


Figure 3.1: Matlab generated frame

Option 4: Build an aluminum monocoque chassis. This concept was borrowed from 1970s Indy cars, and has been used by a very few SAE teams. This would eliminate the difficulty present by the lack of

composites expertise among the senior project. On the other hand, two major drawbacks of this concept were the scarcity of information about this design and the fact that manufacturing it requires someone to develop some degree of skill with an English wheel.

Option 5: Build a skeleton-and-skin hybrid frame under the alternative frame rules. This idea uses a very minimal space frame made of large-diameter tubes, with little to no triangulation, as a skeleton. This skeleton would then have an aluminum skin for stiffness and impact protection, and a flat floor made of a premade composite panel. Problems arose with the weight of the skin and the attachment of the three components.

Option 6: Cut and fold a full composite monocoque from premade panels under the alternative frame rules. This concept evolved from the previous one, as will be discussed at length in the “Cut-and-Fold Monocoque Design Evolution” section later in this chapter. This could achieve many benefits of a monocoque without requiring the investment of time and money or the knowledge of composites analysis and design required to develop a custom layup. One potential downside to this design is the inability to use different layers and thicknesses of material at more or less stressed points on the chassis. Another complication is the planar nature of the panel. The panel only bends in one dimension at once, making complex shapes and abrupt changes in width challenging. This concept can be seen in Figure 3.2 below.

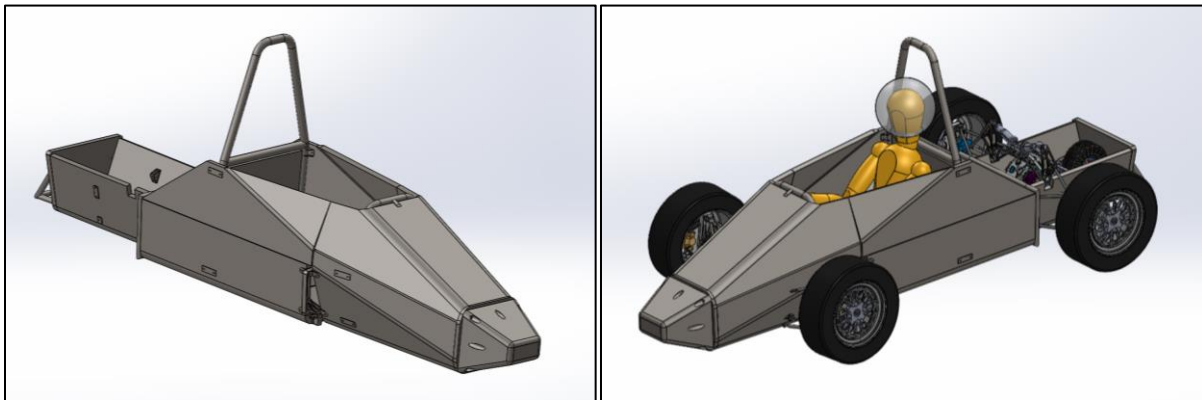


Figure 3.2: Full cut and fold monocoque design

Option 7: Build a hybrid monocoque from an existing half-tub mold. As seen in Figure 3.3, this chassis would be made of three distinct sections. The front section would be laid up in existing molds belonging to Cal Poly’s Formula SAE team. The two rearward sections would be cut and folded from a premade panel. This would bring the Formula Electric team closer to a traditional monocoque but still keep the investment low since the molds already exist. It would also dramatically increase commonality between the two teams, as has been desired for some time now. On the other hand, it would still require enough composites analysis to ensure that an adequate layup schedule was designed. The battery box would not fit fully inside the front half-tub, forcing it to be fully outside. This would shift the drivetrain further back in the car, lengthening the wheelbase and decreasing agility. Another issue with this concept is logistics. Tubs for both teams would need to be laid up in the molds, meaning that if the first team fell

behind schedule with their tub manufacturing, that would delay the second team’s manufacturing timeline as well.

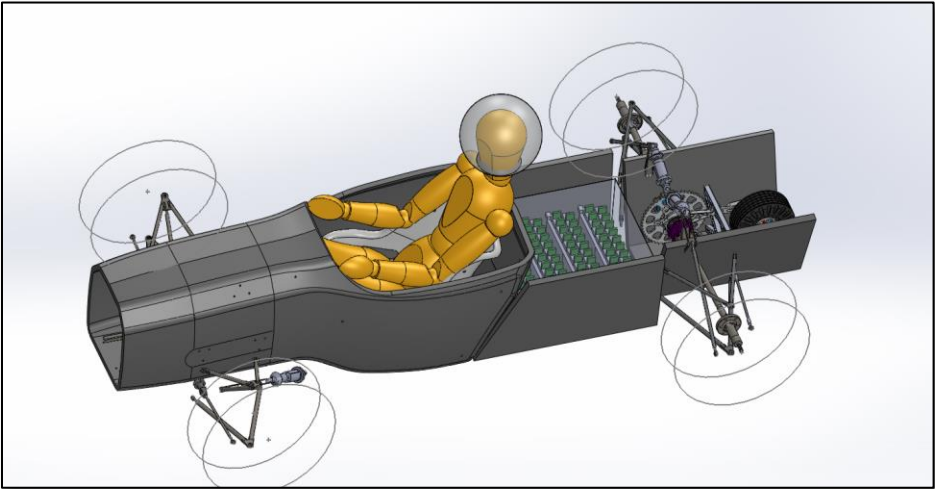


Figure 3.3: Formula shared tub design with cut and fold back

Concept Selection

The 2013-14 tube frame was a logical starting point. It was already very familiar to at least one member of the senior project, and would provide a practical idea of the challenges posed by the alternative frame rules. That chassis had been subjected to extensive FEA testing and appeared to have a remarkably high stiffness-to-weight ratio. The problem came with the fact that torsional stiffness was the only stiffness examined. The frame was designed specifically to maximize the ratio of torsional stiffness to weight, as determined by the Cornell loading case. It accomplished this at the cost of being weak in every other direction and heavier than it needed to be. Cornell found that for FSAE frames, anything less than 1600 ft-lb/degree was too floppy and had negative impacts on handling and driver confidence. Above 2000 ft-lb/degree, the driver could no longer detect increasing chassis stiffness. The past year's chassis was excessively stiff in torsion, at 2800 ft-lb/degree. Its 80 or more pounds of tubes, however, did not help it withstand a front impact or a rollover. As outlined in Table 3, it failed every one of the 7 tests required by AF rules, with an average safety factor of less than 0.5.

Table 3.1: AF Test Results of 2013-14 Chassis

| Rule | Test Name | Stress Safety Factor | Max Deflection | Notes |
|--------|--------------------------------|----------------------|----------------|--|
| AF 4.1 | Main Roll Hoop | 0.57 | 46mm | Main hoop bracing support structure deflects 23mm downward, and the main hoop deflects 23mm relative to that back section. |
| AF 4.2 | Front Roll Hoop | 0.95 | 8.1mm | Very high bending stress at load application point. Max deflection occurs in buckling in the left rearward front hoop support tube. Deflection at load application point is 7.2mm. |
| AF 4.3 | Side Impact | 0.42 | 26mm | Nearly passes in deflection, but because the side impact tubes are so long there is very high bending stress at the load application point. |
| AF 4.4 | Front Bulkhead | 0.13 | 206mm | Very high deflection and stress everywhere in the frame. |
| AF 4.5 | Shoulder Harness | 0.21 | 98mm | High bending stress in the center of the very long harness bar. |
| AF 4.6 | Lap and Anti-Submarine Harness | 0.42 | 68mm | Lap and sub belt attachment was never considered last year, so there is very little structure around that area. |
| AF 4.7 | Front Bulkhead Off-Axis | 0.12 | 208mm | Very high deflection and stress everywhere in the frame |

The failure of last year’s frame does not invalidate the entire steel tube concept. It simply shows that any concept must be evaluated by all applicable standards, not just one. While a tube frame was still under consideration, AF rules seemed to lend themselves much better to more efficient non-traditional structures.

Reasons for why the Matlab-designed frame was not chosen are discussed in depth later in Chapter 3, but in summary the frame generated is too heavy to be competitive. The newest version of the alternative frame rules force the chassis to be heavier than one designed under the standard frame rules.

The decision to not make a chassis based on Formula’s half-tub mold was based mostly on cost. The entire chassis budget for 2014-15 is \$4000. To produce a tub using the same mold would require about \$3000 for the carbon, \$3000 for the film adhesive, and \$1000 for the honeycomb core. This brings the cost of the front half-tub cost to about \$7000, which is far out of budget does not allow for building the rest of the chassis. Even if the funds could be raised, making a tub requires considerable experience to achieve a quality finished product. The layup must be executed precisely as designed for the tub to be effective and safe. This would require massive amounts of help from the Formula team to lend their expertise in carbon tub manufacturing. However, they were in the middle of their project as well and did not have the time to donate to helping with this tub as well.

The aluminum monocoque was quickly eliminated as unfeasible and the skeleton-and-skin hybrid evolved into the cut-and-fold monocoque, leaving only two possible frames from the original list: the standard rules steel tube frame and the cut-and-fold monocoque. For a final decision between the two design options, see trade studies of weight, cost, and time in Tables 3.2, 3.3, and 3.4, respectively.

Table 3.2: Trade study on weight for the two frames.

| Weight | | | |
|--------------------|----------------|--------------------|----------------|
| Monocoque | | Spaceframe | |
| Panels | 24.2 | Body / Floor | 10 |
| Wet Layup | 7.8 | | |
| Tubes | 25.6 | Tubes | 73.9 |
| Tabs / Attachments | 4.7 | Tabs / Attachments | 2 |
| Front Plates | 2.9 | | |
| Total | 65.2 lb | Total | 85.9 lb |

For weight, Table 3.2 shows that the cut-and-fold frame is the clear winner. Table 3.3 compares the cost of making the two cars. The steel tube frame gains an advantage in this category because steel, even chromoly alloy steel, is relatively inexpensive. The costs of the steel tube frame were based on previous steel tube car designs and current material costs. The cost definitely does not eliminate the cut and fold frame however, because both frames come within the \$4000 budget. The carbon option does come close to the maximum budget. If any more unforeseen costs had arisen, more funds might have needed to be raised for the team.

Table 3.3: Trade study on cost for the two frames.

| Cost | | | |
|-------------------|----------------|----------------|----------------|
| Monocoque | | Spaceframe | |
| Panels | 3000 | Notching | 440 |
| Carbon Fiber Tape | 200 | Bending | 610 |
| Microballoons | 50 | Welding | 700 |
| Resin | 100 | | |
| Hardener | 50 | | |
| Tubes | 300 | Tubes | 900 |
| Aluminum Plate | 150 | Aluminum Plate | 300 |
| Total | \$3,850 | Total | \$2,950 |

The final trade study concerns time for construction. Given that the rules changed once one chassis was already designed, requiring a complete redesign of the chassis, time was very important. The monocoque frame shows to be only a slightly better option in this category. Its estimated completion time was only 6 hours less, making the two practically the same.

Table 3.4: Trade study on time for the two frames.

| Time | | | |
|----------------|---------------|--------------|---------------|
| Monocoque | | Space Frame | |
| Panel Prep | 30 | Notching | 40 |
| Panel Assembly | 20 | Bending | 2 |
| Tubes | 6 | | |
| Jigging | 30 | Jigging | 30 |
| Machining | 20 | | |
| Welding | 20 | Welding | 60 |
| Total | 126 hr | Total | 132 hr |

The cut-and-fold frame was chosen to be developed in detailed design. Both concepts were within budget and the carbon would make the lighter final frame. It was Formula Electric's first attempt at a cut-and-fold frame and has proven to be effective for the team.

Formula Electric Subsystem Placement

In the 2013-14 car, the track width and wheelbase were determined by the suspension team. All of the largest components (driver, battery box, drivetrain assembly) were packaged as close to the floor as possible, and within the wheelbase. Extra space was created laterally by means of a very wide chassis structure in front of the rear suspension box. As detailed in the “Shape and Packaging” division of the *Motivation* chapter, packaging was a problem for that car. The most obvious case of this was the battery box, but the battery box might have been less of an issue had other things been packaged differently.

Space Usage

Solving the problems of the previous year’s packaging while using the same basic components required a careful examination of space usage. To make more room for components, the car’s volume needed to expand in one or more of the three dimensions.

Vertical

Each dimension presents its own challenges to expansion. The major problem associated with vertical expansion is an increased CG height. This, in turn, causes greater weight transfer in cornering which, for a traditional suspension configuration, will decrease cornering speeds and increase lap times. In short, it will make the car slower.

Lateral

To expand laterally, a few options exist: widen the track, widen the suspension pickup points (shortening the A-arms), or overhang the pickup points. Widening the track decreases the car’s agility, modifying the racing line and increasing lap times. The existing suspension points are intentionally narrow. Of the possible ways to take up width between the hubs, A-arms are lighter than chassis structure. Longer A-arms allow for better upright packaging and better suspension geometry, which leads to better car handling. The entire car is suspended by the pickup points, so all structures must connect back to those points. As components are placed farther from the centerline of the car, more and more chassis structure must be built back to those points to support the components. In addition to this structural inefficiency, placing weight farther from the center of the car increases both yaw inertia and roll inertia, which degrade the car’s handling.

Longitudinal

To expand longitudinally, the options are to increase wheelbase, overhang the front wheels, or overhang the rear wheels. Chassis structure between the wheels has to support torsional loads where structure outside of the wheelbase, for all practical purposes, does not. This means that structure between the wheels is heavier. Lengthening this structure adds significant weight to the car. In addition, lengthening the wheelbase increases the car's turning radius, decreasing agility and increasing lap times. The main purpose of chassis structure in front of the front wheels is to sustain a front impact. Front impact loading as specified by AF 4.4 is 33000lb applied directly to the front bulkhead, requiring substantial structure to survive. Using space in front of the front wheels means lengthening this structure, adding significant weight to the car. Rear impact requirements are far less stringent. Only high-voltage components must be protected, and only by the same guidelines as apply to side impact structures. While any expansion requires structure to support it, and any extra structure adds weight to the car, this is the least heavy of the available options and allows for weight-saving reconfigurations to other parts of the chassis. The cost to handling is a rearward shift of the car's CG, which tends to increase oversteer.

Changing the dimensions of the overall car volume is not the only way to adjust packaging. Things can be made to fit together better in the same space by changing the sizes and shapes of the components themselves. Any adjustment of the components must be minimally invasive, to avoid a full overhaul of the car. Since fitting the battery pack and related electrical components into the battery box had been just as difficult as fitting the battery box into the car, the battery box needed to change anyway. By changing the battery pack configuration at the same time, the entire battery assembly can be made friendlier to packaging. The entire drivetrain assembly could be flipped so that the motor sits behind the differential rather than in front of it, while maintaining the entire modular mounting system, creating more longitudinal space. The driver could even be put into a more compact position. To examine the related ergonomics and human factors, a full driver cell mockup was constructed and will be discussed in detail in the *Cockpit Mockup* section of Chapter 3.

New Car Layout Concepts

Two new layouts were devised using a combination of updated car volume and updated component configurations.

Sidepod Configuration

The first concept was to divide the battery pack into two halves, placing each half in a long narrow sidepod along the cockpit, as shown in the left half of Figure 7. This would make component packaging very easy, with ample space left between the motor and the driver. This layout would make the carbon half-tub chassis concept theoretically possible. The roomy packaging would come at the cost of doubled battery boxes and electrical equipment. While each box would be smaller, smaller boxes require more wall structure to achieve the same total inside volume. Two boxes would also mean doubled

accumulator isolation relays and fuses, adding significant weight in electrical components alone. The battery pack assembly is one of the heaviest components of the car, second only to the driver. Moving all this weight from behind the driver to beside him will shift the distribution forward, from the desired 45/55 front/rear to 51/49. Such a drastic forward shift could cause dramatic understeer behavior. With the weight of the batteries so far from the car centerline, much extra chassis structure is needed for support and side impact protection. In addition to the extra weight and understeer introduced by this layout, so much weight so far from the center can cause high yaw and roll moments, further harming handling.

Rear Motor Configuration

The second concept, shown in the right half of Figure 7, was to place the motor behind the differential. This can be accomplished by rotating the entire self-contained drivetrain assembly about the inboard CVs. Nothing changes about the assembly except its orientation. The driver is shifted slightly forward, so that the feet of a 95th percentile male would be roughly in line with the front plane of the tires rather than at the wheel centerline. This still provides some impact protection for the driver's feet and legs, although slightly less (in theory) than the previous driving position. In reality, any front impact will be absorbed by the impact attenuator and then the front impact structure, so that things in line with the wheels and tires will never come into contact with an impactor. The battery pack is reconfigured into a more square shape, and takes up no more lateral space than the driver. This new pack configuration allows easier packaging of electrical components and more space between the cells themselves, for better cooling. The weight distribution is kept at or near the desired 45/55. Since the weight of the batteries is in line with the car, no extra structure is needed to the sides for support, and no extra yaw and roll moments are introduced. This layout does require some extra structure behind the differential, but that structure is much less extensive than a sidepod structure.

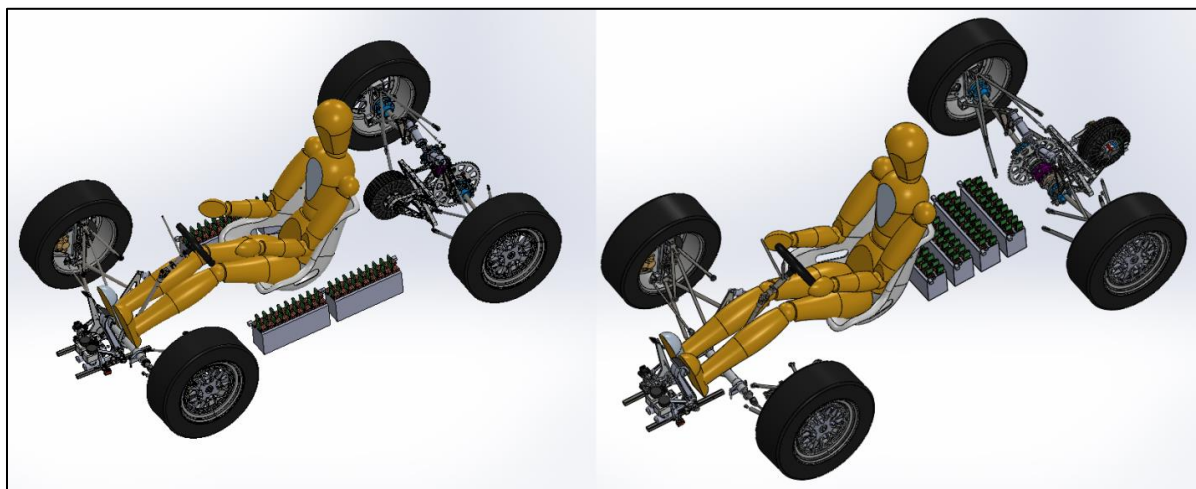


Figure 3.4: CAD of Two Future Formula Electric Concepts.

Left: Sidepod Layout
Right: Rear Motor Layout

Layout Verification

As the Rear Motor layout was clearly the preferred choice by the senior project team, a rules clarification was submitted to ensure that this was, in fact, a viable design. The inquiry regarded what sort of extra structure would be needed for the motor in the rear, and how structural equivalency could be proven in conjunction with the AF rules. The committee's response was prompt and agreeable. Motor protection structure must pass the side impact standards in AF 4.3, the only difference being that the load must be applied to all structural locations behind the main hoop for this case, instead of just all structural locations between the roll hoops.

With this validation secured, the next needed stamp of approval was that of the SAE team. In a Formula Electric team meeting, the senior project team presented the two layout concepts described above. It was collectively decided among the teams that the Rear Motor layout would be most beneficial to all concerned. The SAE team decided to accept the senior project team's proposal, and develop the Rear Motor concept in the 2014-15 school year.

Subsystem Interfaces with Frame

Drivetrain, suspension, steering, battery and electrical boxes, and the entire driver ergonomics system all interface with the chassis. Each of these interfaces supports significant loads, and as such, must be structurally robust. Each joint must be proven adequate for its respective load by FEA, empirical testing, or a combination of the two. Passing technical inspection at the FSAE competition is crucial to the success of the chassis, and to accomplish this, interface testing and evaluation must satisfy the SRCF.

Drivetrain

The drivetrain is a fully self-contained assembly, as shown in Figure 1.3. It is attached to the chassis by four bolts in the four corners of its central mounting plate. The drivetrain plate mounts must resist the forces caused by maximum wheel torque and support the weight and internal loading of the drivetrain components.

Suspension

The suspension interfaces with the chassis through the pickup points at the four corners of the car, the front and rear rocker mounts, and the front and rear shock mounts. Due to the extensive work of the 2013-14 suspension senior project, all forces at the tire contact patch and at every chassis-suspension interface are known for a variety of driving conditions. These forces are presented in Table 3.5, on the next page.

Table 3.5: Suspension Forces

| | | Full Braking (1.65G) | Full Cornering (1.59G) | Full Acceleration (.94G) | Combo Braking (.62G) and Cornering (1.47G) | Combo Braking (1.16G) and Cornering (1.12G) | Combo Braking (1.52G) and Cornering (.61G) | Static | |
|-------------------------------|-------|----------------------|------------------------|--------------------------|--|---|--|---------|------|
| Input Forces (lb) | Front | Fx | 336 | 0 | 0 | 126.25 | 236.22 | 309.53 | 0 |
| | | Fy | 0 | 364.23 | 0 | 354.3 | 324.69 | 279.87 | 0 |
| | | Fz | 211.36 | 232.27 | 93.01 | 254.96 | 258.05 | 243.05 | 134 |
| | | Mx | 0 | 0 | 0 | 0 | 0 | 0 | 0 |
| | | My | 3719 | 0 | 0 | 1325.67 | 2480.29 | 3250.04 | 0 |
| | | Mz | 0 | 199 | 0 | 265 | 300 | 286 | 0 |
| | Rear | Fx | 149 | 0 | -317 | 55.99 | 104.75 | 137.26 | 0 |
| | | Fy | 0 | 395.28 | 0 | 386.3 | 359.55 | 319.1 | 0 |
| | | Fz | 86.83 | 255.94 | 205.19 | 218.91 | 174 | 128.05 | 164 |
| | | Mx | 0 | 0 | 0 | 0 | 0 | 0 | 0 |
| | | My | 0 | 0 | 0 | 0 | 0 | 0 | 0 |
| | | Mz | 0 | 230 | 0 | 158 | 100 | 71 | 0 |
| Resultant Linkage Forces (lb) | Front | UCA F | 432 | 317 | 100 | 411 | 470 | 486 | 144 |
| | | UCA R | 76 | 464 | 140 | 414 | 339 | 255 | 201 |
| | | LCA F | 21 | -456 | -19 | -403 | -332 | -256 | -27 |
| | | LCA R | -407 | -341 | -26 | -469 | -562 | -603 | -37 |
| | | Spring | -547 | -568 | -242 | -627 | -638 | -602 | -349 |
| | | Toe | 330 | 113 | 10 | 201 | 274 | 323 | 14 |
| | Rear | UCA F | -136 | 186 | 350 | 123 | 59 | 4 | 27 |
| | | UCA R | 117 | 75 | -377 | 147 | 204 | 235 | -57 |
| | | LCA F | 288 | -669 | -1108 | -458 | -243 | -62 | -222 |
| | | LCA R | -478 | -664 | 620 | -759 | -810 | -806 | -178 |
| | | Spring | 160 | 438 | 379 | 370 | 290 | 209 | 322 |
| | | Toe | 55 | 224 | 129 | 178 | 132 | 94 | 110 |

Pedals

The acceleration and brake pedals attach to the chassis via two bolts each, in independent custom mounts. These mounts can be updated as needed. Loads on the pedals were measured in last year’s cockpit mockup by attaching a single quarter-car scale to the pedal. The driver was then directed to push on the pedal as hard as he could. Several drivers were tested, yielding a maximum force of 150lb. Force could be applied off-axis up to roughly 30 degrees (eyeballed) before slipping off the pedal.

Seat

The seat mounts to the chassis through one bolt on either side of the upper side edge and two bolts in the lower front edge. Forces applied to the seat during driving can be calculated from the mass of a known driver and expected driving acceleration. In general, the maximum acceleration a human can achieve through the knees is 3 g's. By assuming the driver of known mass leaps into or out of the seat, forces applied to the seat during entry and egress can be approximated. These forces would be assumed to be applied in random directions.

Steering

The steering rack mounts to the chassis via two vertical bolts on either end. These bolts hold down an aluminum collar on either end of the rack, which clamp around the rack to hold it in place. Expected forces through the steering rack have been determined by the suspension senior project. The steering column is supported by a bearing in a steel collar between the top U-joint and the steering wheel. This is mounted to the chassis by welding small-diameter steel tubes to the collar and to the front roll hoop.

Driver Harness

The driver harness can be a 5-, 6-, or 7-point variety, as long as it is FIA certified. The SAE team currently has a 6-point harness, so harness mounting should be designed to accommodate it. Two of the attachment points are shoulder belts, which wrap around a bar at the driver's shoulder level. This bar is welded to the main hoop. Two of the attachment points are the two ends of the lap belt. These bolt to tabs in double shear, at or near the bottom of the frame, and slightly behind the driver's hips. The remaining two attachment points are a dual anti-submarine belt. This attaches to the floor of the chassis under the center of the seat. AF4.4 and T3.41 clearly define the loads, both magnitude and direction, that the frame must support at each harness attachment point. For a full list of these loading cases, see Table 2.1

Head Restraint

The headrest must be 6 inches wide, 11 inches tall, oriented vertically (not tilted forward or rearward), padded, and located such that it supports the head of both the tallest driver and the shortest. Exact specifications for size and location are defined by T5.6.2 in the 2014 FSAE rule book. The restraint, along with its mounting and attachment must be strong enough to withstand 200lb of force applied rearward, as defined by T5.6.3.

Battery Box

The battery box must be removable for charging and maintenance. The mounting system for the box must withstand the forces generated by a 20g acceleration of the batteries parallel to the ground plane, and independently must withstand the forces generated by a 10g acceleration perpendicular to the

ground plane (see rule EV3.4.2). The original concept was to bolt it the floor or to some structure attached to the floor. Further refinement of this concept was left up to the battery box subteam.

Electrical Boxes and Motor Controller

The weight and number of electrical boxes were determined by the SAE team's electrical engineers. Positioning and mounting of the boxes were determined by the senior project team. The forces that these mounts must support have been calculated from the acceleration the boxes were likely to see, and their masses, once known.

Adhesive Testing and Results

Motivation

Four variations on the bonding and riveting method of joining presented themselves: riveting without epoxy, bonding without a rivet, bonding and riveting with the rivet left in, and bonding and riveting with the rivet drilled out. The available information implied that it would be stronger to drill the rivets out than to leave them in, and that merely clamping the metal together while the epoxy cured would be an inferior joining method. Both of these seemed counterintuitive. Definitive answers were needed as to which was the strongest joining method and why. Additional benefits of testing the bond strength were to allow experimentation with surface preparations and to verify that the epoxy would retain its full manufacturer-rated strength under the existing application conditions.

Test Design

Hysol 9460 was chosen as the adhesive to test. Its properties satisfied what would be required of an adhesive, and it was common and easy to find. The joints would be most likely to see high loads in shear, where one piece of metal is pulled or pushed past another. To test for this loading case, a tensile lap shear test similar to the one found in ASTM D1002 was chosen to be run on the Instron tensile test machine in the ME department's composites lab. Aluminum sheet metal was cut into 1x3" strips .06" thick, and holes were drilled in the ones to be riveted. The pieces were prepared for bonding by first roughing the surface on a wire wheel and then sand blasting. The ends were washed in acetone, and adhesive was applied to a 1-inch square for all except the rivet-only samples. Four tests were performed, with three samples in each test group. Group 1 was bonded with the Hysol 9460 and then clamped together with a pair of vise grips and two thick aluminum blocks to distribute the pressure evenly. Group 2 was bonded with the same adhesive but was then held together by a 3/16" structural rivet. After curing, the rivets were drilled out. Group 3 was bonded in the same way as Group 2, but this time the rivet was left in during the shear test. The fourth and final group is bonded with only a rivet. This group was created to be a control of sorts by showing how a rivet alone holds together the two aluminum plates. Sample from groups 1, 2, and 3 can be seen in Figure 3.5.



Figure 3.5: Samples from the Three Adhesive Testing Groups.

Results and Observations

There was data saturation in at least one test out of every group, but there was also at least one test in each group with no saturation. Only the results without saturation are presented. The strength results for Group 1, the bonded and clamped group, were lower than those of the second test group. The adhesive would yield rather suddenly without much strain. Group 2 clearly had the highest stress at failure. This was a result of the rivet being a more effective means of holding the aluminum together while the adhesive cures. The results of groups 1 and 2 are compared in Figure 3.6, below

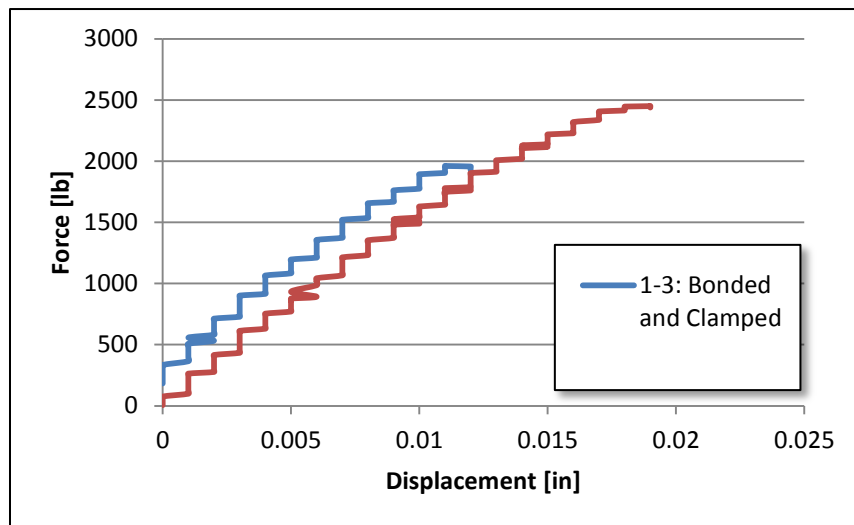


Figure 3.6: Force-Displacement Curves of the First Two Adhesive Groups

Group 3 was bonded just like the second group, however in testing this group showed lower yield strength values than Group 2. This appears to be caused by the rivet forcing the aluminum panels to

bend under tension. The lap joint places the two halves slightly out of alignment with each other, causing a moment under tension. The ductile rivet prevents the epoxy bond from popping apart all at once, but pulls the joint so that the forces on the two halves are aligned. This leaves the bond no longer in pure shear but instead adding a peeling force. The adhesive is very weak in this loading direction and therefore failed at a lower stress. This comparison can be seen in Figure 3.7, below.

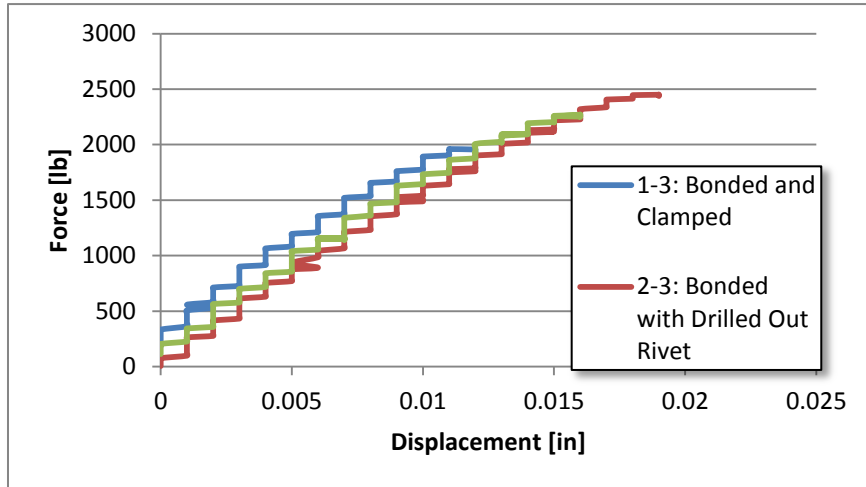


Figure 3.7: Force-Displacement Curves of the First Three Adhesive Groups

Group 4, the rivet-only group, was used strictly to compare the results of the test with the adhesive and rivet bonded panels. The results showed that the panels tend to peel more when under a tensile load with the rivet being used to bind them. The peeling behavior of this group is illustrated in Figure 3.8, below, and Figure 3.8 compares the results of all four tests, showing the low force and high deformation for the rivet-only sample.

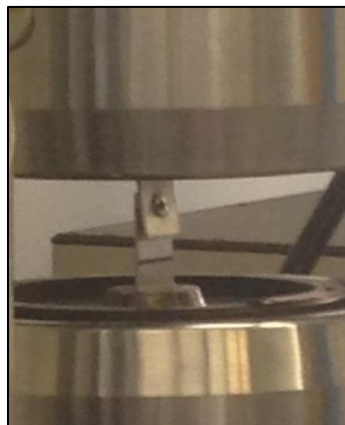


Figure 3.8: Illustration of the Peeling Deformation Caused by a Rivet in Test Group 4

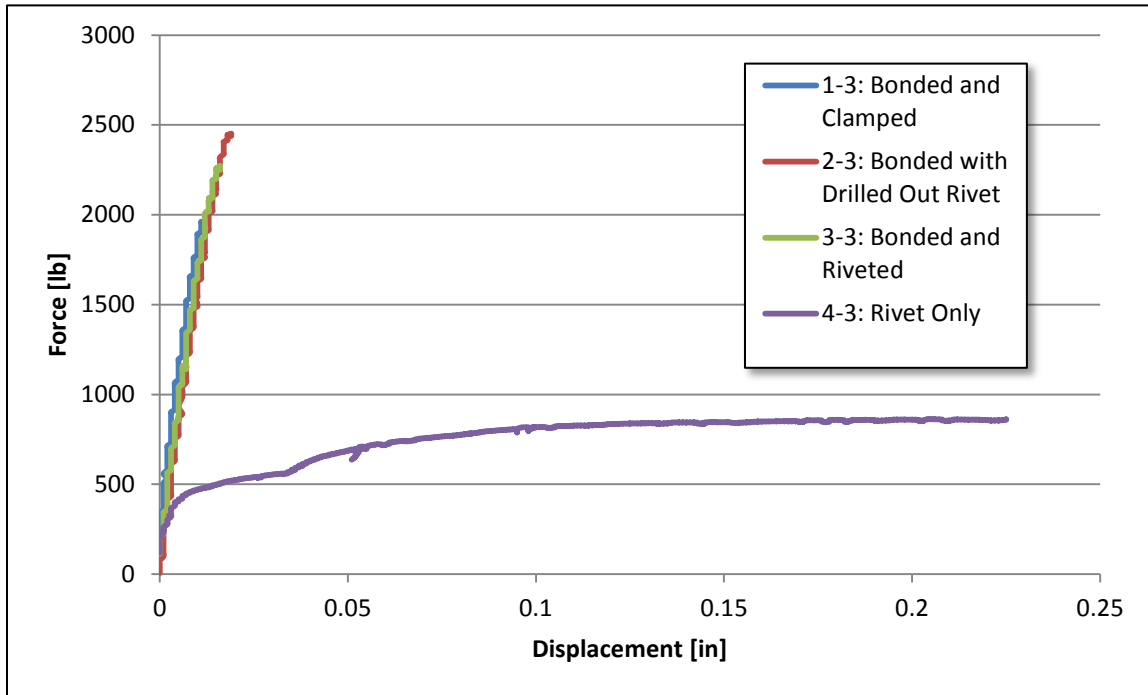


Figure 3.9: Force-Displacement Curves of All Four Adhesive Groups

This testing session confirmed that clamping is weaker than riveting in an epoxy joint, and that drilling out the rivet does, in fact, increase joint strength. Drilling out rivets, however, can be very time consuming. The tests did emphatically confirm the manufacturer’s specifications, with the weakest bonded test failing at the rated 2000psi. This also confirms that the preparation method used is effective. An important takeaway is to avoid placing the bonded joint in any situation where it will experience peeling or tensile forces.

Cockpit Mockup

Construction and Design

A revisit of last year’s cockpit mockup was needed to find a new, more compact driver position and to determine the height limit of the top side impact tubes. The framework for the mockup was repurposed from the 2013-14 chassis jig. The carefully squared 3x10ft rectangular base and upright end sections suited the purpose well. Figure 3.10 shows the framework with the revised mockup.



Figure 3.10: Front View of Entire Cockpit Mockup

To determine the seat position, a kart seat from an older Formula Electric car was used. The seat needed to be moved forward and backward and also rotated to more upright or reclined positions. To accomplish this, vertical pieces of extrusion, from now on referred to as tubes, were bolted to the rear face of the framework. These tubes could move side to side to allow easy centering on the seat. Horizontal forward-pointing tubes were then affixed to these. The horizontal tubes can move up and down on the vertical tubes, forming part of the system for rotating the seat. These horizontal tubes also bolt into holes in the sides of the seat. These bolts allow the seat to rotate relative to the tubes and also slide forward and back on the tubes. The bottom of the seat rests on the longitudinal tube down the center of the framework, but bolts to a lateral tube beneath that for stability. This tube is attached only to the seat and can move forward and back freely, forming the other part of the seat rotation system. This system can be seen to some degree in Figure 3.11.



Figure 3.11: View of Cockpit Mockup Showing Seat Mounting, Top Tube Mounting, and Steering Wheel

The steering wheel needed adjustment in both translation and rotation front-to-rear, and also in height. A dummy steering wheel was made of foam and bolted to two vertical tubes. This allowed vertical adjustment and stability. The vertical tubes bolt to the center tube with two brackets, to allow for both rotation and longitudinal translation (see Figure 3.12).



Figure 3.12: Double Bracket System to Allow Rotation of Vertical Mockup Components

The pedals needed all the same dimensions of adjustment as the steering wheel, and also needed to be adjusted closer together and farther apart. To accomplish this, the same sort of rotating vertical structure was built as was built for the steering wheel. The pedals themselves were made of pieces of 80/20 extrusion to rest the feet against, and lateral adjustment was achieved by bolting the pedals to a horizontal tube affixed laterally across the double upright tubes. The pedal mockup is illustrated by Figure 3.13.



Figure 3.13 Pedals in Cockpit Mockup

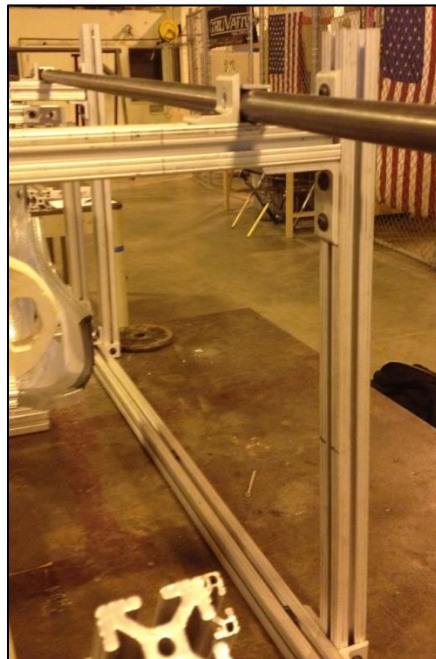


Figure 3.13a: Top Side Impact Tube in Cockpit Mockup

Side impact tubes were integrated into the mockup, as seen in Figure 3.13a, by attaching vertical tubes to the side rails of the framework. Horizontal lateral tubes were then bolted between these uprights at

the front and rear. These lateral tubes can be moved up and down independently of each other, allowing height and slope adjustment of the side impact tube. The tube itself is held to the lateral rails by bolted-on brackets, which allow lateral adjustment of the two ends of the side impact tube independently of each other.

Intended Outputs

The seat can move by angling up and down (more upright or reclined). This will establish what is a reasonably comfortable seat angle for the driver. All other dimensions will be measured relative to the seat. The steering wheel position can move forward and backward, up and down, and be angled up and down. This will establish how compact the arm position can be before the driver begins to feel cramped, and what is the best steering wheel angle for a compact arm position. The pedal position can move forward and backward, up and down, can adjust wider or narrower, and can rotate up and down. This, like the steering wheel, will establish the most compact position for the driver without causing discomfort. By establishing the seat position and angle, the mockup will also help to establish harness attachment points. This is important for accurate modeling and analysis, since harness attachment structure is an important part of AF rules. The width, height, and slope of the top side impact tube have an important bearing on the ease of 5-second egress as required by rules. FEA has also shown that higher side impact tubes tend to make stiffer frames by essentially increasing the cross-sectional moment of inertia of the chassis. It is important to find the highest possible location of this tube and the possible effect of a slope up or down so that it can be exploited in chassis design. The cockpit parameters established by this mockup are reported in the dimensioned sketch below (Figure 3.14).

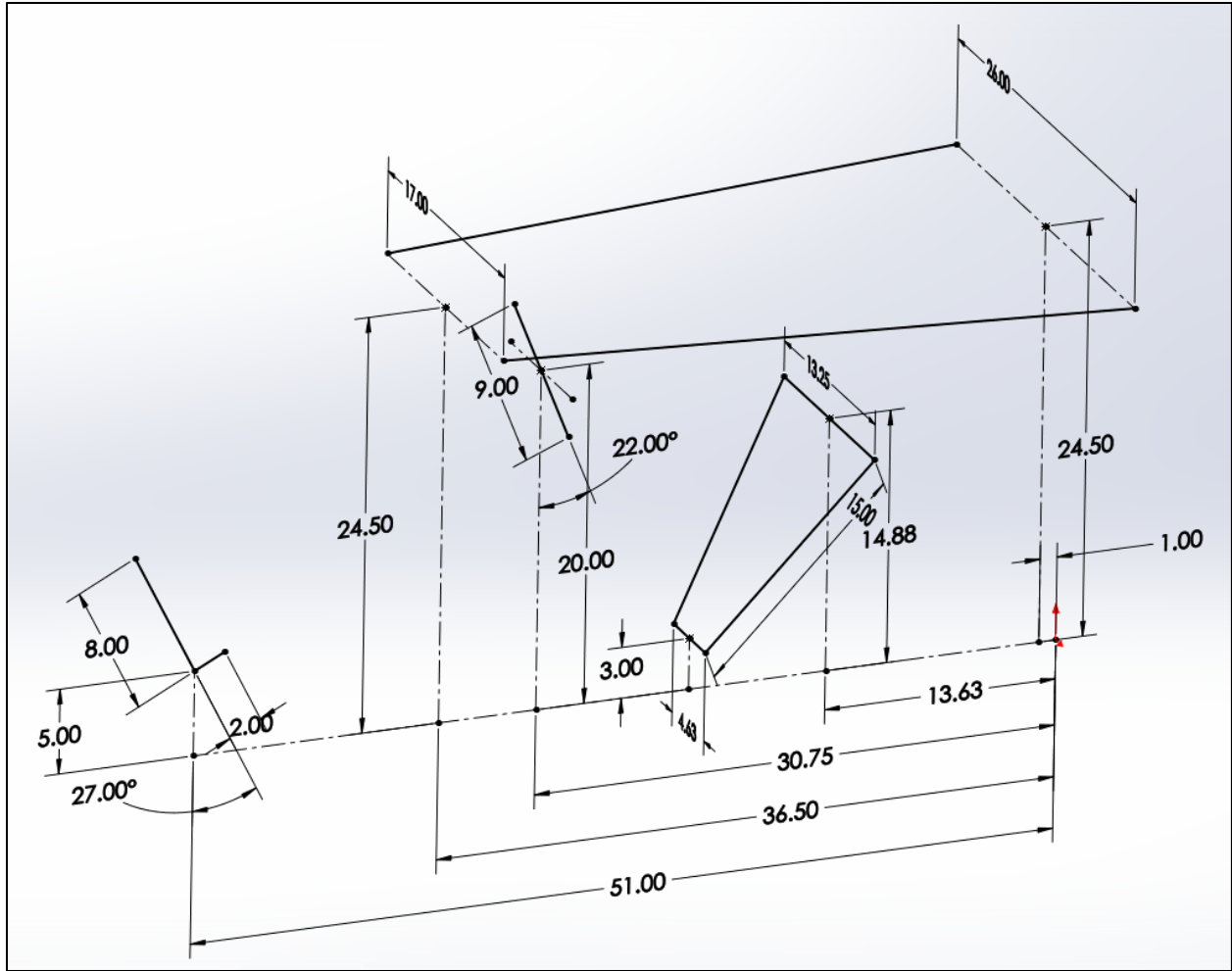


Figure 3.14: Dimensioned Sketch of Final Cockpit Mockup

FEA-Based Evolutionary Design in MATLAB

Purpose

The purpose of this MATLAB code is to speed up steel tube frame design from rough concept to final design. The steel tube frame makes up most of the structure of the chassis, and therefore must withstand various loads, including those required by AF rules in Table 3.1. Designing a single steel tube frame doesn't take long, but very rarely does the first design meet all structural requirements. Repetitive finite element analysis (FEA) in commonly used CAD programs like Solidworks takes a very long time. It is also very time inefficient to be doing the same setup procedure over and over again. This task is perfectly suited to MATLAB code, where it is very easy to loop repetitive processes. With an FEA method written in MATLAB code, the program could quickly test and iterate many frame designs. Coding

a logical selection process to make the MATLAB code generate new frame iterations based on previous results would exponentially increase steel tube design productivity.

Program Summary

The main inputs to this program are arrays called 'Node Coordinates' and 'Element Data'. Nodes are where more than one frame tube intersect. The node coordinates array is a list of the x,y,z locations of every node in the frame. The element data array is a list of which nodes each frame tube connects, and the outer diameter (OD) and wall thickness of those tubes. The program takes the input node coordinates and element data and creates a 3D wireframe representation. Each tube is represented as a line connecting two end points. The program then creates a meshed version of the wireframe. Meshing each line adds a defined number of evenly spaced points on that line. Those points are new nodes, which create new, smaller elements between them. In general, smaller elements in FEA model yield more accurate results.

Once the program has established a meshed model of the frame, it can apply the stiffness method. The stiffness method starts with calculating the stiffness matrix for each individual element. The stiffness matrix for a 3D frame element is a 12x12 matrix, with a row and column for each degree of freedom for each end point. The matrix values are functions of the material and geometric properties of the element such as area, moment of inertia, and modulus of elasticity. The stiffness method adds the individual element stiffness matrices according to the global shared degrees of freedom to form the global stiffness matrix. The global stiffness matrix is a square matrix of size equal to 6 times the total number of nodes. The global stiffness matrix represents way the entire frame deforms under load. The stiffness method is essentially Hooke's Law: displacement is equal to force divided by stiffness. To get the displacement of every degree of freedom in the frame, stiffness method just divides the applied force by the global stiffness matrix.

Once the program gets the displacement of every degree of freedom of every node in the frame, it can calculate the total linear displacement of each node by taking the root-sum-square of the linear degree of freedom displacements at that node. From this, the maximum total displacement of any node on the frame can be found. This is the final output of the FEA function in the MATLAB code.

Once the program has found the maximum deflection for each loading case, the only frame performance information left to find is weight. From the non-meshed 3D wireframe found earlier along with the known tube OD and wall thickness, the program can calculate the length and weight of each tube. Now, having deflection and weight information about the current frame design, the program can compute a numerical score for the frame. The numerical score allows for comparison between frames. Details about the numerical scoring method are explained below in the Scoring Method section.

There are two other functions aside from the FEA that make this MATLAB program a design tool, not just an analysis tool. The first function has three inputs: node coordinates, element data, and a user-defined set of parameters: some that are allowed to change and some that are held fixed. The function

creates a new frame design based on the input information, but with random slight variations according to the user's set of parameters. In combination with the FEA and scoring method, this function allows the program to randomly generate a set of frame designs, analyze them, and compare them to find the best one. The second function controls and loops this process. It takes in the frame data and respective scores for each frame, chooses the best design to re-iterate on, and sends it back through the loop of randomization, analysis, scoring, and selection. More details of this process are explained in the Evolutionary Algorithm section below.

Outputs

This MATLAB program can output any information about the frame design as it changes throughout the iterative design process. Often useful to the user is a 3D plot of the deformed result of a given loading case for a given frame design. If this is not desired, the program can simply output the history of design changes and the final frame design of the iterative process. For these results, see the Results section below.

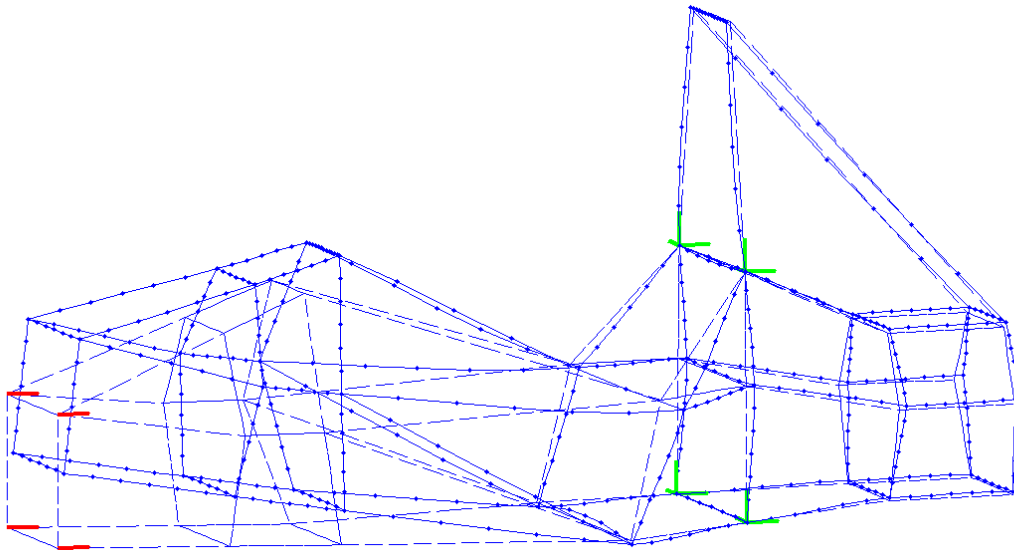


Figure 3.15: Deformed FEA Result in MATLAB

Figure 3.13 shows a frame being tested under the front impact loading case. The green lines represent fixed displacement constraints, and the red lines represent applied forces. The dashed lines with no dots represent the undeformed shape of the frame, and the solid dotted lines show the mesh and deformed shape.

Model name: Front Box FEA
Study name: Study 1
Plot type: Static displacement Displacement1
Deformation scale: 41.3514

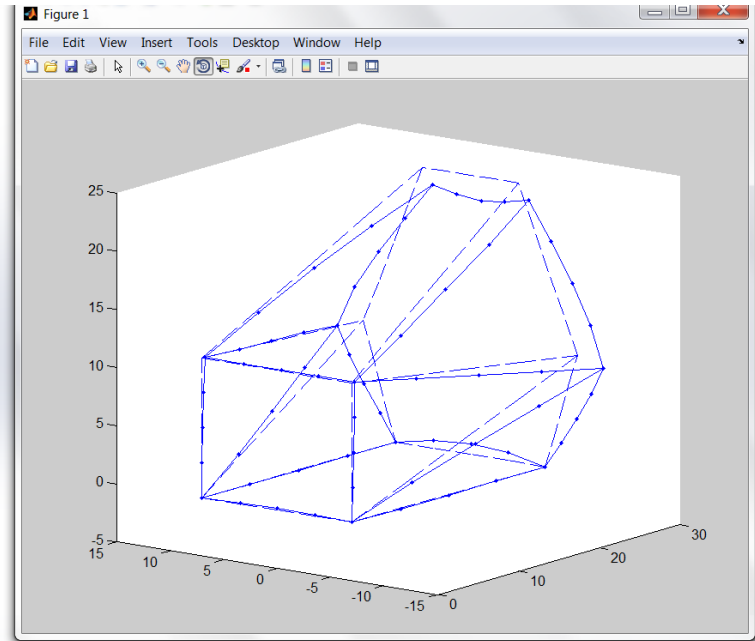
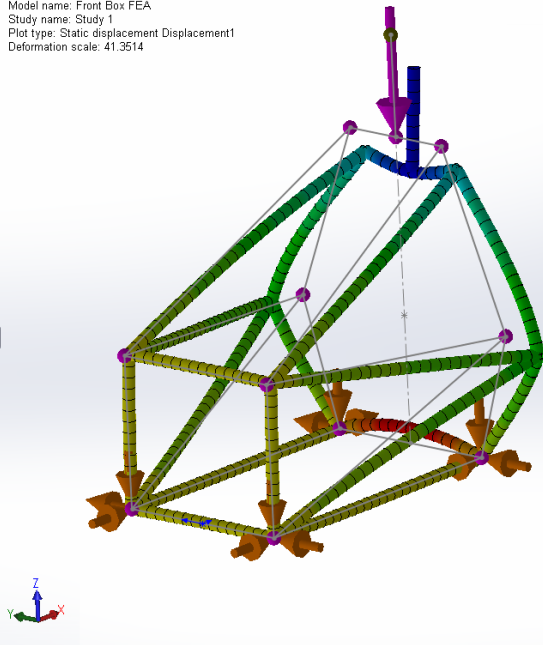


Figure 3.15: SolidWorks and MATLAB FEA on a Sample Tube Structure

Figure 19 shows the deflected result of a sample tube structure in both Solidworks and MATLAB. Through a series of tests similar to this one, MATLAB consistently outputs deflection results 1-2% lower than Solidworks. This difference could be caused by different simplifications made by the Solidworks software and the stiffness method used in MATLAB.

Scoring Method

The purpose of the scoring function in the overall MATLAB program is to take in weight and deflection results from one frame and compute a single numerical score. That score is then used to compare different frame designs to each other, no matter how different the individual deflection results are. The purpose of the scoring method is to shape the way the composite score favors certain results over others in order to give the best score to the result that is closest to what the user desires.

The current scoring method has inputs of weight, six maximum deflection results from the AF loading cases, and one max rotation result from torsion. In general, a lower score is better. The score starts out by giving a base number of points equal to the weight of the frame in pounds multiplied by 2. The current max deflection requirement is 0.75, which corresponds to a safety factor of 1.33 to the maximum deflection allowed by the AF rules. For each max deflection result, if the deflection is under the threshold of 0.75, the score gets a bonus of 2 points subtracted from the total. For the max rotation result, the bonus is 20 points with a threshold of 0.35 degrees, which corresponds to a torsional stiffness of 1800 ft-lb/deg. The rotation score effects are weighted 10 times larger than each individual deflection score because there are more deflection results. This step bonus means that once a design passes a new test it previously hadn't, it's more likely to not fail that test again even after further dropping weight.

Finally in the scoring method, all deflection results are multiplied by 3, the rotation result is multiplied by 30, and those point values are added to the total score. This gives slight pressure to constantly improve results without valuing stiffness over weight too excessively. Figure 3.17 illustrates this scoring method.

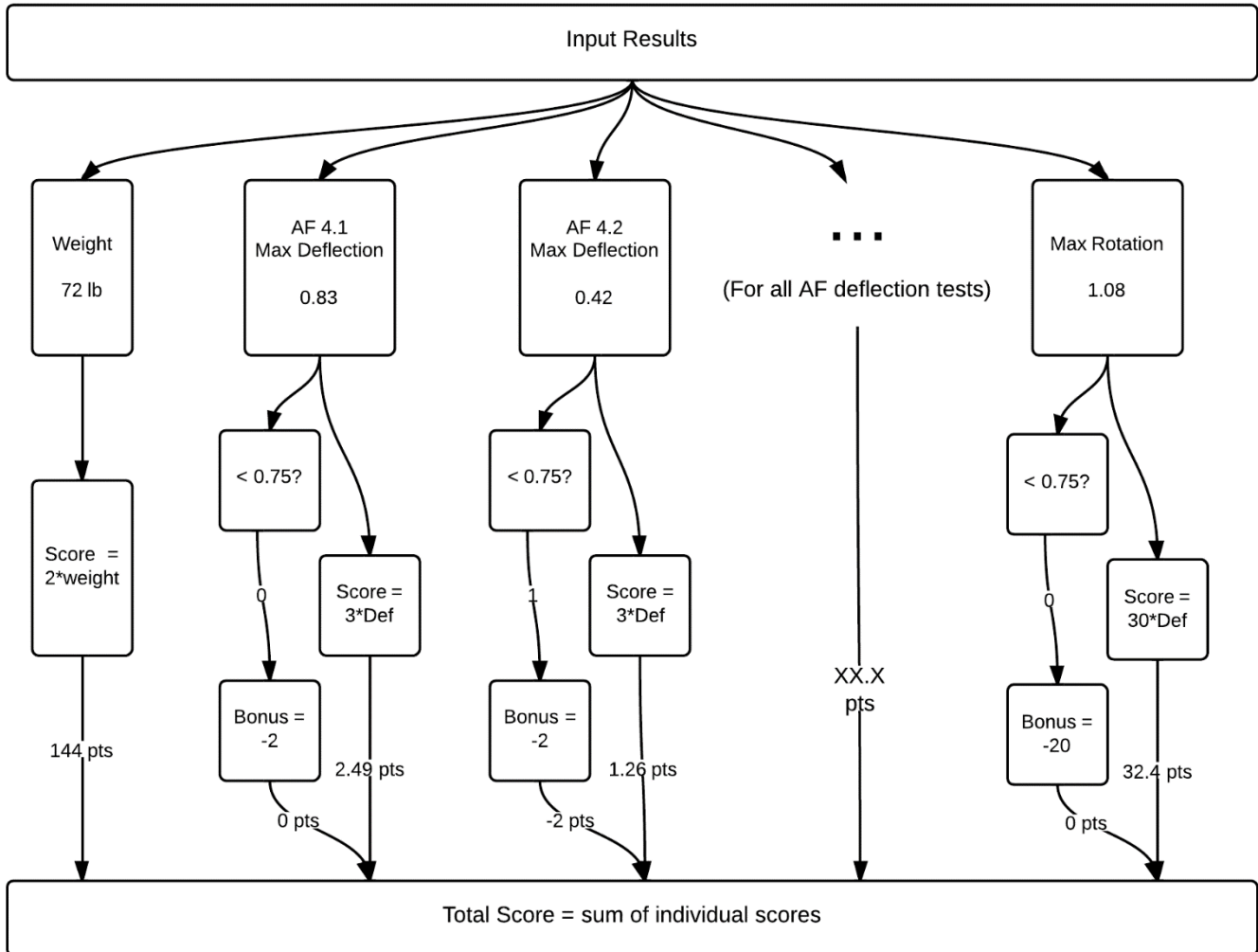


Figure 3.17: MATLAB Program Scoring Method Flowchart

The end result of design iteration is highly dependent on the scoring method. If the scoring favors stiffness over weight too much, the end result can be a 120 pound frame with safety factors of 10 everywhere. The same extreme behavior could also work for weight, yielding a very light frame that fails structural requirements. The goal of the scoring method is to make the desired frame results score the best.

Evolutionary Algorithm

Before running the code, the user defines which aspects of the frame can change, such as node geometry or tube size. The user also defines which dimensions must change together, such as to keep the frame symmetric or ensure a continuous roll hoop doesn't change tube size between nodes. These sets of dimensions are called parameters. Sets of frames analyzed in parallel with each other are called generations. In order for the frame design to evolve and accumulate changes, the program must create a new generation based on the results of the previous one. The set of patterns and rules that determine how that is done is called an evolutionary algorithm.

Our current evolutionary algorithm picks the single best scoring frame from the previous generation as the winner. To create a new frame based on the winner, it randomly picks a few of the parameters and changes them in a random way. The rest of the parameters that were not chosen to change stay the same as those of the previous winner. The program populates the new generation with these randomized mutations. This is how beneficial changes can be passed on from generation to generation. Take the upper side impact frame tubes as one example of parameter randomization. One dimension can define the z-height of the upper side impact tubes. The associated parameter would simultaneously change both the right and left upper side impact tubes to keep the car symmetric. This parameter would be expressed as a range of possible z values this tube could be, such as 12.5 to 16 inches above the ground plane. If this parameter is chosen at random to change, the program will pick a random number between 12.5 and 16 to be the new z-height of the upper side impact tube.

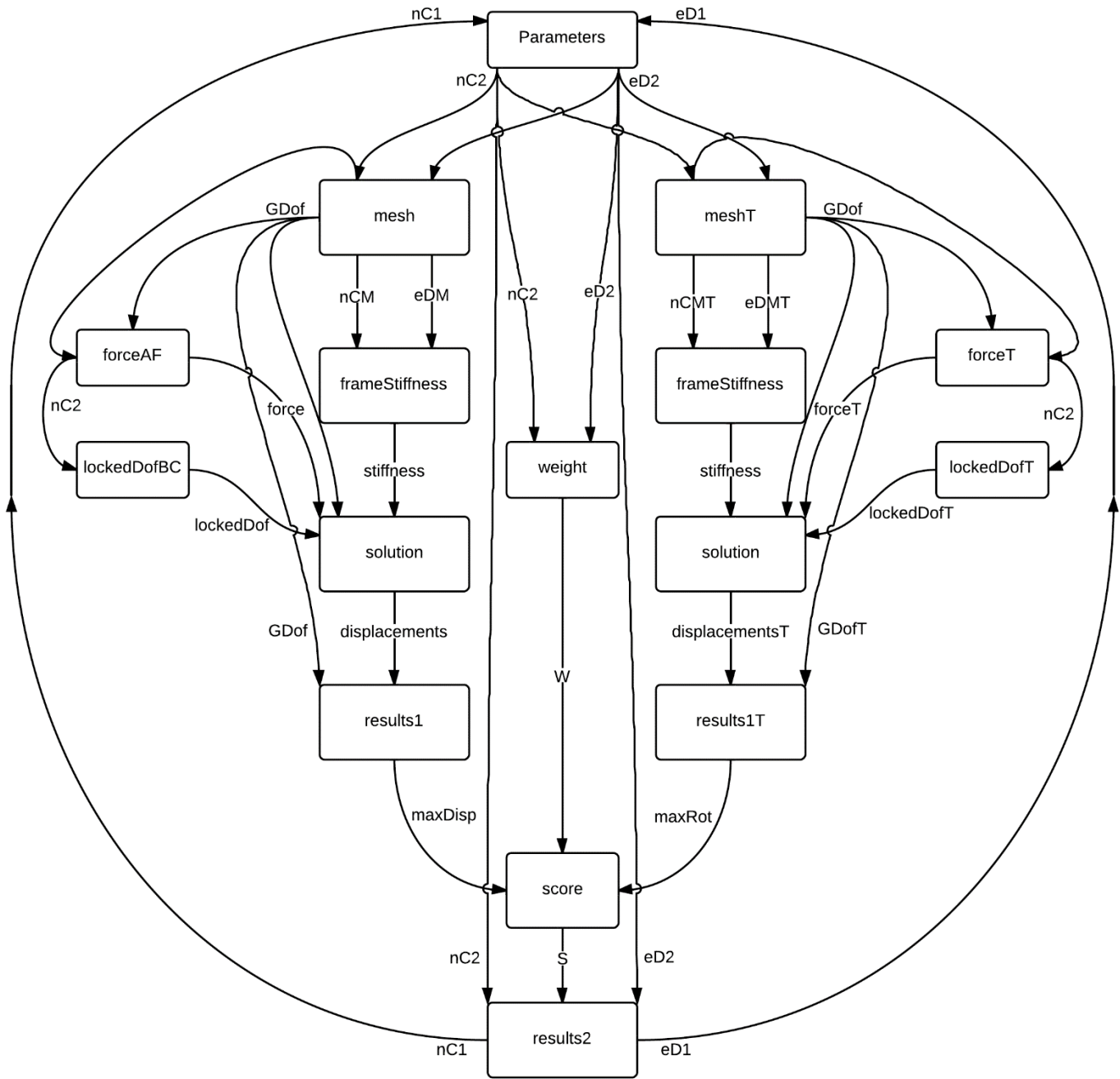


Figure 3.18: Overall MATLAB Program Map

Figure 3.16 illustrates the iterative process the program follows. Each cycle starts and ends at the top Parameters block, which takes the winning generation 1 data and creates a random set of generation 2 frames. The frames individually go through the middle FEA section until they get to the score block. The score block is expanded in Figure 20. The score block passes on the frame data and its respective score to the results 2 block. The results 2 block compiles all the frames in the generation, picks the best one, and passes it back to the top to restart the cycle.

NASA has used similar techniques to design evolved antennas for the ST5 spacecraft. Because of unusual radiation patterns the spacecraft may encounter, their evolutionary algorithm can develop complicated asymmetric antenna shapes that could not be designed with traditional methods. NASA's evolutionary algorithm eliminates a few of the weakest designs in a generation and repopulates the next generation with mated children of the strongest designs. This method closely approximates the natural selection process. It finds high-performing designs more efficiently than our simpler method because it mutates multiple high-scoring designs in a generation and only eliminates a few of the worst designs, instead of simply picking the single best design in a generation to iterate on. Because of the complexity of a large space frame, it will be beneficial to us to develop a more intricate evolutionary algorithm similar to one like NASA's.

Results

The initial design for the results in this section is a full steel tube frame with no floor. The program was run with a generation size of 200 frames, over a total of 80 generations. The loading cases considered by the program were AF4.1-4.5, rear side impact, and torsion. The scoring method and evolutionary algorithm used in this run are described in the Scoring Method and Evolutionary Algorithm sections above.

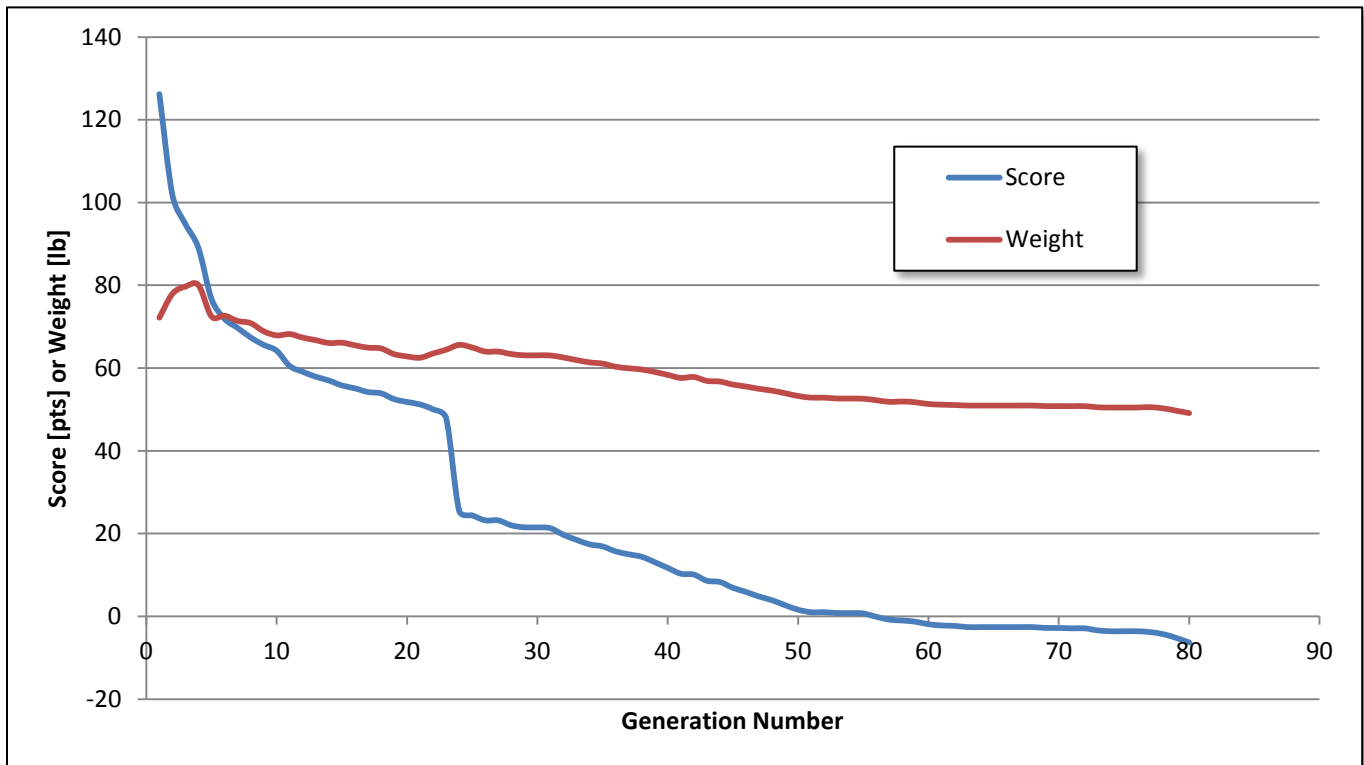


Figure 3.19: Weight and Score Change Across 80 Generations

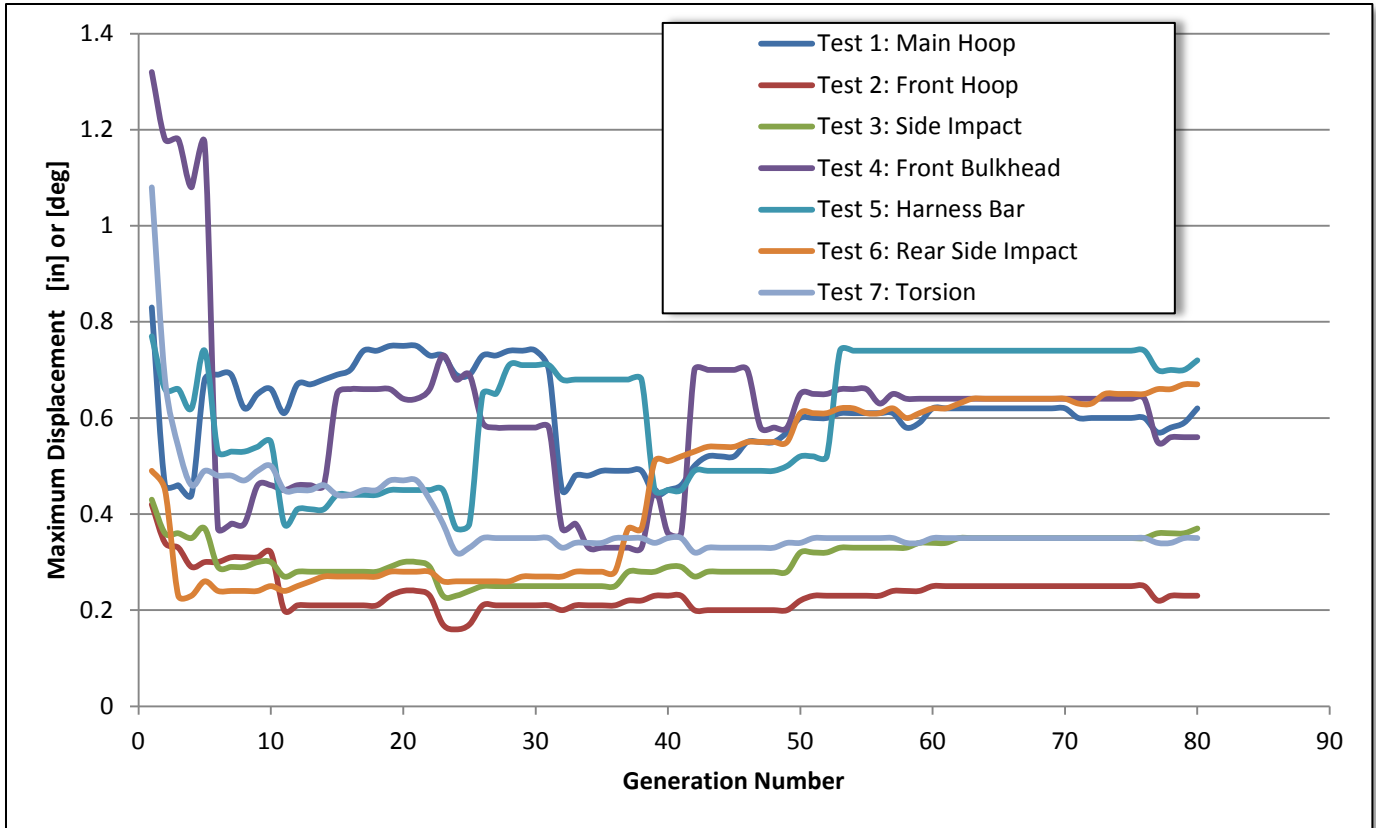


Figure 3.20: Maximum Deflection Change Across 80 Generations for 7 Loading Cases

In the first 4 generations, the frame gets heavier in order to greatly improve stiffness results. In the next few generations after that, the frame loses all the weight is just gained, but with greatly improved stiffness. By generation 6, every deflection and rotation result is under 0.75. From generations 7-20, the frame gradually loses weight and increases in stiffness. In generations 20-23, it starts to gain weight again. In this period, the score is still slowly decreasing. This is driven by a strong improvement in torsional stiffness, as seen in Figure 3.19.

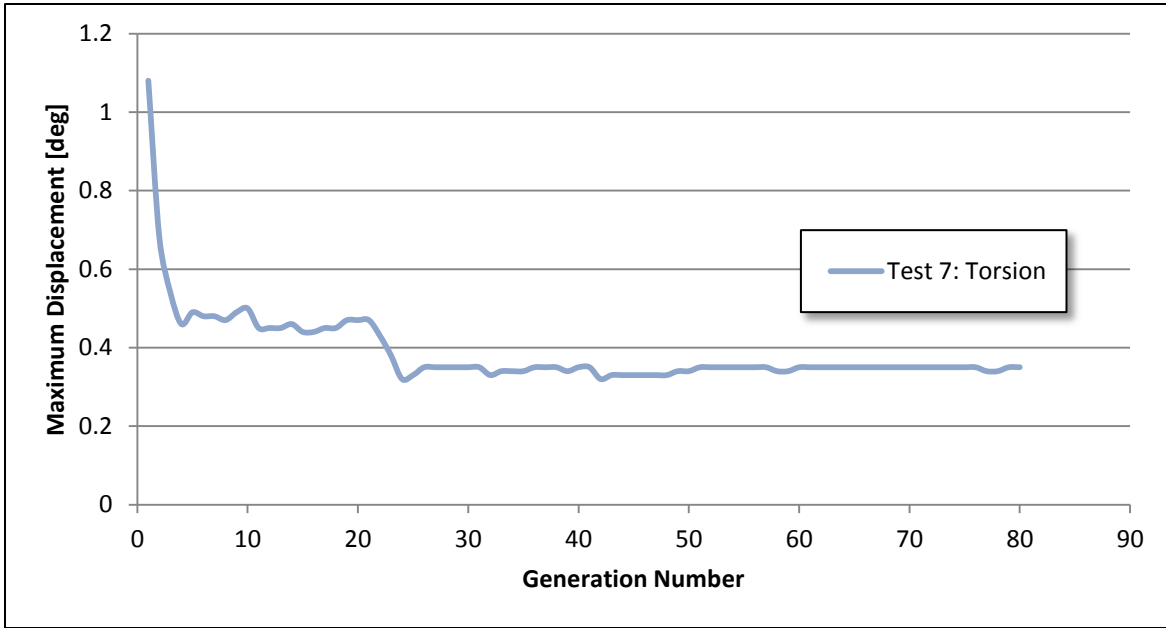


Figure 3.21: Maximum Rotation Change Across 80 Generations

At generation 24, the score suddenly drops. This is caused by the rotation result dropping below the bonus score threshold of 0.35 degrees, which corresponds to passing our torsional rigidity goal of 1800 ft-lb/deg. After generation 24 until the end, the frame continues to become lighter and lighter while still passing all deflection requirements and holding torsional rigidity at our goal.

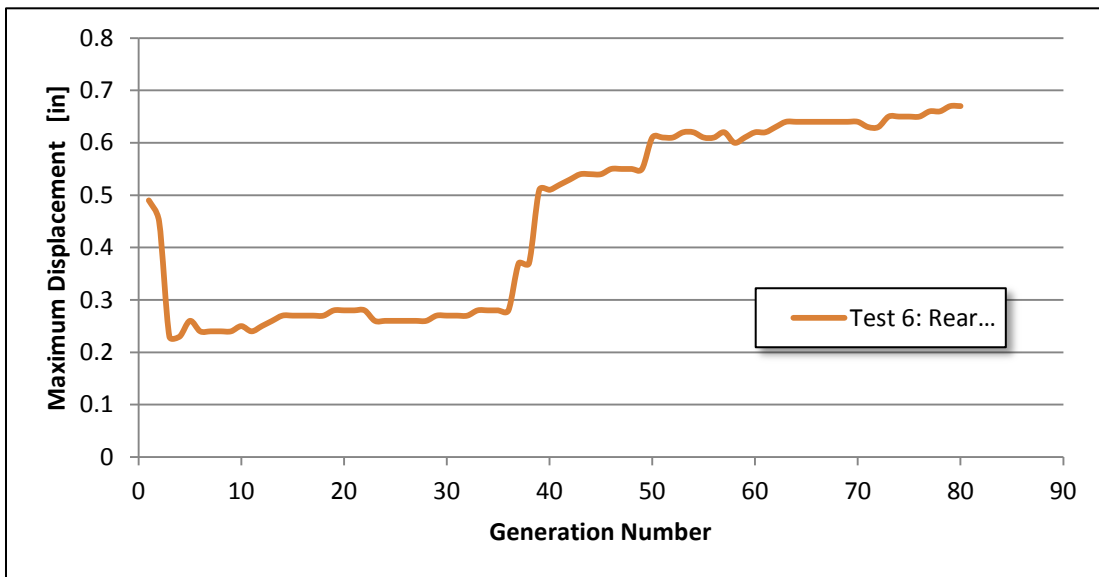


Figure 3.22: Maximum Deflection of Rear Side Impact Test Across 80 Generations

As seen in Figure 3.20, the deflection of the rear impact structure increases up to the threshold of 0.75 in order to save as much weight as possible. The rear side impact structure is mostly isolated from the rest of the frame, so it can freely adapt to what makes it help the frame score the highest

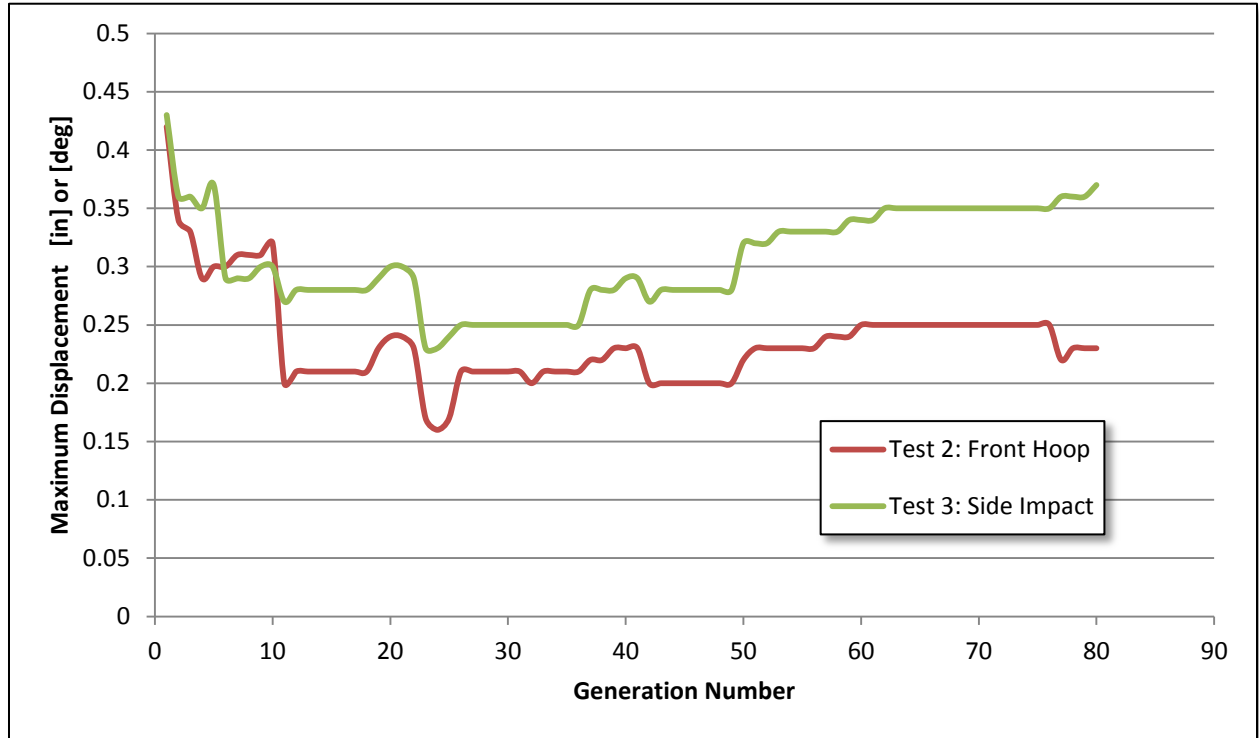


Figure 3.23: Maximum Deflection of Front Hoop and Side Impact Tests Across 80 Generations

A similar type of behavior to the test 6 results can be seen in the test 2 and 3 results in Figure 26. These two deflections start increasing after generation 50, but never get as close to 0.75 as the test 6 deflection did. The front hoop and side impact structure affect other tests like front impact and torsion, so they have to stay stronger than necessary for just test 2 and 3.

These results prove that this program can develop steel tube frame designs in a few hours of run time that would be nearly impossible to manually design in any FEA program in the same amount of time. The starting design was 72 pounds, failed 3 of the 6 AF tests, with a torsional stiffness of 500 ft-lb/deg. The final output design was 49 pounds, passed all AF tests, with a torsional stiffness of 1800 ft-lb/deg.

Program Refinement

Further development and implementation of new features improved results even more. Consolidating every program input into a single spreadsheet made it faster and easier to run the program and observe how it behaves. Using deflection results to calculate stresses in the tubes made for more thorough

design development and resulted in more refined output designs. Improving the scoring method and evolutionary algorithm improved the program duration as well as the quality of the output design.

Zodiac Aerospace and Composite Sandwich Panels

For research on all things related to sandwich panels, Hexcel was the go-to information source. The difficulty came when Hexcel's panels proved very difficult to acquire. In the search for Hexcel panel suppliers, it came to light that Hexcel and Zodiac Aerospace had recently collaborated to develop a new carbon composite airline seat. This recalled the fact that C&D Zodiac, the Santa Maria, CA division of Zodiac Aerospace, has a very close relationship with Cal Poly. Previous tours with the Cal Poly's Manufacturing Engineering department and Zodiac's prior sponsorship of the combustion FSAE team's carbon tub prompted hope that the company would be willing to help this project as well. An email was sent inquiring about their interest in the project and requesting panel scraps for testing and any advice they could offer. Their response was quick and encouraging, offering an array of panel test samples and a tour of the facility.

The tour was conducted by a former FSAE member who had worked on the carbon tub, so his advice was both about composite panel design in general and about things he learned while working with sandwich structures on an SAE car. C&D Zodiac purchases their materials from a supplier that is also owned by the same mother company, so buying panels from their source was not an option. They did, however, state that they would likely be able to provide an entire panel or two to donate to the project. Flat panels are only a small fraction of the materials the company uses. Zodiac makes much more extensive use of prepreg skins and honeycomb cores, shaped and bonded in enormous heated presses. Another small part of their business involves the cut-and-fold technique, where part of the panel is removed to allow the rest to bend around a corner. For large-radius bends, many small parallel cuts are made through the skin on the inside of the corner. This forms a wide, smooth, sweeping curve. For small-radius bends, a single wide strip of skin is removed from the inside of the corner. This allow the panel to bend in a much smaller arc, as there is less skin left to get in its own way. For very tight corners, a part of the core is removed along with the skin, leaving just the outside skin and a small part of the core. Where extra structure is needed, an aluminum plate is bonded to the panel. The plate is acid etched before bonding for the best possible bond strength. Honeycomb sandwich structures are very stiff, but are terrible for bearing stress. Anything attached to the panel must be bonded, or if using a fastener the fastener must be placed in an insert. To scale test results from a small sample, force and displacement data must be converted to stress-strain curves. Stresses and strains should be the same regardless of panel size.

When asked about the torsion properties of the panels, the response was that these panels are not designed to support torsional loads. For torsion, there must be shear flow from the top skin to the bottom. With raw edges, the only way for this to happen is through the core. The core, however, is very weak in shear. To route the shear stress somewhere besides the core and prevent core shearing, the edges of the panel must be closed out. To close out the edges, the core should be cleaned away and the

edge filled with resin or lightweight glass microspheres. A composite wet layup can then be wrapped around the resin-filled edge.

Another very useful point is that panels do not behave isotropically. There are usually two plies of 0-90 weave composite for the skin, leaving the 45 degree direction weak. Data sheets usually give the most conservative data: that of the weak direction of the panel. To examine how that will affect behavior in real-life scenarios (for example, the floor of a chassis), the panels should be tested in a point loading case on a plane, not just in beam bending.

They proceeded to send us home with four large pieces of honeycomb panel, as follows:

- 3/8" thick: 11.25" x 18"
- 1/2" thick: 17.625" x 27.75"
- 3/4" thick: 12" x 35"
- 1" thick: 12" x 24"

Once it became clear what materials were available to work with, test fixture design began in earnest. With fixtures made and data collected and analyzed (see next section for details), a decision was made that the 1" thick panel would be the best option. An email was sent back to Zodiac requesting three 24"x96" panels. The first was intended for use as the final floor panel for the chassis, the second for a full-scale chassis prototype, and the third for large-scale testing and validation of designs as required by the AF rules and SRCF.

Sandwich Panel Testing

Panel Mass Properties

First, each panel was weighed and measured, and the area densities were calculated for each of the four thicknesses.

Table 3.6: Measured Panel Mass Properties

| Thickness (in) | Width (in) | Length (in) | Area (ft ²) | Weight (lb) | Density (lb/ft ²) |
|----------------|------------|-------------|-------------------------|-------------|-------------------------------|
| 3/8 | 11.250 | 18.000 | 1.406 | 0.679 | 0.483 |
| 1/2 | 17.625 | 27.750 | 3.396 | 1.748 | 0.515 |
| 3/4 | 12.000 | 35.000 | 2.917 | 1.689 | 0.579 |
| 1.000 | 12.000 | 24.000 | 2.000 | 1.292 | 0.646 |

Volumetric density of the core is found in Table 3.7. The area density of one panel is subtracted from that of another, cancelling out the two skin layers and leaving only a difference in core thickness. This allows us to find the volumetric density of the core, in terms of pounds per square foot for 1 inch of thickness. This comparison was performed for all 6 possible combinations of the 4 panels and the average core volumetric density was found out to be 0.26 (lb/ft²)/in. The sample standard deviation between the 6 calculated densities was 0.0048 (lb/ft²)/in, which demonstrates that these panels and measurements are highly consistent.

Table 3.7: Average Core Volumetric Density

| Comparison | Difference in Thickness of Core | Difference in Total Density (lb/ft ²) | Density per Inch Thickness of Core ((lb/ft ²)/in) |
|------------|---------------------------------|---|---|
| 1/2 to 3/8 | 0.125 | 0.032 | 0.255 |
| 3/4 to 3/8 | 0.375 | 0.096 | 0.256 |
| 3/4 to 1/2 | 0.250 | 0.064 | 0.257 |
| 1 to 3/8 | 0.625 | 0.163 | 0.261 |
| 1 to 1/2 | 0.500 | 0.131 | 0.262 |
| 1 to 3/4 | 0.250 | 0.067 | 0.268 |

Table 3.8 subtracts the average core volumetric density multiplied by the core thickness from the total panel density, leaving just the area density of the two skin layers. The average skin density from this was about 0.385 lb/ft². The sample standard deviation was 0.00084 lb/ft², which again shows the consistency of the panels and repeatability of measurements.

Table 3.8: Measured Panel Mass Properties

| Panel Thickness (in) | Overall Area Density (lb/ft ²) | Area Density of Core | Area Density of Skin (both sides) (lb/ft ²) |
|----------------------|--|----------------------|---|
| 3/8 | 0.483 | 0.097 | 0.385 |
| 1/2 | 0.515 | 0.130 | 0.385 |
| 3/4 | 0.579 | 0.195 | 0.384 |
| 1 | 0.646 | 0.260 | 0.386 |

Testing Setups

Testing methods were taken from Hexcel’s paper “Mechanical Testing of Sandwich Panels,” which is based on the military testing standard MIL-STD-401B, and augmented by other relevant loading cases. From Hexcel, the useful tests were long beam bending, short beam shear, and core crushing. The long and short beam tests were selected because they give basic panel properties like maximum shear and bending stresses before failure. Core crushing shows the maximum preload that can be placed on bolts through the panel. While bolts need to pass through inserts rather than the panel itself, crush properties are still useful to know and compare. If one panel fares significantly worse than the others, then that panel should be approached with greater caution. Added to these tests were also a plane bending test and a torsion test. These two tests most closely simulate other loads the panels would experience in the car. Plane bending is most relevant to a floor. It is the loading case that will be present when a driver stands on the floor or when the battery box rests on the floor. This floor must contribute heavily to the overall torsional rigidity of the frame. The panel’s torsional stiffness is important for handling characteristics and driver feel, but even more important is that the panel’s delamination threshold must be higher than any torsional load the chassis will see.

Long Beam

The long beam test consists of a simply supported beam with a span of 20 inches. Two forces with a span of 10 inches are applied to the beam, centered on the support span. The expected failure modes for this test are tension/compression failure of the skin or skin wrinkling. The geometry of the test is taken from MIL-STD-401B Sec.5.2.4 or ASTM C-393, with the exception that these beams were chosen to be 2” wide in order to fit all the needed samples within the available test material.

Short Beam

The short beam test consists of a simply supported beam with a span of 4 inches. A single force is applied to the center of the beam. The expected failure modes for this test are core shear or delamination of core from skin. The geometry of the test is taken from MIL-STD-401B Sec.5.2.4 or ASTM C-393, with the exception that these beams were chosen to be 2” wide in order to fit all the needed samples within the available test material.

Plane Bending

The plane bending test consists of four simple supports in a square pattern, 7.5 inches apart on a side. A single force is applied to the center of the square. The expected failure modes for this test are tension/compression failure of the skin or skin wrinkling. The area of this test was chosen based on what appeared to be a large enough area to bend without simply shearing the core, but was small enough to still fit within the available test material.

Core Crushing

The core crushing test consists of a 2x2" square panel sample that is compressed between two 1.25" round rods. The expected failure modes for this test are shearing of the skin and then crushing of the core. The rod diameters were chosen based on what appeared to be the largest reasonable washer diameter for a bolted joint on the car.

Torsion

The torsion test consists of a 6"x11" panel, held 1" deep in jaws by the narrow ends. Expected failure modes for this test are shearing of the core or delamination of the skin from the core. The area of this test was chosen based on what appeared to be a large enough area to not twist easily, but was small enough to still fit within the available test material.

Testing Fixtures

Long Beam



Figure 3.24: Long Beam Fixtures

The long beam support, pictured above, is made of one long 2"x2" square tube that spans the entire width. It has two upright 1" round tubes to allow for more beam deflection, with horizontal round tubes welded on top of the upright tubes to make the simple beam supports. On the other side of the square base tube is a 3/8x1" steel tab that is gripped by the Instron machine. The long beam force applicator has a 2"x2" square tube spanning 10", with horizontal round tubes welded to the corners. Since the beam will curve away from the center of the force applicator, no upright tubes are necessary. The other side of the square base tube has the same steel tab as the support. Once in the testing lab, the 24" support was found to be too long to fit between the columns of the Instron machine. The steel tabs had to be cut off of both support and applicator so that they could be placed diagonally in the machine on flat plates.

Short Beam

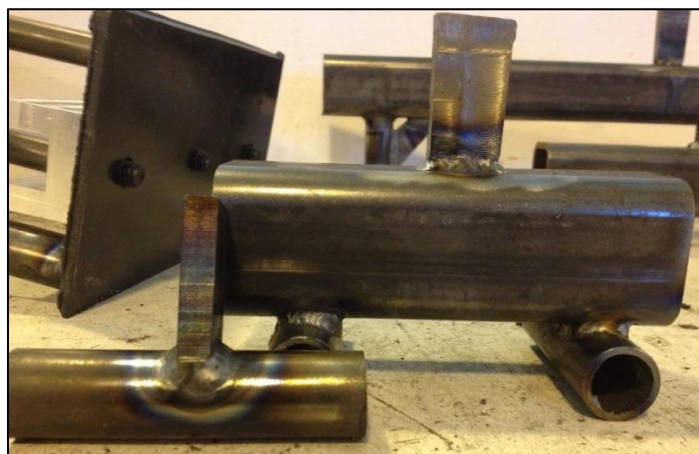


Figure 3.25: Short Beam Fixtures

The short beam support, shown above, is a 2"x2" square tube with 1" round tubes welded across it at a 4" span as the simple beam supports. On the other side of the square base tube is a 3/8x1" steel tab that is gripped by the Instron machine. The short beam force applicator is a single tube with the same tab welded perpendicular to it.

Plane Bending



Figure 3.26: Plane Bending Fixtures

The plane bending fixture, shown above, consists of three 2"x2" square tubes welded in a plus-sign formation. Holes are drilled in the ends and carriage bolts are threaded into those holes for the supports. The spherical tops of the carriage bolts make smooth-topped support points. Washers were added under the bolt heads to increase available room for panel deflection. The force applicator was originally a 1"x1" square aluminum bar with a 3/8"x1" tab milled on the back to be gripped by the machine jaws. On the other end was another hole with a carriage bolt threaded in. This applicator was too small, so it promptly punched through the panel skin. A new force applicator, found in the testing lab, was a 3" round steel disk that applied force in the middle of the panel. This solved the problem of the force applicator punching through the skin before bending the panel.

Core Crushing



Figure 3.27: Core Crushing Fixtures

The core crushing support and loader are the same: a 1.25" round steel rod with the 3/8"x1" tab milled into the end. For a few of the tests, noted on the results plots, the bottom support was substituted for a flat plate, which distributed the forces through the core differently.

Torsion

For the torsion test, a device was needed to turn the pulling motion, applying a tension force, into a twisting motion, applying a torsional force. Two concepts were generated for this purpose: the externally-rifled cylinder and the 2-bar linkage.

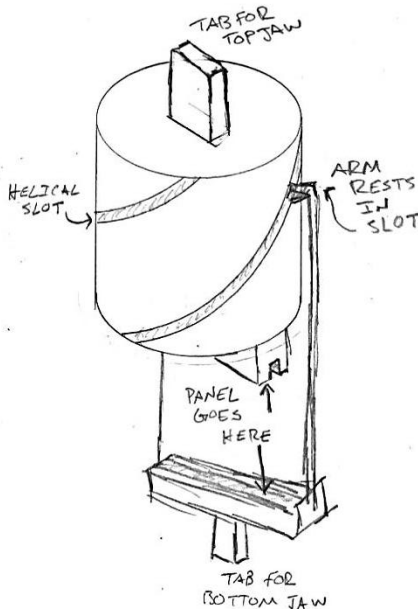


Figure 3.28: Concept Sketch of the Externally-Rifled Cylinder Torsion Test Concept

The externally-rifled cylinder concept above has an aluminum cylinder with 2 helical slots cut down its length. This cylinder is gripped by the upper Instron jaw. On the bottom is a piece that fits in the helical slots and can rotate freely. The panel is rigidly attached to both the upper and lower pieces. As the lower Instron jaw is pulled down, the slot forces the lower piece to rotate at a constant speed which applies a torque to the panel. This design will convert a constant applied force into a constant torque, so that converting measured force data to applied torque data is a simple matter. However, it will be very difficult to manufacture the slotted cylinder. It would need to be machined on a 4th axis CNC mill or cast. Another problem with this design, not noticed until after it was already rejected, is that as the cylinder is pulled upwards, the jaws that hold the panels will be pulled farther apart. This will pull the top jaw right off the end of the panel, causing the fixture to spit out the test piece.

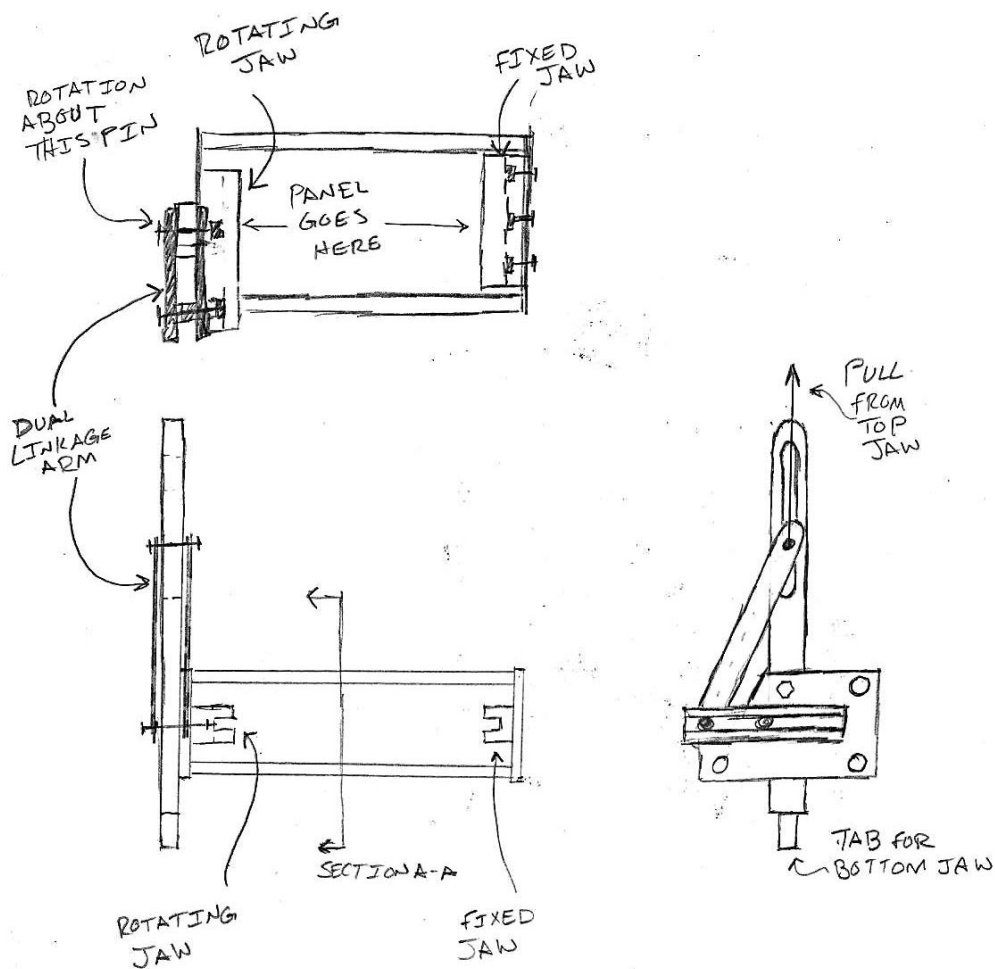


Figure 3.29: Concept Sketch of the 2-Bar Linkage Torsion Test Concept

The 2-bar linkage concept centers around a vertical aluminum bar, as seen above. This bar has a tab machined onto its lower end so that the Instron machine can grip it. The upper end of the bar has a

vertical slot cut into it. One end of a dual linkage arm is pinned in the slot, while the other end is pinned to the end of the rotating jaw. The center of the rotating jaw is pinned to the same vertical aluminum bar. At the top of the dual linkage arm, where Figure 3.29 has only an arrow to indicate the pull of the Instron, there is a bar pinned with a tab machined into it just like the bottom tab. See Figure 33 for the actual part. The top jaw of the Instron can grip this top tab and pull the end of the dual linkage up, which rotates the rotating panel jaw. The other panel jaw is fixed in a frame that bolts to the vertical aluminum bar. While this setup involves many more parts than the rifled setup, they are all simple manual mill or welded parts. The biggest downside to this design is the nonlinear force to torque relationship. To find applied torque from measured force data, force-to-torque curves must be calculated from kinematics. The tradeoff in this case was between a system that was difficult to make and easy to analyze or one that was much easier to make but required a bit more analysis. In the end the choice was not that hard. Any upper-division ME student should be able to do kinematics, but CNC machining is both a special skill and a special certification that not just everyone has, aside from the fact that 4th axis machines are not common on campus. On top of that, the rifled system requires that the difficult step be done before data collection, where the linkage allowed data collection sooner and then data processing at our leisure. The linkage design was built. The finished result, as seen in Figure 3.30, is heavy but very sturdy. The aluminum jaws are interchangeable to hold panels of different thicknesses. The jaws are easy to change, and operation is smooth.



Figure 3.30: Torsion Fixture

Panel Failure Observations

Torsion

The squared edges of the test machine jaws crushed the core, then sheared the skin of the $\frac{3}{4}$ " and 1" panels (Figure 3.32, below). In the $\frac{3}{8}$ " panel the core shear deformation was distributed more evenly down the length of the panel. The test ran its full range of motion – just over 30 degrees – without ever causing the panel to fail, however after the test the panel stayed permanently warped. The $\frac{1}{2}$ " panel showed a mix of thick and thin panel behavior (Figure 3.31, below). It permanently deformed like the thin panel, but started to shear the skin at the jaw edge like the thick panels. A single test was also run on the empty torsion test machine to determine the pull weight of the machine itself. The force required to simply move the linkage was measured to be 14lb.

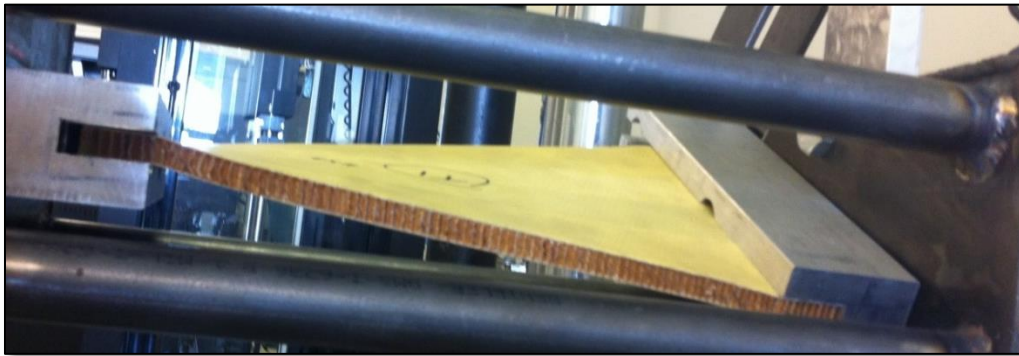


Figure 3.31: Thin Panel During Torsion Test

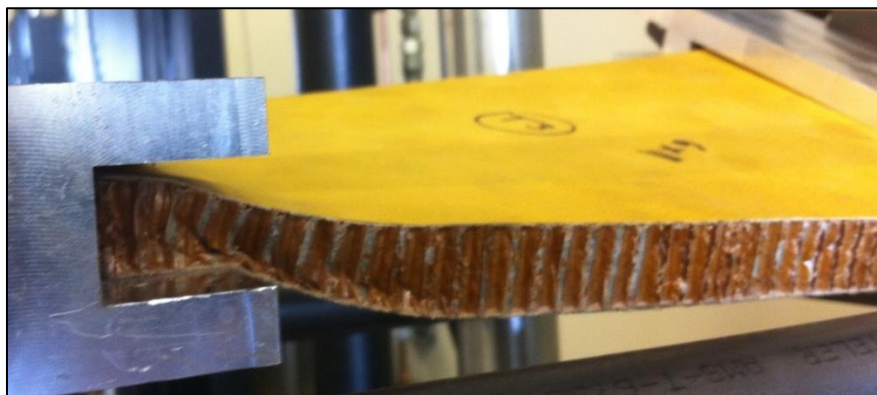


Figure 3.32: Thick Panel During Torsion Test

Long Beam

The pictures below show the failure mode of the long beam tests. Thinner beams were less stiff and failed less suddenly, deflecting more before failure. Thicker beams, as expected, were stiffer, failing more suddenly and at less deflection. The failure mode, however, was the same for all panels: the skin wrinkled and snapped, leaving the core with much less damage than the skin. For skin damage see Figure 3.34.

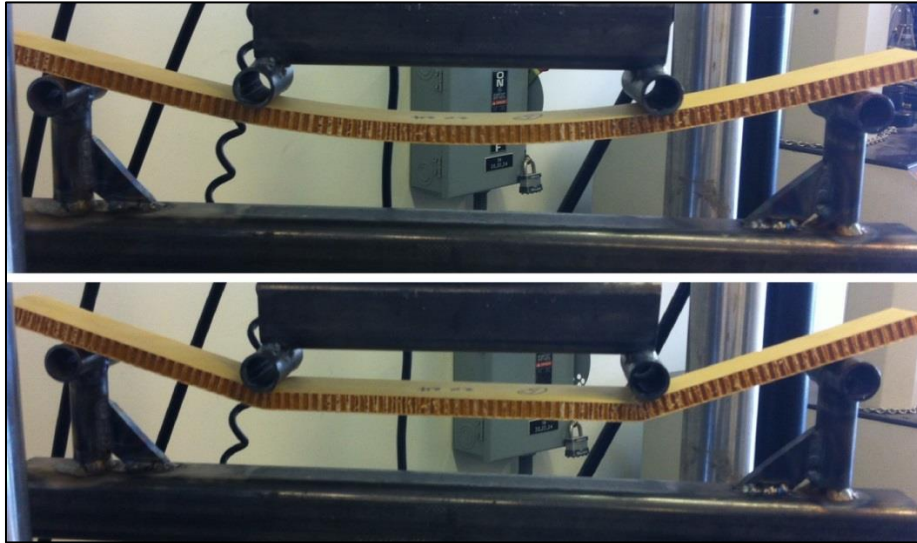


Figure 3.33: Long Beam Testing Before (Top) and After (Bottom) Failure



Figure 3.34: Thinner (Top) and Thicker (Bottom) Panel Failure Modes For Long Beam Test

Core crushing

All thicknesses sheared more cleanly in the tests run with a bottom flat plate compared to tests with a bottom round peg. The thicker samples warped less before ultimate failure, but caused cracks to propagate through the skin to the edges, radially out from the circle. The thinner panels warped more before the hole punched through, with the corners lifting up around the pusher. Fewer cracks formed in the skin of the thinner samples. Failed samples are shown in Figure 3.35, below.

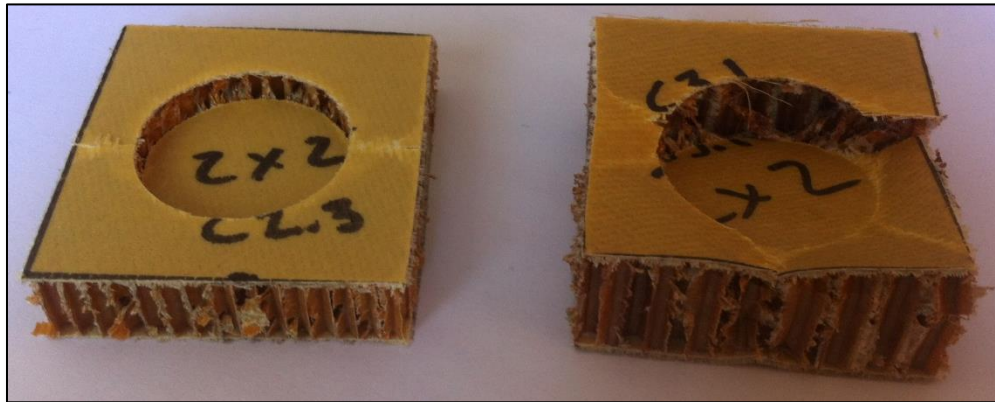


Figure 3.35: Crushing Failure of Thinner Sample Using Bottom Plate and Thicker Sample Using Bottom Peg

Plane Bending

The plane bending test showed a sharp distinction between the thinner panels (Figure 3.36, top) and the thicker ones (Figure 3.36, bottom). The thinner panels ($\frac{3}{8}$ " and $\frac{1}{2}$ "") stayed flat on top of the corner supports and near the center pusher, with a step down in between. The skin of these panels indented slightly at the contact points. The thicker panels ($\frac{3}{4}$ " and 1"") did not show this smooth bend. Cracks formed in the top skin in a circle around the edges of the round pusher, then propagated radially out from the circle to the midpoint of each edge. The panel then folded sharply along these cracks.

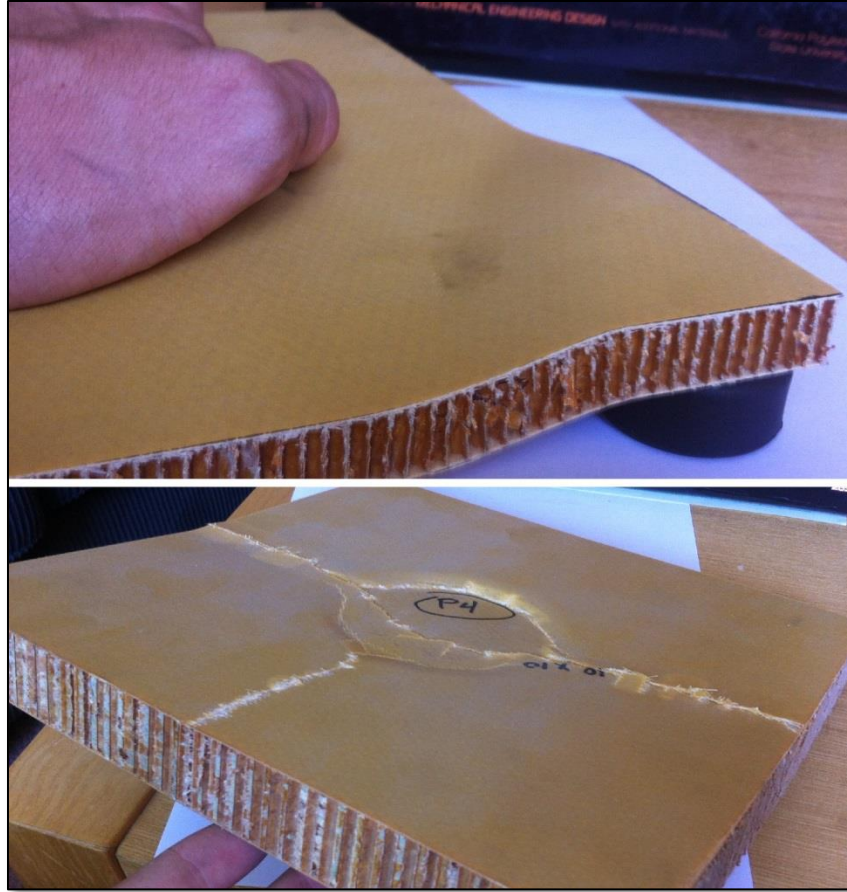


Figure 3.36: Thinner (Top) and Thicker (Bottom) Panels Showing Different Failure Modes in Plane Bending Test

Short Beam

The purpose of the short beam test was to test for shearing properties of the core. In order to gain a full picture of those properties, samples were test with both the paper ribbon running the length of the sample (parallel) and the ribbon running across the sample (transverse). The only $3/8$ " thick sample was a transverse sample (shown in Figure 3.37, top left), but behaved much more like a long beam. The skin cracked in the center, at the force application point, but the only other damage was the core bending down. The $1/2$ ", $3/4$ ", and 1 " transverse samples, with a representative shown in the bottom left of Figure 3.37, all behaved similarly to each other. The seam between one paper ribbon and the next sheared, so that a whole section of core pushed downward under the force applicator, causing the bottom skin to delaminate from the remaining core. In the $1/2$ " parallel sample, shown in the bottom right of Figure 3.37, the core sheared in a clean diagonal line across the panel. The line very clearly runs from the pusher contact point to the support contact point. The $3/4$ " and 1 " parallel samples in the top right of Figure 3.37 behaved much more like core crushing samples. The top skin snapped at the sides of the pusher and the core just underneath began to crush. The samples also show the bottom of the panel beginning to stretch and splay slightly.

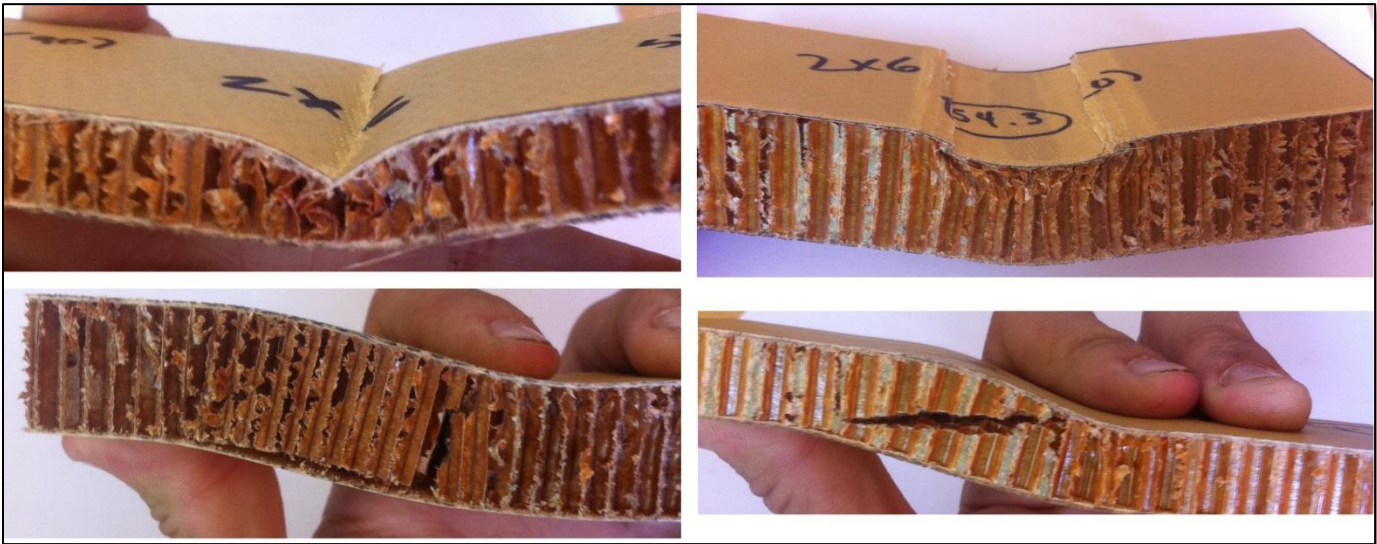


Figure 3.37: The Four Major Failure Modes of the Short Beam Test
 Counterclockwise From Top Left: 3/8" Thick Transverse Ribbon, 3/4" Thick Transverse Ribbon,
 1/2" Thick Parallel Ribbon, 1" Thick Parallel Ribbon

Results

Long Beam

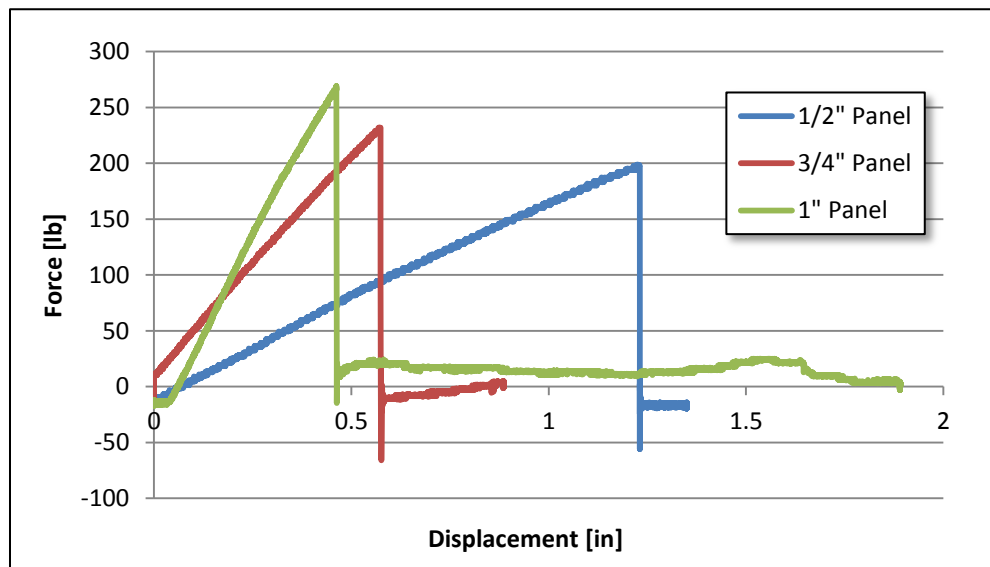


Figure 3.38: Long Beam Bending Results

The long beam testing, plotted in Figure 3.35, resulted in nearly perfectly linear force-displacement curves. The bending stiffness was calculated with the slope of this curve, and the failure point is the

sharp end in the linear region. Not surprisingly, as panel thickness increased bending stiffness increased as well, with maximum displacement before failure decreasing quickly.

Short Beam

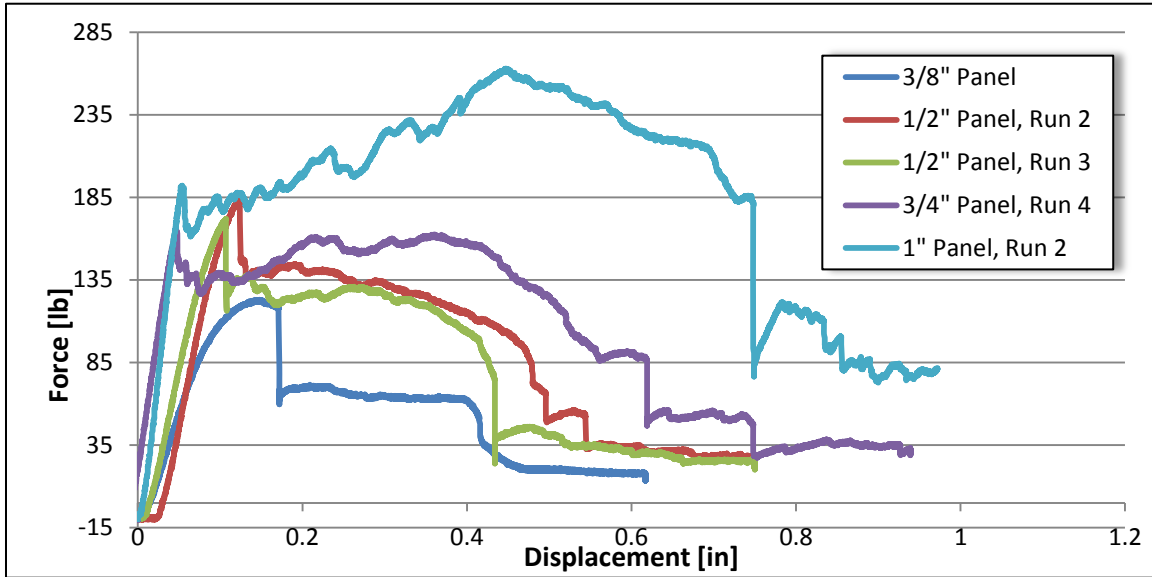


Figure 3.38: Short Beam Shear Results: Transverse Paper Ribbon

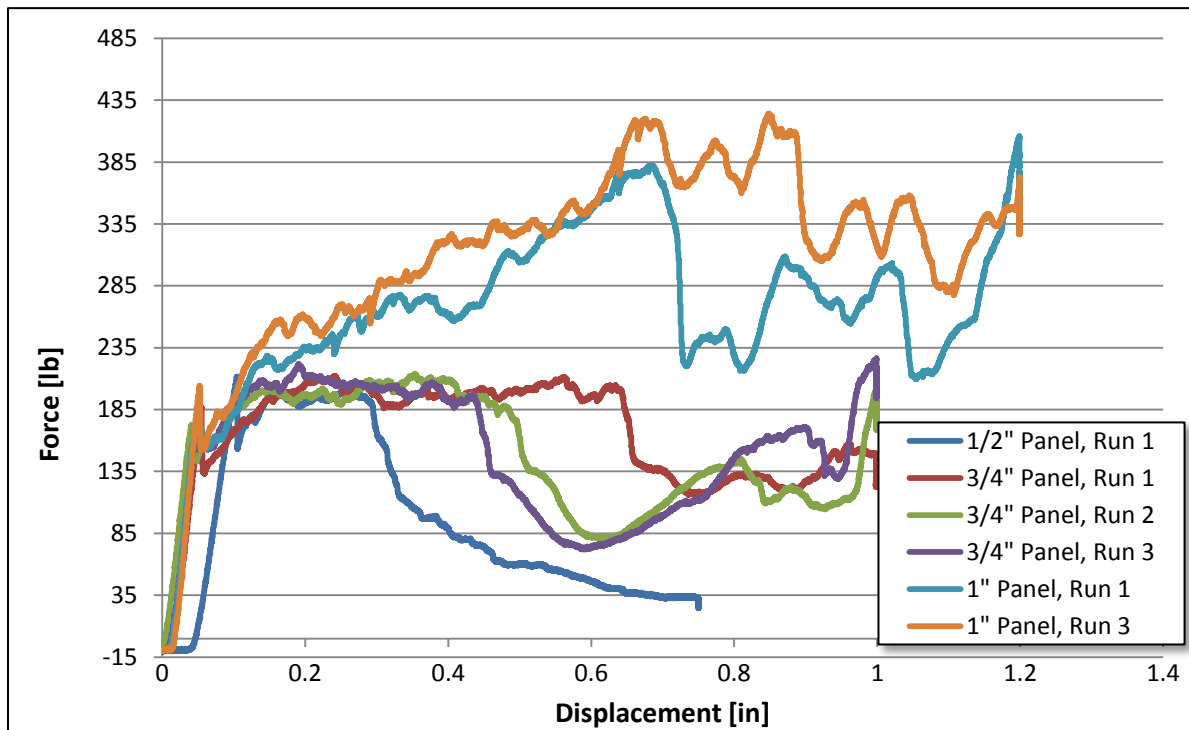


Figure 3.39: Short Beam Shear Results: Parallel Paper Ribbon

The short beam shear was performed with the paper honeycomb running in two different directions. The paper ribbons will run with the seam lengthwise with the bend and run the other across the bend. This would hopefully show use the best way to use the panel for the cut and fold frame. Because there was very little deflection before failure, and the failure modes were different for the different categories, it didn't make sense to try to calculate panel stiffness from these tests. The failure point in the crossways paper ribbon category corresponds to the sharp vertical drop in force towards the end of each data series. The failure point in the lengthways paper ribbon category corresponds to the first steep (but not vertical) drop in force.

Plane Bending

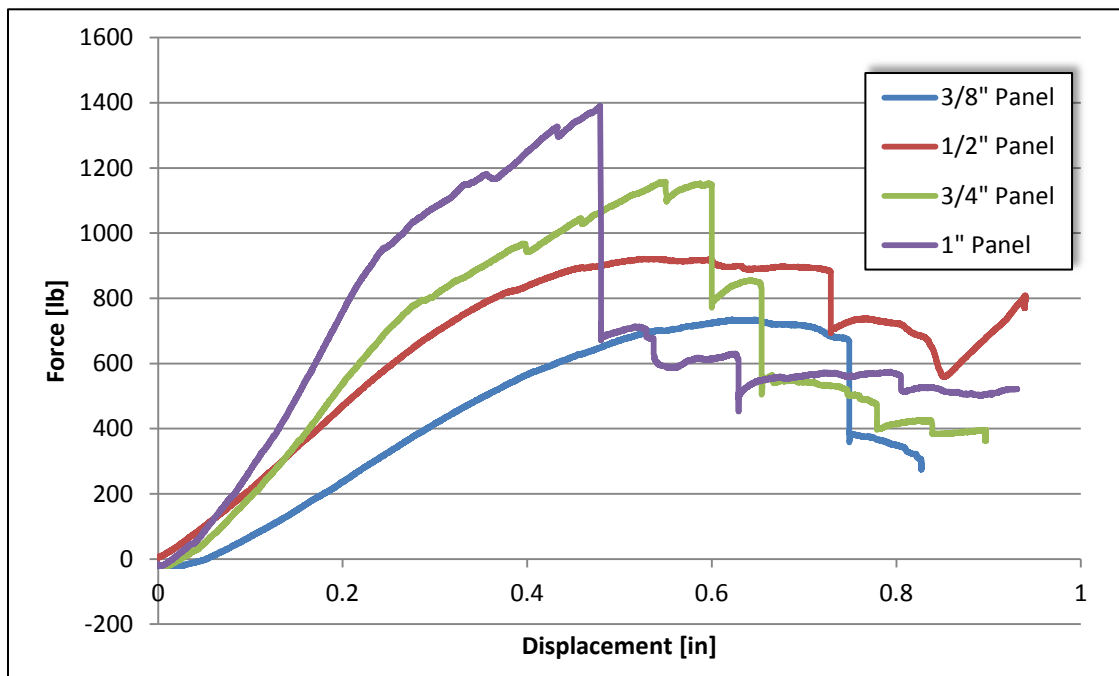


Figure 3.40: Plane Bending Results

The plane bending testing resulted in good, clean force-displacement curves, which more closely resembles stress-strain curves of real isotropic materials. The bending stiffness was calculated with the slope of the linear portion of this curve (after the concave up portion and before the concave down portion), and the failure point is the sharp vertical drop in force, which is where the panel loses all structural integrity.

Core Crushing

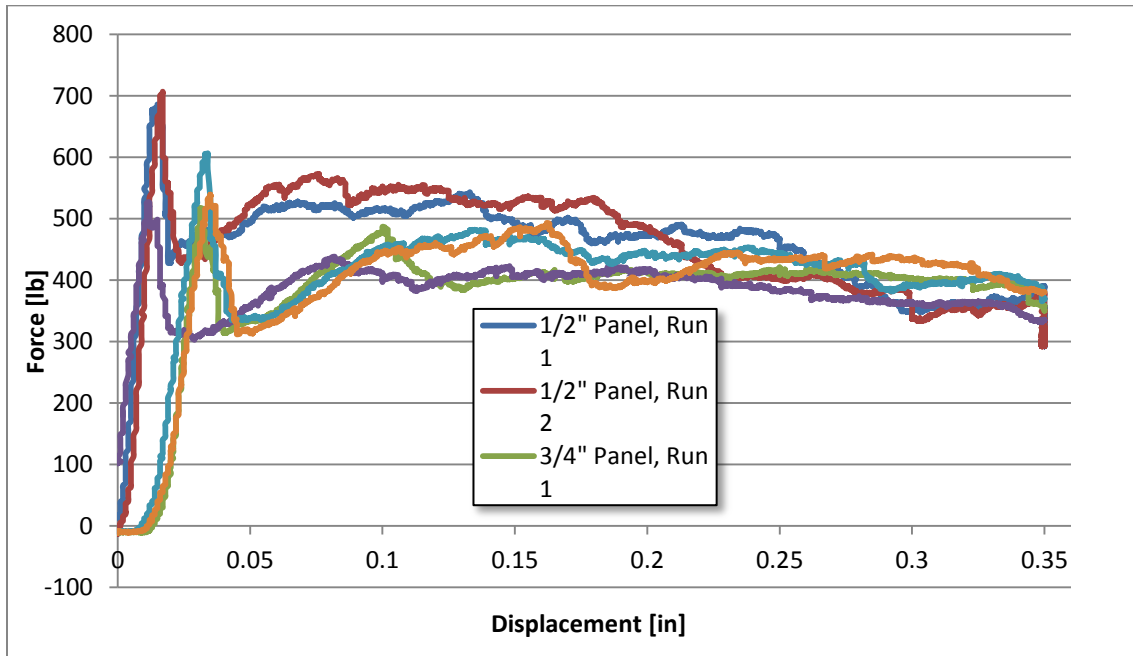


Figure 3.41: Core Crushing Results: 1.25" Round Against 1.25" Round

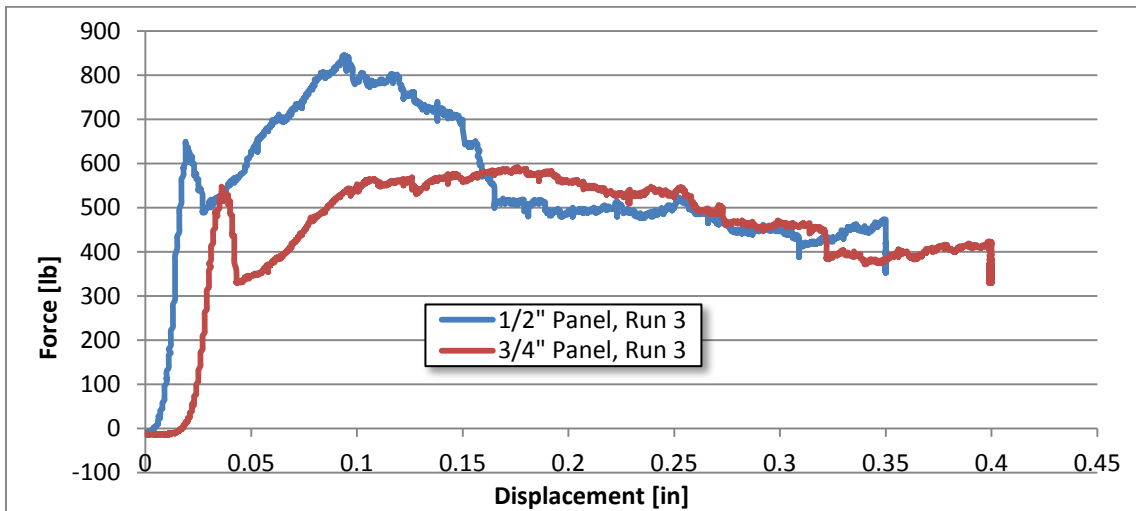


Figure 3.42: Core Crushing Results: 1.25" Round Against Flat Plate

There were two categories of core crushing tests, the round on round rod crushing and round rod on flat plate. The failure point for each of these tests is the sharp end of the initial linear region. The crushing stiffness is irrelevant in the context of bolted joints or frame stiffness. The failure point is directly related to the amount of pre-load and clamping that can be put on a bolt through the panel without an insert.

Torsion

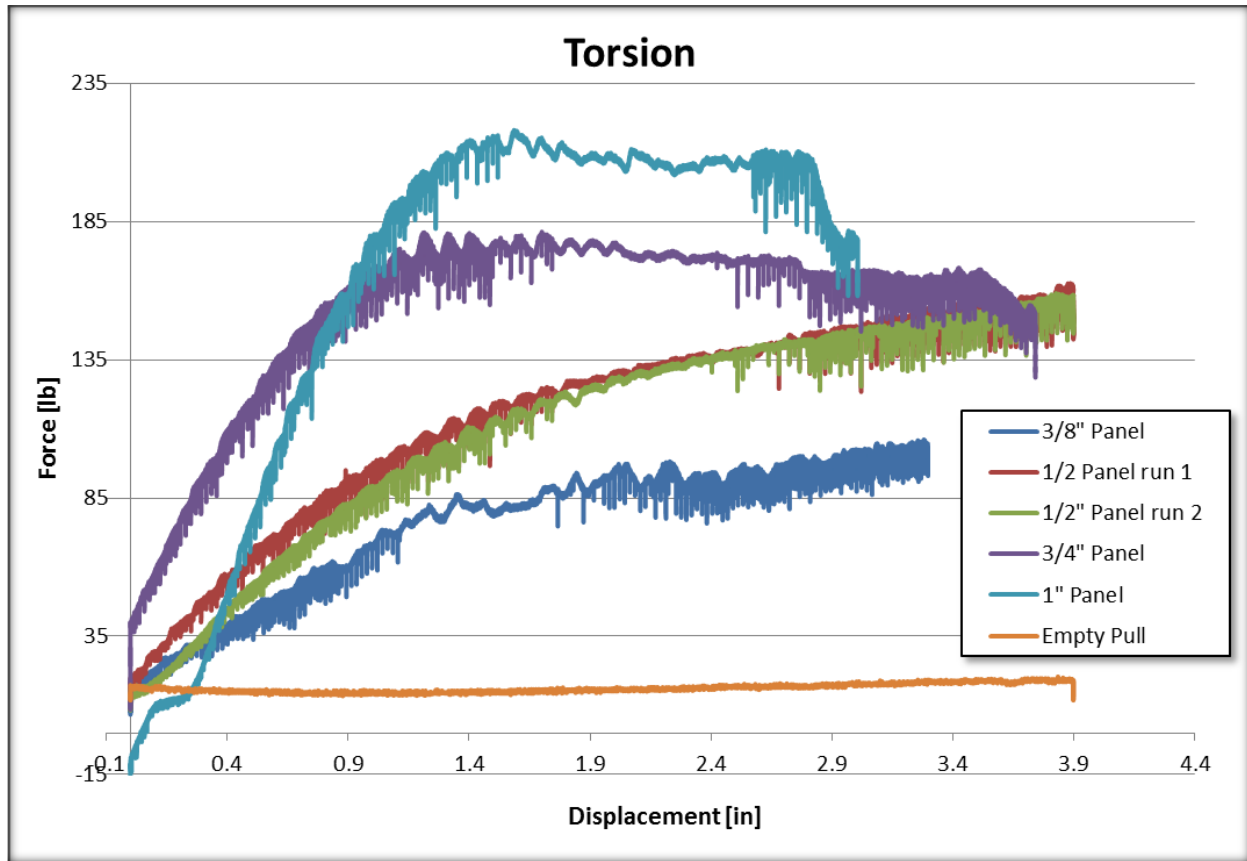


Figure 3.43: Torsion Results

The torsion results were noisy because of the complicated fixture setup, but otherwise yielded good smooth curves. These results are force to displacement, where it really should be torque to angle data. Because of the changing angles in the linkages of the mechanism, it is not a constant conversion from force to torque. The conversion from force-displacement to torque-angle results could be made with a simple kinematics model of the system. However, because this test is used only to compare between panels, the relative force-displacement results should still be valid. The force-displacement stiffness was calculated from the initial linear region of the graph. Since these panels either did not fail or failed in an unexpected way, and since the frame will never torsionally deflect enough to make the panel fail, the failure point can be disregarded in the torsion test.

Final Decision

Table 3.9 shows the results of the graphs and data selection process described above.

Table 3.9: Tabulated Results

| Category | | 3/8" Panel | 1/2" Panel | 3/4" Panel | 1" Panel |
|-----------------------|------------------------------|------------|------------|------------|----------|
| Torsion | Stiffness (lb/in) | 36.977 | 74.894 | 160.599 | 288.400 |
| | Stiffness (lb/in) | 1675.478 | 2148.870 | 3455.602 | 5038.800 |
| Plane Bending | Failure Point (lb) | 680 | 890 | 1150 | 1360 |
| | Stiffness (lb/in) | x | 169.141 | 402.913 | 676.486 |
| Long Beam Bending | Failure Point (lb) | x | 200 | 230 | 270 |
| | Failure Point (lb) | x | 190 | 193.333 | 395 |
| Short Beam Shear (0) | Failure Point (lb) | 120 | 175 | 165 | 185 |
| Short Beam Shear (90) | Failure Point (lb) | x | 700 | 500 | 550 |
| Core Crushing | Weight [lb/ft ²] | 0.483 | 0.515 | 0.579 | 0.646 |

NOTE: Torsion units are in force applied by Instron per distance moved by Instron. This is adequate to compare one panel to another, but for any other use of the data, this must be converted to units of torsional stiffness through test setup kinematics.

For the un-weighted decision matrix, the weight results use the inverse of density to make a higher score better (square feet per pound). Because the data spans multiple orders of magnitude (plane bending stiffness vs long beam stiffness for example), each set of results was normalized to the highest result within that set. This allows us to then weight each result without having to worry about scale affecting the weighted importance of each factor.

Table 3.10: Un-weighted Decision Matrix

| Category | | 3/8" Panel | 1/2" Panel | 3/4" Panel | 1" Panel |
|-----------------------|--------------------------------|------------|------------|------------|----------|
| Torsion | Stiffness | 0.13 | 0.26 | 0.56 | 1.00 |
| | Stiffness | 0.33 | 0.43 | 0.69 | 1.00 |
| Plane Bending | Failure Point | 0.50 | 0.65 | 0.85 | 1.00 |
| | Stiffness | x | 0.25 | 0.60 | 1.00 |
| Long Beam Bending | Failure Point | x | 0.74 | 0.85 | 1.00 |
| | Failure Point | x | 0.48 | 0.49 | 1.00 |
| Short Beam Shear (0) | Failure Point | 0.65 | 0.95 | 0.89 | 1.00 |
| short Beam Shear (90) | Failure Point | x | 1.00 | 0.71 | 0.79 |
| Core Crushing | 1/Weight [ft ² /lb] | 1.00 | 0.94 | 0.83 | 0.75 |
| Score | | 2.61 | 5.70 | 6.47 | 8.53 |

The chosen weights were integer values. Initially each weight was 1, with the weight then increasing for the results that appeared to be more directly applicable to the panel's application in the floor. Greatest emphasis was placed on the floor application because that was the primary intended use of the panel at

the time of these tests. The most obvious was plane bending – because the floor was to be supported by the steel structure at bolted joints with weight suspended in the middle of a planar area between those joints, supporting loads like the driver’s weight and the battery box. This was weighted result as 3. The other applicable result was torsion – because the floor panel would see similar torsional loading while driving. However, because of the advice from Zodiac about these panels (see Zodiac and Composite Sandwich Panels section, a skin will be laid up around the perimeter of the panel. This means the torsional stiffness results from testing might not be directly related to what actually happens with the floor. Because of this, it was decided to weight the torsional stiffness result by a factor of 2. Finally, there are 11 total weighted points on stiffness or strength related results, and only one weight result. To offset this outnumbered difference, the weight result was weighted by a factor of 11. The table below shows the final weighted decision matrix with final results at the bottom.

Table 3.11: Weighted Decision Matrix

| Category | | Weight Factor | 3/8" Panel | 1/2" Panel | 3/4" Panel | 1" Panel |
|--------------------------------|-------------------|---------------|------------|------------|------------|----------|
| Torsion | Stiffness | 2.00 | 0.26 | 0.52 | 1.11 | 2.00 |
| Plane Bending | Stiffness [lb/in] | 1.00 | 0.33 | 0.43 | 0.69 | 1.00 |
| | Failure Point | 3.00 | 1.50 | 1.96 | 2.54 | 3.00 |
| Long Beam Bending | Stiffness | 1.00 | x | 0.25 | 0.60 | 1.00 |
| | Failure Point | 1.00 | x | 0.74 | 0.85 | 1.00 |
| Short Beam Shear (0) | Failure Point | 1.00 | x | 0.48 | 0.49 | 1.00 |
| short Beam Shear (90) | Failure Point | 1.00 | 0.65 | 0.95 | 0.89 | 1.00 |
| Core Crushing | Failure Point | 1.00 | x | 1.00 | 0.71 | 0.79 |
| 1/Weight [ft ² /lb] | | 11.00 | 11.00 | 10.32 | 9.17 | 8.22 |
| Score | | | x | 16.65 | 17.05 | 19.01 |

This strongly points to the 1” panel as the best to use for the floor. The only other negative effect of a thick panel is raising the CG of the car by having heavy components like the driver or battery box sitting on a 1” panel instead of a 1/2” panel. After talking with the previous years’ suspension senior project, who performed extensive trade studies on parameters like CG height, it was decided that the 1/2” difference would not be enough to offset the stiffness benefits of a thicker panel. This 1” panel was to be a major component of an early frame design, described in the *Cut and Fold Monocoque Design Evolution* section later in Chapter 3.

2015-16 Rule Changes and Rules Clarifications

Rule Changes

For the new set of rules the largest changes were seen in the alternative tube sizes for chassis construction. The 2013 rules stated that the baseline steel tube size was 1"x0.095" for the front hoop main hoop and harness bar. The side impact, front bulkhead, and hoop bracing were to be made of 1"x0.065" and every other tube on the car needed to be at least 1"x0.049".

Alternatives to this size were allowable according to the rules set in T3.6. These alternatives allowed for a tube of the same weight but a much higher stiffness. This would have allowed use of a 1.50" x .065" tube. There were rules to the diameter and wall thickness of the rest of the car under standard rules, but they did not apply directly to the alternative frame rules because only the front and main hoop were required to be made from steel tube. When using alternative tube sizes, a weld test must be performed and the results submitted in a Structural Equivalency Spreadsheet (SES). The test is a destructive test of an H pattern welded set of the chosen tubes (Figure 3.44)

Table 3.12: Alternative tube calculations

| OD | wall | ro | ri | A | I |
|-------|-------|--------|--------|----------|----------|
| 1 | 0.095 | 0.5 | 0.405 | 0.135049 | 0.027957 |
| 1.125 | 0.065 | 0.5625 | 0.4975 | 0.108228 | 0.030516 |
| 1.25 | 0.065 | 0.625 | 0.56 | 0.120991 | 0.042602 |
| 1.375 | 0.065 | 0.6875 | 0.6225 | 0.133753 | 0.057525 |
| 1.5 | 0.065 | 0.75 | 0.685 | 0.146516 | 0.075582 |

| | | | | | |
|-------|-------|--------|--------|----------|----------|
| 1 | 0.065 | 0.5 | 0.435 | 0.095465 | 0.020965 |
| 1.125 | 0.047 | 0.5625 | 0.5155 | 0.079586 | 0.023165 |
| 1.25 | 0.047 | 0.625 | 0.578 | 0.088814 | 0.032182 |
| 1.375 | 0.047 | 0.6875 | 0.6405 | 0.098043 | 0.043281 |

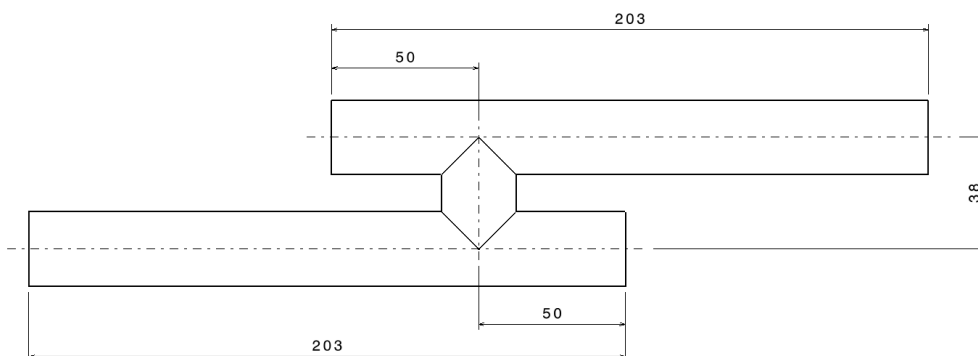


Figure 3.44: Rule 3.6.2 describing the weld test for SES.

The 2015 rules require the same baseline tube sizes and the alternative tube rules allow for 0.079" wall on the main and front hoop and the harness bar. It also allows for 0.049" for the side impact, front bulkhead and main and front hoop bracing. The alternative sizes do not need testing to be used. 0.065" and 0.035" can be used respectively, but they require physical testing of the weld in order to be used. Area moment of inertia (I) and cross sectional area (A) must be the same as the baseline steel tube sizes by rules. With a smaller wall thickness, this means the OD of the tube must increase. Since I is proportional to radius⁴ and A is proportional to radius², as OD increases I will exceed that of the baseline tube before A does. Since A is proportional to weight of the tube, decreasing wall thickness to the minimum will not make the frame lighter, but it will make it much stiffer. SAE rules state "Teams using the alternative frame rules must comply with rule T3.6" which is minimum wall thickness and maintaining A and I of baseline tube, meaning the frame would be no lighter going with AF than standard frame if a steel tube frame was pursued. The alternative tube calculations can be found earlier in the report in Chapter 2 under the design specifications. By using a structural firewall, the battery box is allowed to support only 20g loads instead of 40g loads.

Rules Clarifications

For the parts of the design that were not explicitly clear, rules clarifications were requested from the Formula SAE rules committee. Some of these clarifications are as follows:

To validate the cut-and-fold manufacturing method, a lap joint test must be performed with the same materials used for the chassis. This can be accomplished by constructing a lap joint on a sample of the panel material and pulling the sample apart on an Instron machine. The lap joint must be equivalent with the strength of the original panel.

Because composite panels are used for the chassis, certain monocoque frame rules apply. These rules include T3.32, which specifies that the panel must have equivalent A and EI values to 2 baseline steel tubes.

Finally, material properties cannot be taken from manufacturer data sheets as previously assumed. Instead, they must be derived from the 3-point bend test and punch through (shear strength) test as defined by T3.31.

Cut-and-Fold Monocoque Design Evolution

Design development began with a steel tube frame as our base design. It is what Formula Electric has always used and it was a good starting point (Figure3.45).

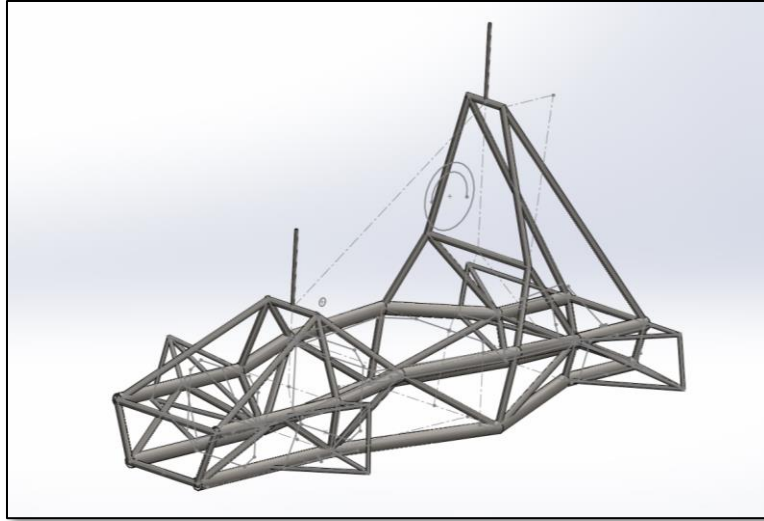


Figure 3.45: Original steel tube frame.

The Matlab-generated steel tube frame in Figure 3.45 was used to start the design evolution. This frame passes the alternative frame rules but leaves room for improvement. The bottom tubes were replaced with a fiberglass panel floor (Figure 3.46). It is lighter than the steel tubes but it does have a lower yield stress. However, it makes it much easier to mount various components to the floor such as the battery box and harness attachments. This also allows for much less welding time because there are fewer tubes.

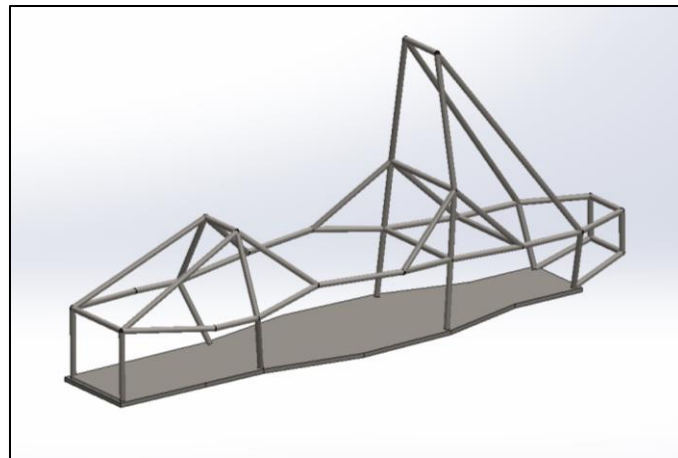


Figure 3.46: Fiberglass composite floor frame design.

After the new floor design was finished, the rear end was redesigned as in Figure 3.47 to help eliminate even more tubes. This allowed for even less welding and jiggling for final manufacture. It did require the addition of the cut and fold production time as well as wet layups, but this was still less than the welding. The cut-and-fold rear end allowed for a much stiffer rear section. It also made the impactor test trivial in the folded up side sections.

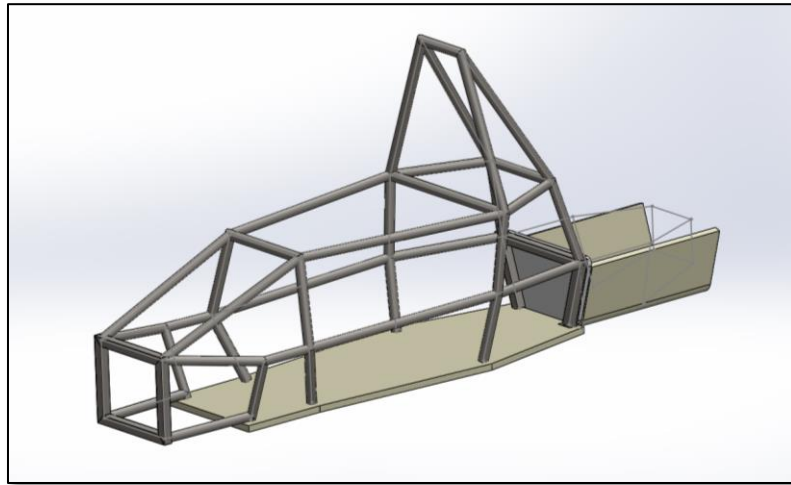


Figure 3.47: Cut and fold rear end frame design

Once the cut and fold rear section of the car was designed, the same method lent itself to being useful elsewhere too. Even more tubes and welding could be eliminated by replacing the sides with cut and fold panel as well, shown in Figure 3.48. This made manufacture more complex, but it was a much stiffer frame design. Now with the folded sides the impactor test, which had been so hard to pass previously, was now trivial on the entire car. As more and more pieces of panel were folded up around the car, the chassis became lighter and stronger, resulting in the full monocoque seen in Figure 3.49.

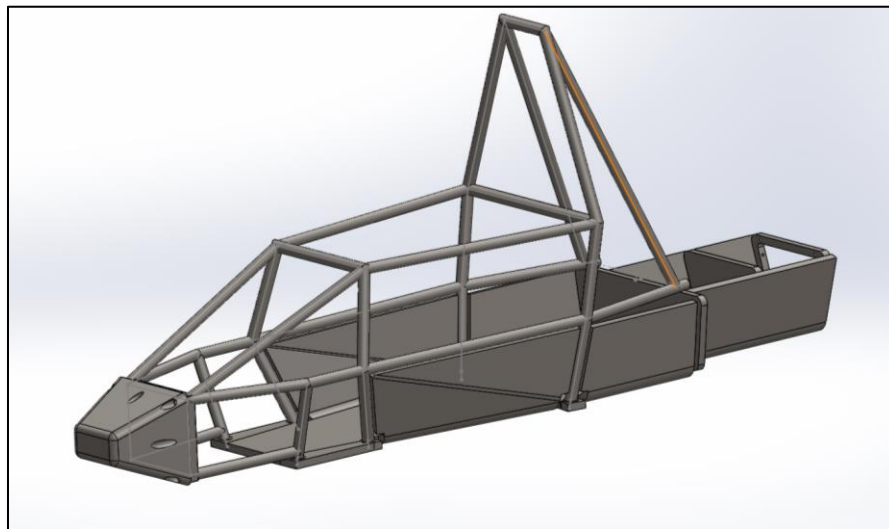


Figure 3.48: Cut and Fold side and back frame design.

After finalizing the design in SolidWorks, the model was analyzed in Abaqus and it was found that the frame would not pass the alternative frame loading. It was fine under normal driving conditions but the

stresses were above the ultimate strength of 27,000lb in the front impact test. A similar carbon panel would not yield under this test. This caused the decision to switch to a carbon panel for the cut and fold frame. This switch allowed a decrease in the size of steel needed for the frame, making the car even lighter.

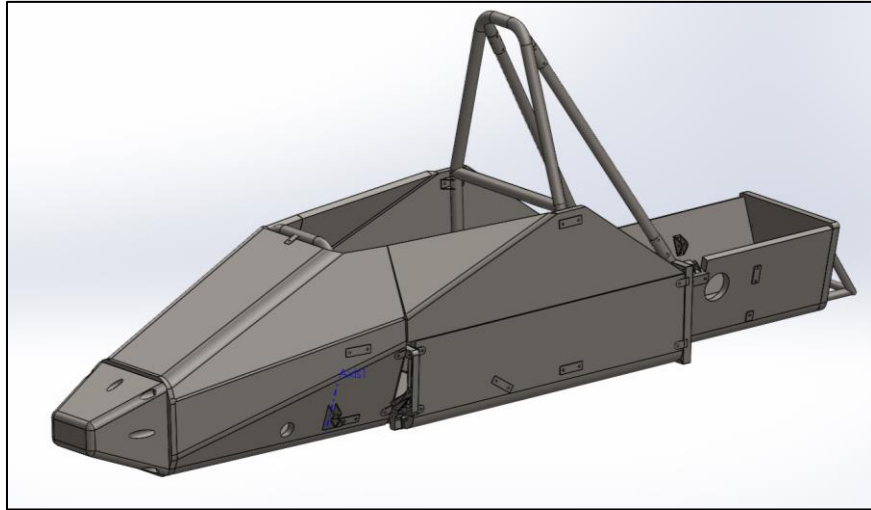


Figure 3.49: Full monocoque cut and fold frame design.

The final iteration of the design is the full cut and fold carbon monocoque. Since the yield strength of the carbon panel is so much higher than that of the fiberglass panel, all tubes were eliminated from the chassis except for the required front and main hoops. This is by far the lightest iteration of the chassis and is one of the stiffest as well.

Chapter 4: Description of the Final Design

Detailed Design Description

Material

The basic form of the chassis is a cut and fold panel monocoque. The materials used are composite honeycomb panels with 2 ply, 0-90, plain weave, 3K carbon fiber skins and 1" thick Nomex honeycomb core. The panels were prefabricated by ACP Composites, in Livermore, California.

Geometry

The panel chassis is split into two disconnected pieces, with the nose and cockpit one unified piece and the rear compartment for the drivetrain attached through a bulkhead. These two pieces can be seen in Figure 4.1. The entire length of the chassis is 117". There are no prefabricated panels in production more than 96" long, and a custom-made panel of this size would be enormously expensive. That means that there must be a joint between panel pieces somewhere along the length of the car.

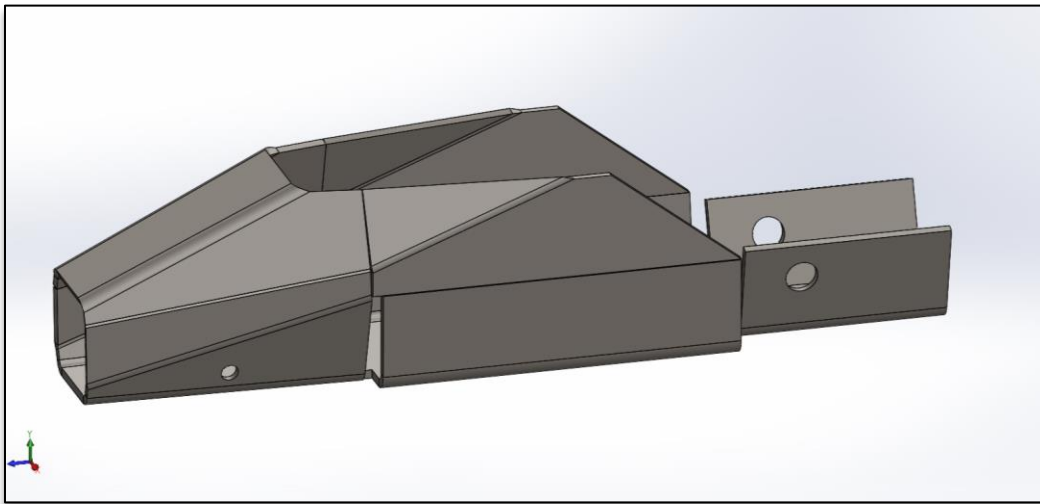


Figure 4.1: Cut-and-Fold Panel Geometry

It makes the most sense to make such a break here, since the battery box is a full 6" wider than the rear suspension points. This difference in width means that the chassis must neck down sharply from the wide battery compartment to the narrow suspension box. This can be accomplished much better by dividing the panel here than by trying to fold it at such a sharp angle and maintain chassis integrity. This division also makes a good place for removing the battery box, as will be discussed in the Battery Box Removal section.

The front panel section extends from just behind the battery box to the front bulkhead. The front section comprises four separate folded panels, all bonded together. This, again, is due to normal stock sizes. The biggest prefabricated panel is 48"x96".

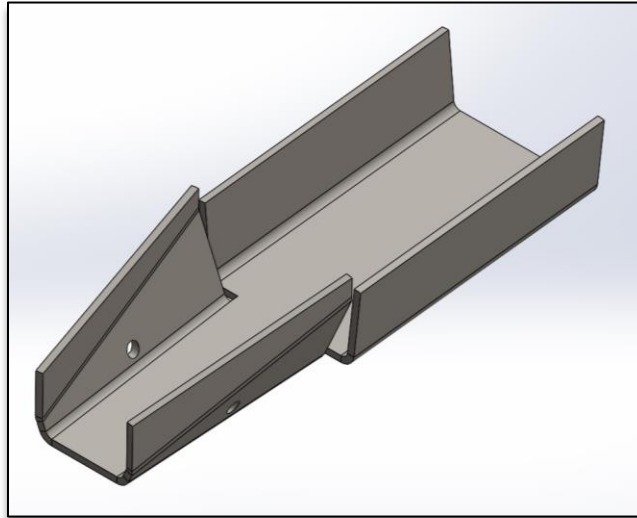


Figure 4.2: The Main Bottom Panel

The main bottom panel can be seen in Figure 4.2. This includes the floor and side impact structure as required by rules. The hole near the bottom of the main panel allows clearance for the steering rack. The rear half of the main front panel is sized to fit the battery box, while the front half is sized to fit the suspension points. Three of the four pieces in Figure 4.3 finish off the front section.

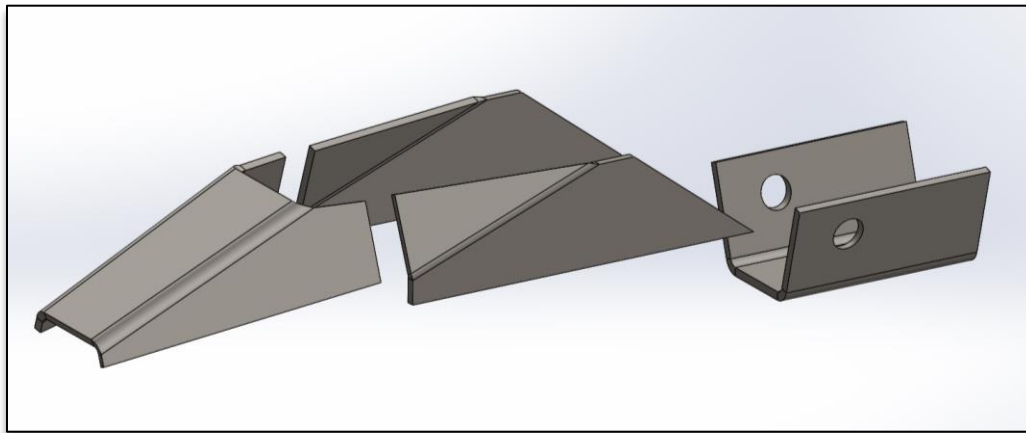


Figure 4.3: Front Top Panel (Left), Side Panels (Middle), and Rear Section (Right)

The rear section of the chassis is also shown in Figure 4.3. The circular holes in the panel allow enough drive shaft clearance that the entire CV joint can pass through. This allows for easier disassembly of the drivetrain. The panel itself is sized to fit the rear suspension points, and is long enough to completely enclose the rear-positioned motor.

Reinforcement

To allow for shear flow, the edges of the panels are closed out in a similar method to Formula SAE's process as described in the 2013 senior project report, "Formula SAE Hybrid Carbon Fiber Monocoque/Steel Tube Frame Chassis" by Hagan, Rappolt, and Waldrop. A small amount of core is cleared away from the edges of the panel and the space filled with a slurry of resin and glass microballoons. Carbon tape is then laid up over this and allowed to cure at room temperature. Bends are reinforced in a similar manner, with the cut line being filled with microballoons and the inner skin reinforced with carbon tape. This process is verified via a lap joint test.

The various panel pieces are attached by the same process as bend reinforcement, also used in the 2013 FSAE senior project to attach the two clamshell halves of the carbon tub. The gap is filled with resin and microballoons, and the skins are connected with a simple lap joint of 2 plies of tape per side.

Mounting

All mounting and attachments are accomplished through aluminum tube inserts, bonded in with resin and microballoons. Backing plates are used at every mounting point to distribute shear forces. The standard foam Formula SAE impact attenuator is mounted to the 0.060" thick steel anti-intrusion (AI) plate required by rules. The front bulkhead is a carbon panel bonded to the front of the frame by same method as the bend reinforcement. A hole in the front bulkhead panel allows access to the pedal box and any other components inside the nose of the car. Both the impact attenuator and AI plate mount to the front bulkhead with four 5/16" bolts, as dictated by rules. These components are shown exploded in Figure 4.4 and assembled in Figure 4.5.

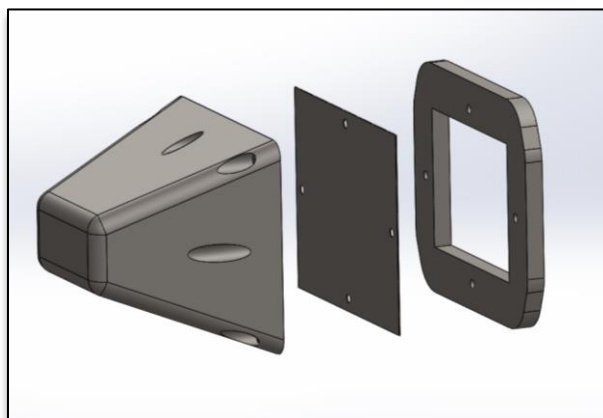


Figure 4.4: Exploded View of Impact Attenuator, Anti-Intrusion Plate, and Front Bulkhead, Shown in Order Left to Right

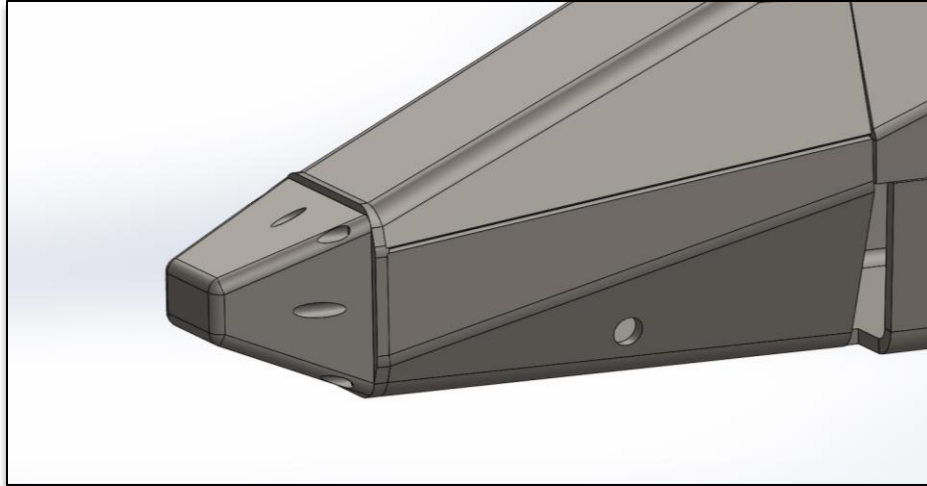


Figure 4.5: Assembled View of Impact Attenuator, Anti-Intrusion Plate, and Front Bulkhead

Roll Hoops

The front roll hoop (FH), main roll hoop (MH), and main hoop braces (HB) are 1.5"x0.065" round 4130 steel tube. By the area and moment of inertia requirements of rule T3.6, this is the minimum wall thickness that can be used to increase stiffness while maintaining weight. This wall thickness will require a weld test to verify joint strength. The main hoop braces are mechanically attached as described in T3.40, with 0.080" steel plates and two 5/16" bolts per attachment point, for a minimum of four attachment points per hoop. These roll hoop assemblies are shown in Figure 4.6, with the hoops assembled into the car shown in Figure 4.7, both below. The harness bar is welded into main hoop. The bottoms of the hoops require small amounts of notching to better fit the bend of the panel.



Figure 4.6: Roll Hoops and Mounting

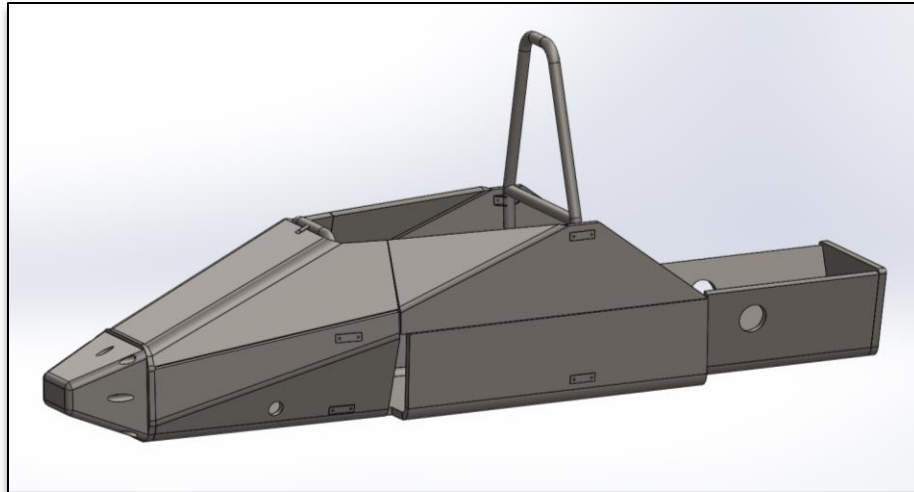


Figure 4.7: Chassis with Roll Hoops

Firewall

The firewall is made of the same carbon panel, with a single fold in it, as seen in Figure 4.8, below. It is structural, to satisfy the battery-driver separation in rule (AF4.8), so that the battery box need not support 40g loads. By making the structure between the driver and the batteries equivalent to side impact structure, the battery box can be allowed to support loads of only 20g. By the definition of side impact structure, this structural firewall only needs to reach 350mm from the ground. The structure of our firewall reaches the required 350mm, while additional fireproof layers extend all the way to the harness bar (not shown). The top of the firewall structure bolts directly to the main hoop through an attachment point on either side. The bottom attachment to the chassis is similar to roll hoop attachments. The firewall structure can be seen in its place in the car in Figure 4.9.

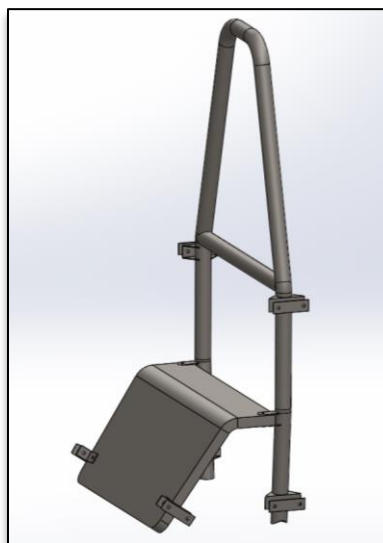


Figure 4.8: Structural Firewall and Mounting

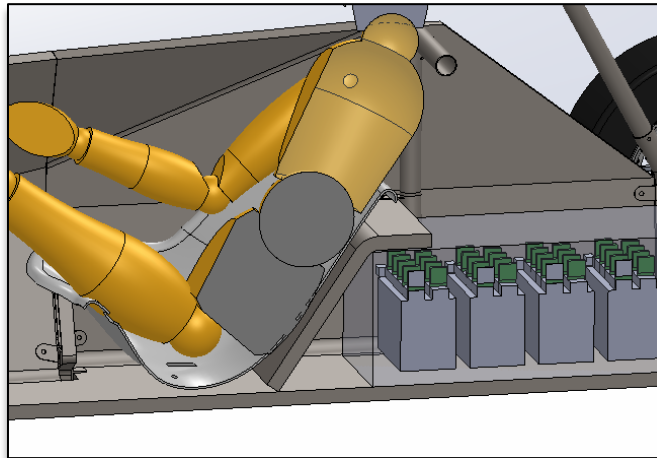


Figure 4.9: Structural Firewall Placement Between Driver and Battery Box

Drivetrain Plate Attachment

The drivetrain support plate is attached via 0.080" steel sheet metal tabs. The flat components will be cut out on a waterjet cutter, then welded together to make the mounts shown in Figure 4.10. In this way, the chassis can interface with the previous years' main drivetrain mounting plate, shown in position in Figure 4.11.

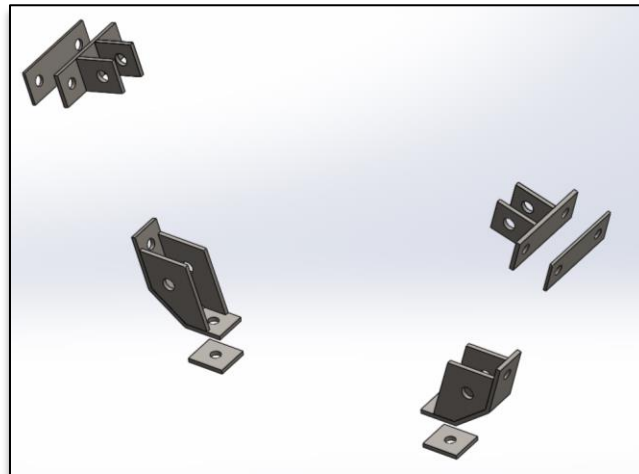


Figure 4.10: Drivetrain Support Plate Mounts

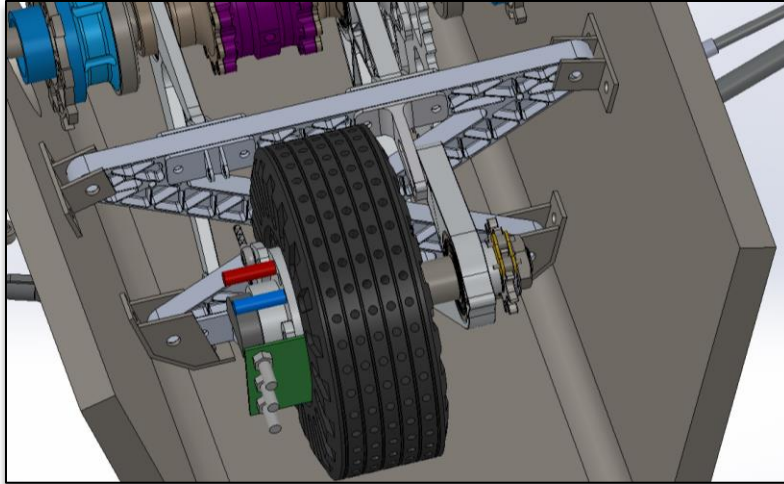


Figure 4.11: Drivetrain and Support Plate Shown in Place in Rear of Car

Front Machined Plates

Machined aluminum plates, shown in Figure 4.12, join the wide rear panel section (which accommodates the battery box) to the narrow front panel section (which accommodates the suspension points). At the same time, this provides a very strong mounting point for the front shocks. The plates are CNC milled from 7075 billet, with weight-saving pockets, achieving 1.5lb each, and are identical between the left and right sides of the car, to simplify machining. Aluminum tabs bolt to the plates for mounting of panels and shocks, as shown in Figure 4.13. The tabs are waterjet-cut flat pieces, which are then welded together. Of the five tabs per plate, each tab is anchored by two bolts, yet only six bolts are needed because of bolts being shared by multiple tabs on both sides of the plate. The plates are shown in place in the car in Figure 4.14.



Figure 4.12: Front Machined Plate

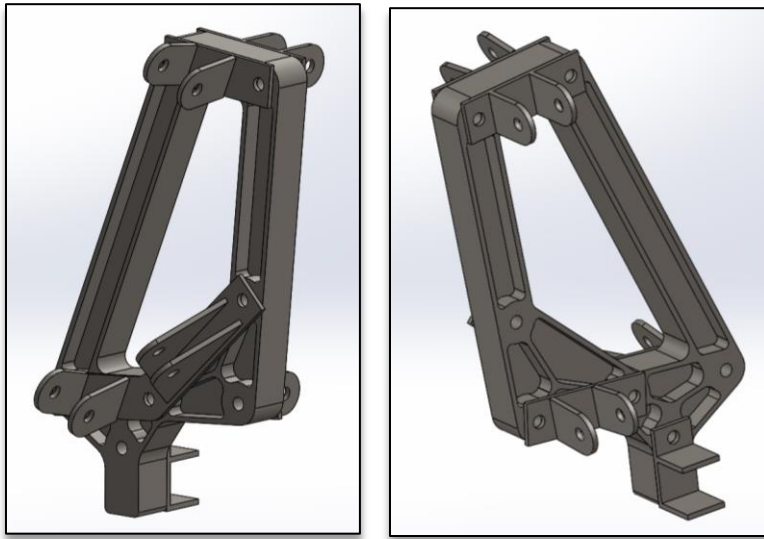


Figure 4.13: Front Machined Plate, Front View (Left) and Rear View (Right)

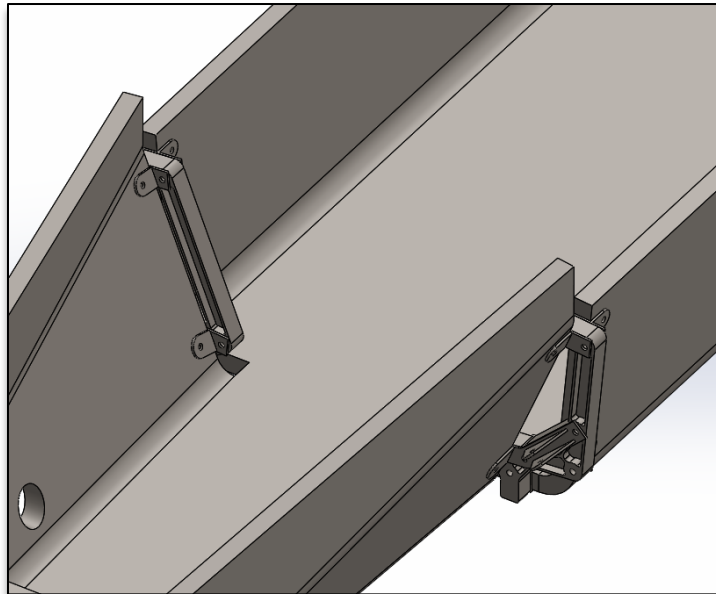


Figure 4.14: Front Machined Plates in Position in the Car

Jacking Point

The jacking point is required by rules to be a round steel or aluminum tube at 1" diameter. The tube must be at least 12" long (laterally) and between 4" and 10" from the ground. The original jacking bar

design, in Figure 4.15, bolted to a rear carbon panel bulkhead which was bonded to the rest of the frame like the front bulkhead. End caps would hold a nut welded on the inside of the tube.

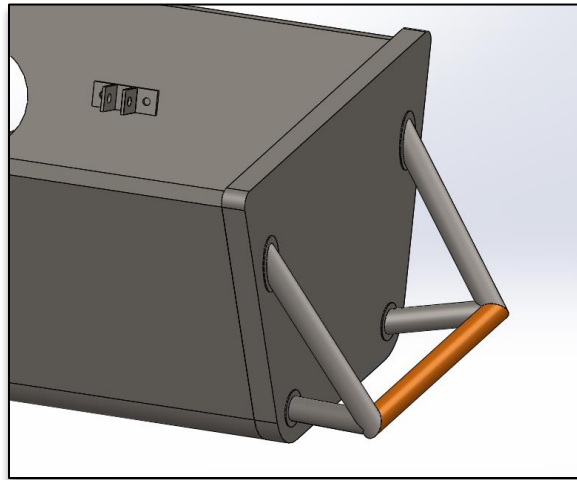


Figure 4.15: Original Jacking Point Configuration

The jacking point was revised and simplified, as shown in Figure 4.15a. The rear section panel was extended in an overhang, and the jacking bar attached to the bottom of this overhang by tabs. This revision eliminates 4 steel tubes, saving welding and extensive jiggling. It also allows the jacking bar to strengthen the rear section laterally, eliminating the need for a rear panel bulkhead and its associated wet layup. The attachment is simpler, as all bolts and nuts can be easily accessed, and this revised design is 1.2lb lighter than the original.

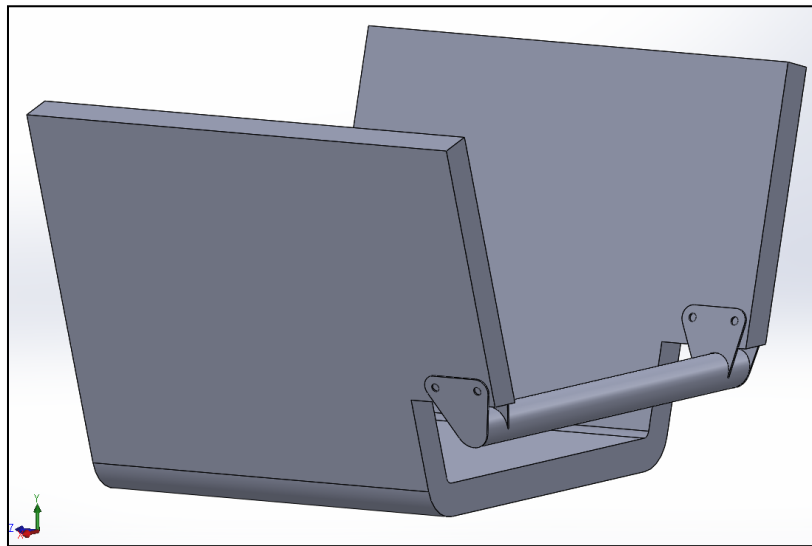


Figure 4.15a: Redesigned Jacking Point

Middle Bulkhead

The middle bulkhead, seen in Figure 4.16, is positioned just behind the battery box and connects the front and rear panel sections. The battery box is 6 inches wider than the rear suspension points (3 inches wider per side). The middle bulkhead allows the frame shape to neck down after the battery box and also provides two sturdy suspension points. The bulkhead is made of 1.125 x 0.049" square steel tube. The 1.125" size was chosen so that any tabs welded on the sides would be far enough apart for the panel thickness. This is needed because the panel has 1" core plus skin thickness, making the overall panel more than an inch thick. Waterjet-cut 0.060" steel sheet metal tabs are welded to the bulkhead for attachment to the panels. The bulkhead is shown in position in Figure 4.17.

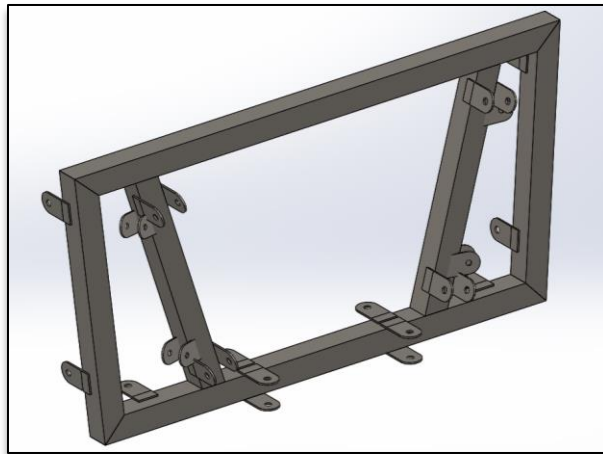


Figure 4.16: Middle Bulkhead with Tabs

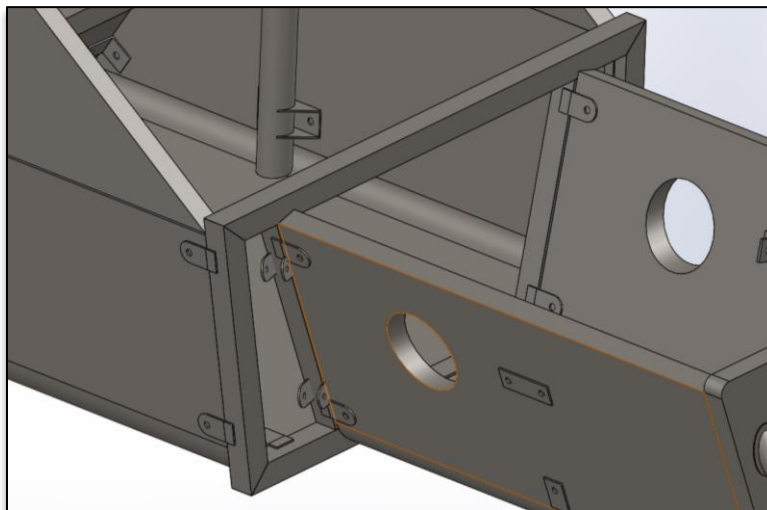


Figure 4.17: Middle Bulkhead in Position in the Car

Main Hoop Bracing

The main hoop is braced by removable 1.375" x 0.049" round 4130 steel tubes. 3" long tube stubs are welded to the top of the main hoop for the mechanical connection points of these braces. The long lower tube sections are bolted onto the stubs with sleeved butt joints (shown in Figure 4.18), forming a continuous tube as dictated by rule T3.17. The joint sleeves are 1.375" inner diameter and 0.049" wall thickness, with two 1/4" bolts per half, making 4 per joint.



Figure 4.18: Sleeved Butt Joints for Removable Main Roll Hoop Braces

Rear Suspension Bridge Mounting

The suspension bridge, shown in position in the car in Figure 4.19, is last year's machined billet structure for rear rocker and shock mounting. The panels at the ends of the bridge have a notch cut out for rocker clearance. A bent 0.125" aluminum sheet metal tab (Figure 4.20) fits in the notch. Two flat 0.125" aluminum tabs then weld to the bent tab. This bent tab wraps all the way over the edge of the panel, allowing bolts to go through the panel back into the tab in double shear. This can be seen by the hole locations in Figure 4.20.

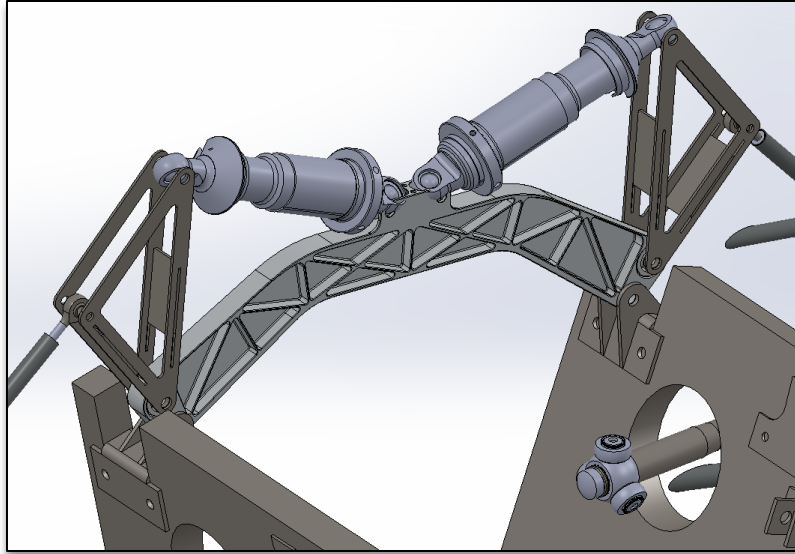


Figure 4.19: Rear Shock and Rocker Assembly Showing Suspension Bridge Function

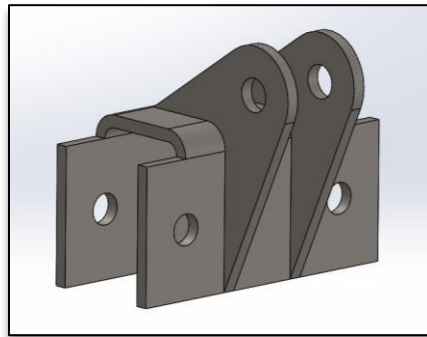


Figure 4.20: Rear Bridge Mounting Tab

Suspension Points

On the front suspension corners, the rocker and bottom rear suspension point share the same tab and bolt as the bottom front hoop backing plate (Figure 4.21). The bottom front and both top suspension points all bolt to tabs that have 3 bolts each: flat tabs with a bolt on either side and one on top. Two vertical tabs welded on to those flat tabs meet the rod end of the a-arm.

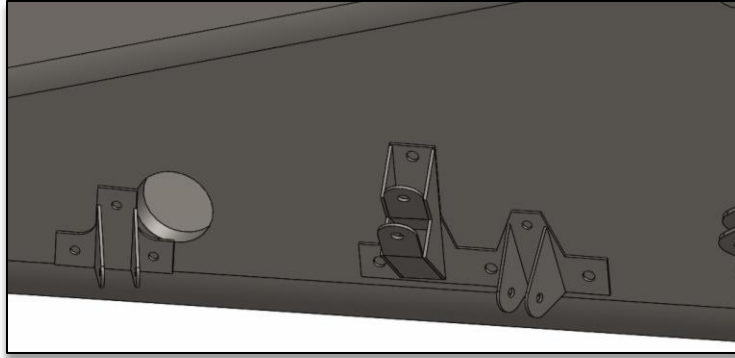


Figure 4.21: Front Suspension Mounting Tabs

On the rear suspension corners, the front points attach to tabs welded to the middle bulkhead. The rear points attach to the same 3-bolted tabs. The rear bottom point is merged with the backing plate for the drivetrain support mount. The rear suspension mounting system is shown in Figure 4.22.

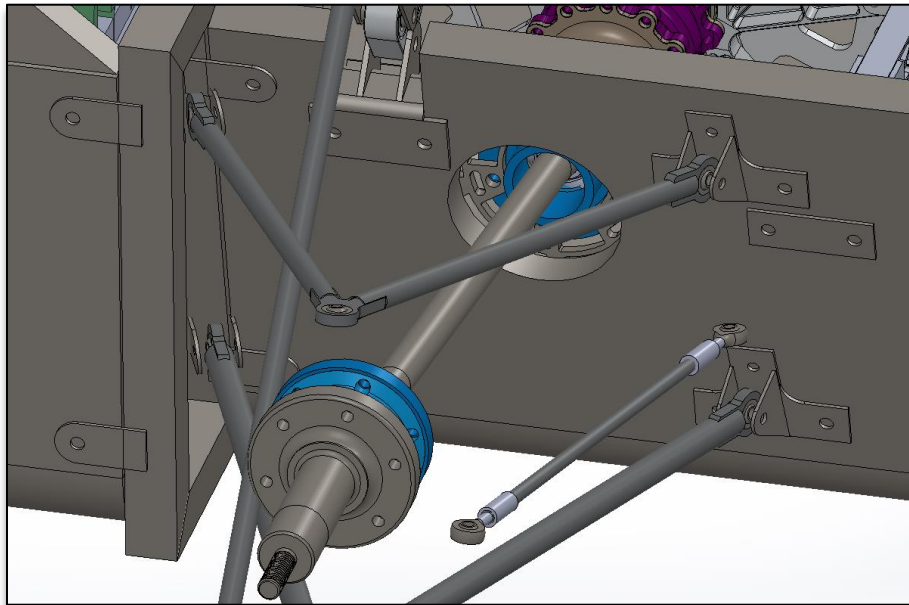


Figure 4.22: Rear Suspension Mounting

Battery Box Removal

To remove the battery box, the rear half of the car unbolts at the middle bulkhead. The middle bulkhead, suspension, and drivetrain all stay attached to the rear half. The roll hoop braces disconnect from the sleeve joints at the top of the hoop and the top of the bulkhead. The entire back half of the car is moved aside enough to get the battery box out, as shown in Figure 4.23. Electrical lines have quick disconnects in this area, and a coil of extra soft brake line is reserved by the joint. In this way the rear of

the car can be removed without needing to re-bleed the brakes every time. The two halves of the car are supported by dollies when doing this. This method of removing the battery box leaves a wide open bay with extremely easy access to the heavy battery box.

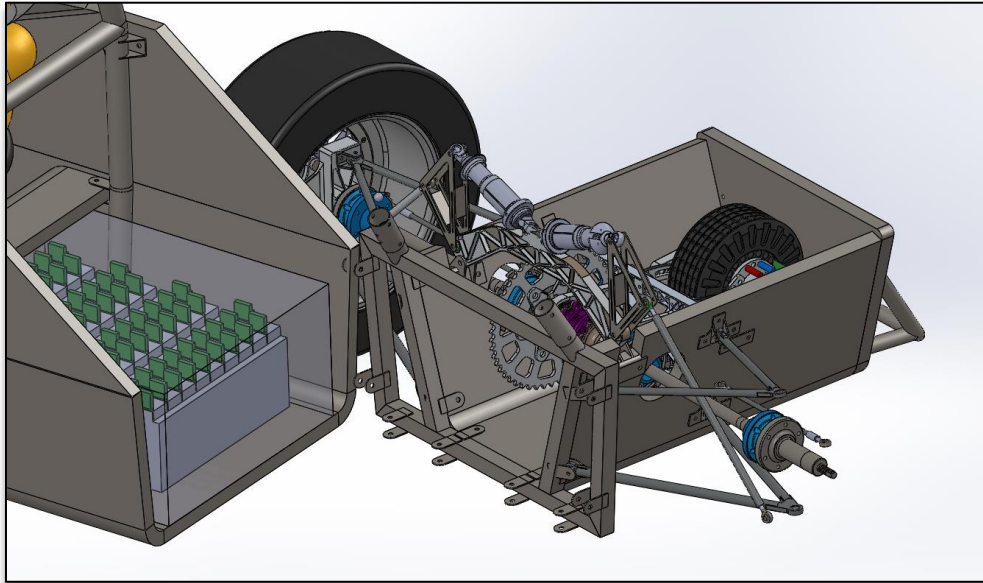


Figure 4.23: Removing the Back Half of the Car to Remove the Batteries

Analysis Results

All analysis for the chassis was finite element analysis (FEA) done in Abaqus CAE. The geometry of the model was simplified in SolidWorks to surface and sketch entities and then imported into Abaqus. The Abaqus assembly consists of two parts: one part contains all of the shell bodies in the model and the other part contains all the wire bodies in the model. Figure 4.24 shows how the shell and wire elements fit together and interact.

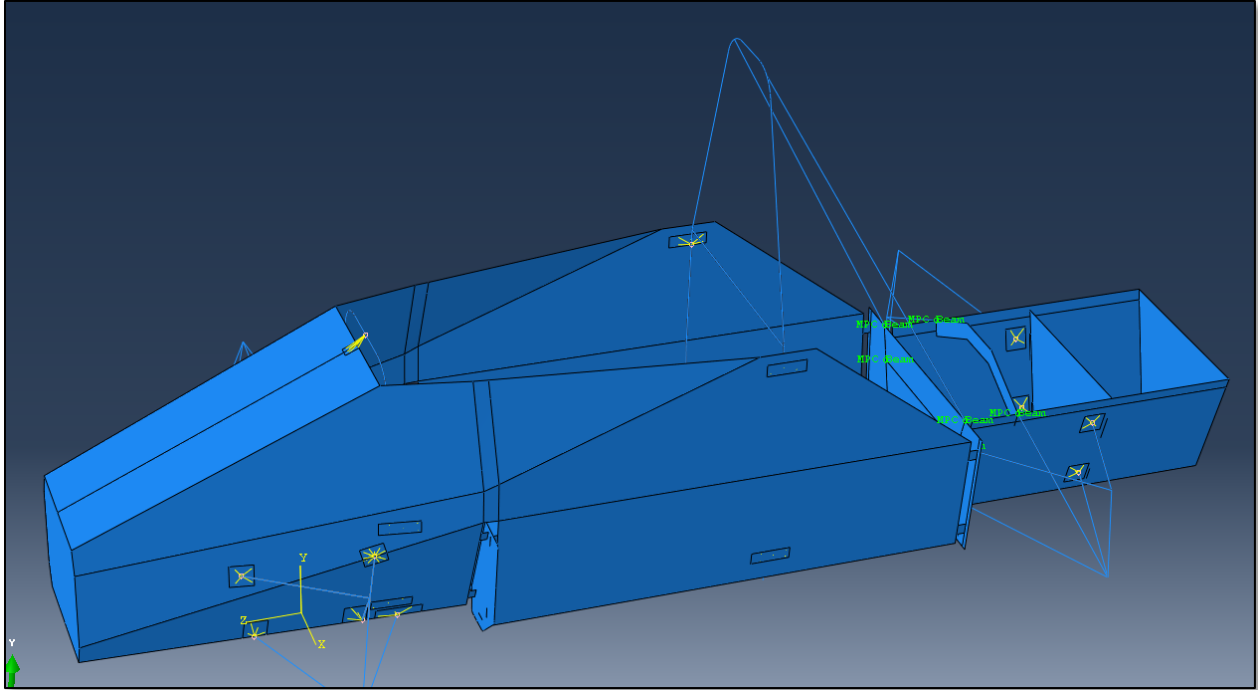


Figure 4.24: Abaqus model assembly with interactions shown in yellow and green.

The shell part was partitioned into multiple faces. Each different region as seen in Figure 4.24 is assigned different section properties. The main panel area was assigned a composite layup section, composed of two layers of 0.012" thick carbon fiber per side, with 1" thick core material in the middle. This composite layup section uses composite laminate theory in addition to the 3-dimensional plate theory which is default in the Abaqus/Standard solver. The small square faces representing tabs are assigned the same composite layup section, but with one layer of aluminum or steel on the outside. All of the wires seen in Figure 4.24 exist in the same part, but disjoint sections do not directly influence each other during the analysis. The yellow and green lines and labels in Figure 4.24 represent the interactions between the wire elements and shell elements, which represent bolted tab connections. These interactions simply force the deflections of the two connected regions to be the same, even if they don't physically touch. The suspension members were modelled at truss elements in order to accurately transmit forces to the chassis.

Table 4.1: Composite Material Properties used in Abaqus

| Carbon (plain weave) - Type: Lamina | | | | | |
|-------------------------------------|-----|------|--------|--------|--------|
| E1 | E2 | Nu12 | G12 | G13 | G23 |
| 1e7 | 1e7 | 0.05 | 0.25e7 | 0.25e7 | 0.15e7 |

| Honeycomb - Type: Engineering Constants | | | | | | | | |
|---|-----|-----|------|-------|-------|-----|------|------|
| E1 | E2 | E3 | Nu12 | Nu13 | Nu23 | G12 | G13 | G23 |
| 100 | 100 | 3e5 | 0.05 | 0.002 | 0.002 | 100 | 5000 | 5000 |

The composite material properties used in this finite element model are outlined Table 4.1. These values are conservative estimates based on the material properties listed on the Fibreglast website. Once destructive testing was completed on the actual carbon panels used, material properties were derived based on those tests to use in FEA.

Table 4.2: Analysis Results for the AF Loading Cases and Cornell Torsion Loading Case

| Rule Number | Description | Max Deflection (in) | Deflection Safety Factor | Max Stress (ksi) | Stress Safety Factor |
|--------------------|--|----------------------------|---------------------------------|-------------------------|-----------------------------|
| AF4.1 | Main Hoop Rollover | 0.254 | 3.94 | 35.2 | 1.99 |
| AF4.2 | Front Hoop Rollover | 0.067 | 14.93 | 11.6 | 6.03 |
| AF4.3 | Side Impact | 0.327 | 3.06 | 29.1 | 2.41 |
| AF4.4 | Front Impact | 0.321 | 3.12 | 52.4 | 1.34 |
| AF4.5 | Shoulder Harness Bar | 0.197 | 5.08 | 47.3 | 1.48 |
| AF4.6 | Front Impact Off-Axis | 0.576 | 1.74 | 55.9 | 1.25 |
| AF4.7 | Lap/Anti-Sub Harness | 0.181 | 5.52 | 33.5 | 2.09 |
| AF4.8 | Battery Box Loading | 0.408 | 2.45 | 50.1 | 1.40 |
| N/A | Torsion - 1000lb applied upward to one wheel | 1.324 | 0.76 | 7.8 | 8.97 |

The results of this finite element analysis are outlined in Table 4.2. All of the stress and deflections pass the criteria in the AF rules: no more than 1 inch deflection and no failure anywhere in the structure. The yield stress of the carbon was approximated as 70 ksi, which is slightly lower than the values given by F Fibreglast. The force applied in the torsion loading case was 1000 lb, which is given by the suspension senior project as the maximum wheel force caused by hitting a large bump at full speed. The torsional stiffness was about 1200 ft-lb/deg, which is below our goal of 1800 ft-lb/deg. However, this was likely caused by tab approximations in the analysis which made them weaker than they actually are. The main source of torsional stiffness loss in the chassis was the middle bulkhead connection to both halves of the car.

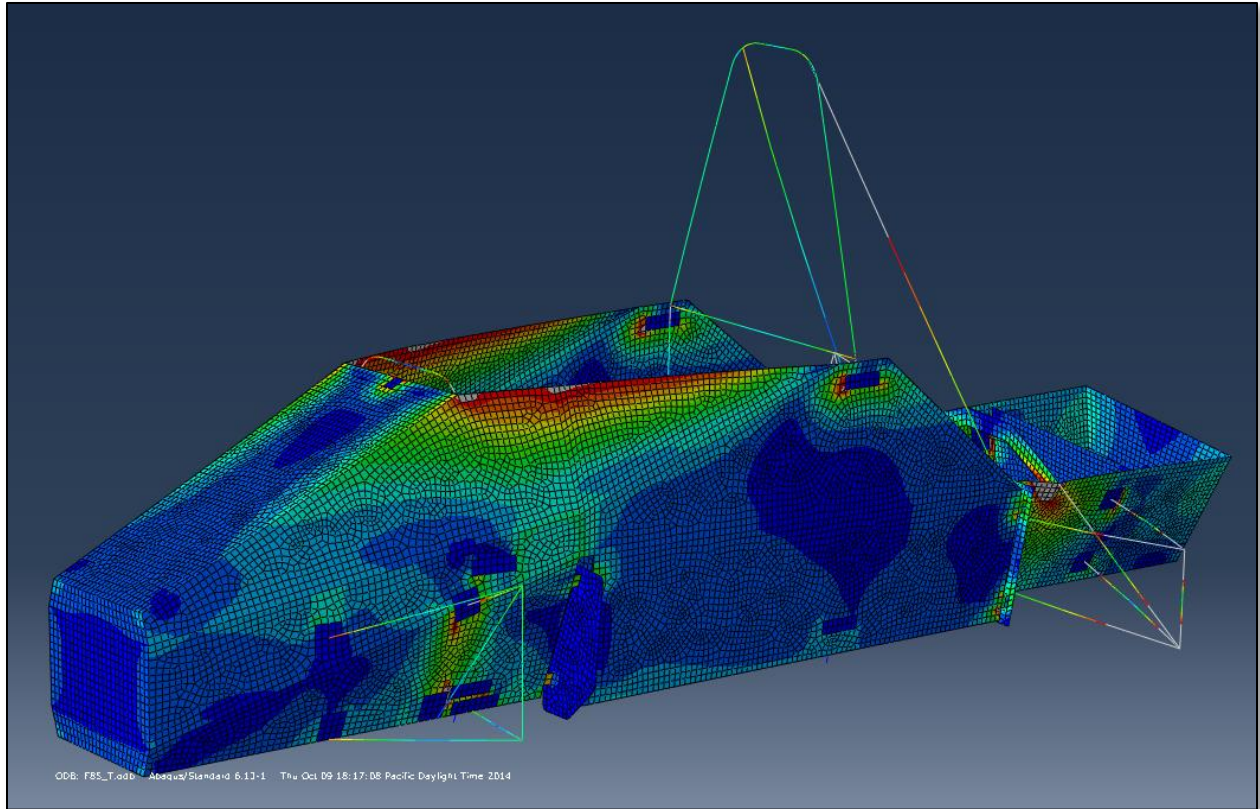


Figure 4.25: Von Mises Stress Contour Plot for the Torsional Loading Case
Blue: ~0.1 ksi, Green: 3.5 ksi, Red: 7 ksi, White: up to 9 ksi

The stress distribution caused by the 1000 lb wheel load is shown in Figure 4.25. The small square areas on the panel representing tabs show much less stress than the surrounding material, verifying the accuracy of the way tabs are attached to the composite layup. The mesh shown is small and unrefined, and was improved for SRCF documentation of the frame for technical inspection later. Overall, this finite element model is enough to assure that the designed frame construction will safely pass the AF loading cases. More model refinement occurred after material testing was completed.

Cost and Weight Analysis

Table 4.3: Weight Analysis of the Final Design

| Panels | Area (in ²) | Weight |
|----------------|-------------------------|----------------|
| Main Front | 3035 | 11.6 |
| Top Front | 863 | 3.3 |
| Front Bulkhead | 106 | 0.4 |
| Middle Left | 435 | 1.7 |
| Middle Right | 435 | 1.7 |
| Firewall | 370 | 1.4 |
| Rear Taco | 892 | 3.4 |
| Rear Bulkhead | 192 | 0.7 |
| Total | | 24.2 lb |

| Tubes | Weight |
|---------------------------|----------------|
| Main Hoop | 8.5 |
| Front Hoop | 4.9 |
| Harness Bar | 1.7 |
| Jacking Point (incl caps) | 1.1 |
| Main Hoop Braces | 3.6 |
| Middle Bulkhead | 5.8 |
| Total | 25.6 lb |

| Tabs/Attachments | Weight |
|------------------------|---------------|
| Hoop Tabs | 1.9 |
| Drivetrain Tabs | 0.5 |
| Front Plate Tabs | 0.9 |
| Front/Rear Attachments | 1.4 |
| Suspension Points | 3.2 |
| Total | 7.9 lb |

| Resin | | |
|-------------|--------------------|-------------------------|
| 0.55 | lb/ft ² | Panel area |
| 633 | in | bond/fold |
| 237 | in | open edge |
| 0.0361 | lb/in ³ | Water (resin) |
| 0.0090 | lb/in ³ | resin+microballoons |
| 0.5 | in ² | resin fill per length |
| 0.0045 | lb/in | resin weight per length |
| 3.93 | lb | resin weight |

| Carbon Tape | | |
|-------------|--------------------|--------------------------|
| 0.0003 | lb/in ² | carbon cloth weight |
| 4 | | total number of plies |
| 0.0011 | lb/in ² | carbon weight per area |
| 4 | in | width of tape |
| 0.0044 | lb/in | carbon weight per length |
| 3.83 | lb | carbon weight |

| Other | Weight |
|--------------|---------------|
| Front Plates | 2.9 |
| Total | 2.9 lb |

Total: 68.3 lb

Table 4.4: Bill of Materials and Cost Analysis for Final Design

| Part | Dimensions | Cost | Supplier |
|-----------------------|-------------------------------------|----------------|-----------------|
| Carbon Panels | one 48"x96", one 48"x72" | \$2,500 | ACP Composites |
| Roll Hoops | 16ft - 1.5"x0.065" round 4130 | \$320 | Online Metals |
| Main Hoop Braces | 8ft - 1.375"x0.049" round 4130 | \$50 | Online Metals |
| Middle Bulkhead Tubes | 10ft - 1.125"x0.049" square 4130 | \$64 | Discount Steel |
| Impact Attenuator | one standard item | \$150 | SAE |
| Front Machined Plates | one 12"x12"x1" thick 7075-T6 | \$150 | McMaster |
| Carbon Tape | one 30yd roll x 4" wide | \$199 | Fibreglast |
| Series 2000 Resin | one gallon | \$69 | Fibreglast |
| 2020 Resin Hardener | one quart | \$49 | Fibreglast |
| Glass Microspheres | one carton (6 gallons) | \$69 | Fibreglast |
| Sheet Metal for Tabs | one 24"x48"x0.125" thick 6061-T6 | \$93 | McMaster |
| Sheet Metal for Tabs | one 24"x24"x0.080" thick mild steel | \$44 | McMaster |
| Sheet Metal for Tabs | one 24"x24"x0.060" thick mild steel | \$42 | McMaster |
| Total | | \$3,799 | |

Chapter 5: Manufacturing

Fiberglass Chassis

It was decided that the senior project team would construct a mockup chassis from the Zodiac fiberglass panels while waiting for the new carbon panels. This would give all the following benefits:

- Allow the team to test fit other subsystems into the chassis as designed
- Build familiarity and skill with the cut-and-fold layup process
- Identify issues to solve before beginning work on the final product

The flat patterns for the panels were generated from the SolidWorks model. All cuts were straight lines, so Matlab was used to generate CNC router (Shop Bot) code from the endpoints. The panels' outer shapes and bend lines were machined in the Shop Bot, using the team's extra billet material as weights to hold the panel down in the machine, as seen in Figure 5.1. The same Matlab program that generated the shop bot code was used to run a simulation of the cut path. This ensured that the panel was cut correctly and the machine would not collide with the billet weights. The machined panels are shown in Figure 5.2.

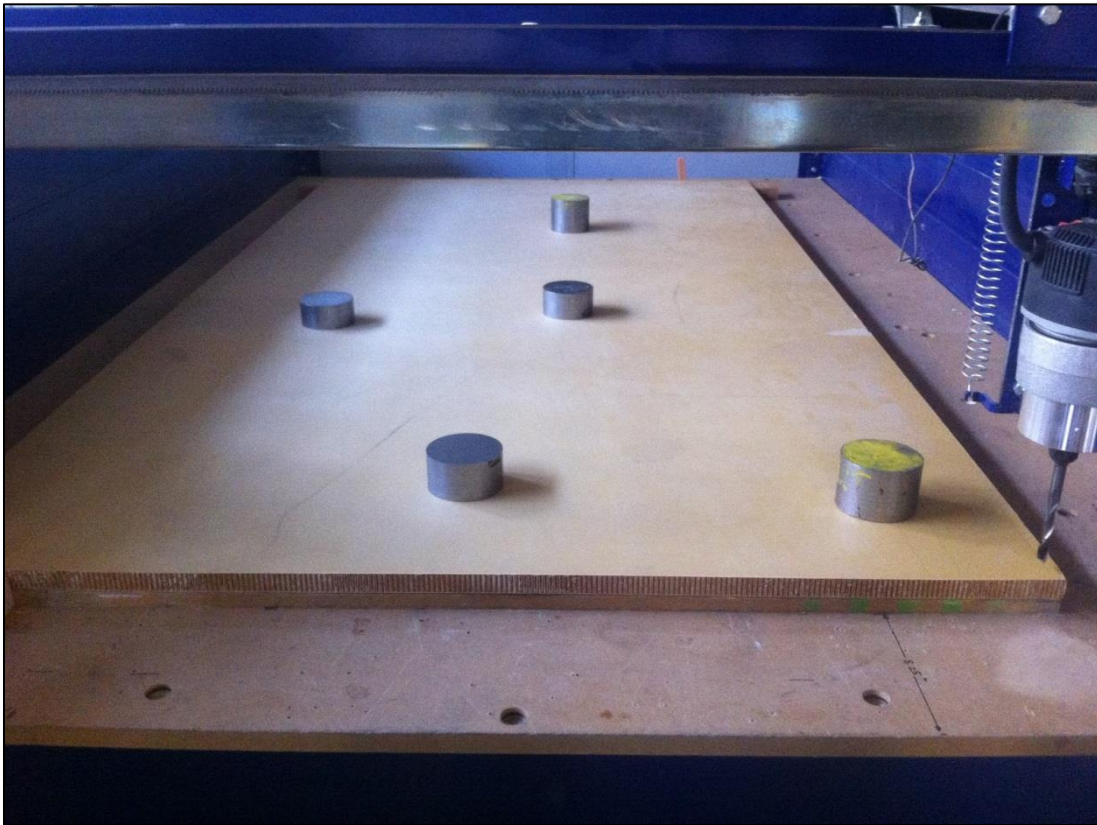


Figure 5.1: Fiberglass panel in CNC router.



Figure 5.2: Fiberglass panels after CNC routing.

The fiberglass chassis constructions helped us to build the carbon chassis by proving our construction methods and allowed us to modify jigs and techniques without sacrificing expensive materials. Each jig was thoroughly tested on the fiberglass chassis and modified before being used on the carbon. This allowed for more consistent bend angles and cleaner joints. It also allowed us to practice the wet layup technique and prove out the process. The wet strips required delicate handling and were easily wrinkled up. Holding the peel ply and breather with tape proved to be effective and was continuously used throughout constructions.

Carbon Chassis

Panel Machining and Prep

The final product was made with carbon panels pressed by ACP Composites. The panels used 3 plies per side of plain weave carbon cloth over .75 inch-thick nomex honeycomb core. These panels were machined in the same way as the fiberglass panels, with one exception. A shorter endmill was used with these panels to reduce chatter and so improve cut quality. This meant that the endmill would not reach far enough down to cut the panels.

In order to raise the panel high enough for the cutter to reach, a work table was constructed from a 4'x8' MDF panel supported by a framework of 4"x4" wooden beams. The table was leveled through the use of wooden shims under the legs. In this way the cut depth could be kept consistent, allowing for accurate bends.

Each panel was cut in a series of two operations. In the first operation, the panel was clamped to the table using C-clamps and wood blocks to distribute the load, and the insert holes were drilled, as shown in Figure 5.3. The holes were then used to bolt the panel to the table, allowing full access to the edges for cutting outer profiles and bend lines in the second operation.

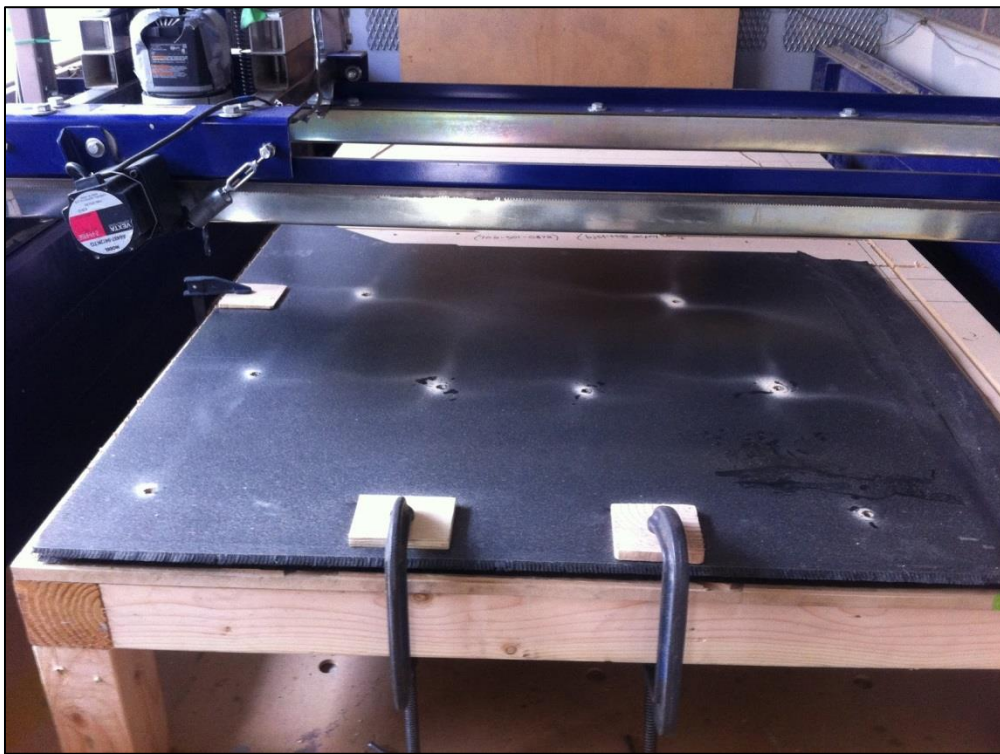


Figure 5.3. Carbon panel clamped to work table. Insert holes are drilled through both panel and table.

With machining finished, the panels (shown in Figure 5.4) are removed from the router and prepared for the cut and fold layup. The excess nomex core is removed from the edges of the cuts, leaving a small channel to be filled by the microballoon mixture. The smooth outer surface of the panel is sanded and roughed up for better wet layup adhesion.

The existing jigs from the fiberglass mockup chassis were reused for the carbon chassis, with adjustments as needed. Angles, alignment, and fits were double-checked by test-fitting the carbon panels together in the jigs. Pieces of masking tape were used to mark the jig locations on the panels. This would help the layup process to run smoothly.



Figure 5.4: Finished carbon panel after removal from the router.

Wet Layup-Bend

Along with preparing the panels, the layup materials must also be prepared. A vacuum bag was cut for each layup out of Stretchlon 600% elongation stretchy bagging purchased from Fibreglast. Tacky tape was used to seal three sides of the bag, reducing time between when the resin was mixed and when a vacuum could be pulled on the part. The bags were made with about a foot of extra space on each side of the part and jig. This allowed the bag to suck tightly into all corners without popping or tearing. In most cases, the entire panel would be sealed inside of the bag. In some cases the panel in progress was too big to reasonably fit inside a bag, so vacuum bagging was sealed to the panel itself with tacky tape. This method is not preferred, as it is more difficult to seal well.

Two layers of carbon tape, a layer of peel ply, and a layer of breather were cut for each bend. The carbon was cut to the exact length of the bend, while the peel ply and breather were cut to have about two inches of excess on all sides of the carbon. This prevented the bag from contacting wet resin, allowing some of the bags to be reused and avoiding messy bits of Saran wrap stuck in the joint.

Resin and hardener were mixed, usually in batches of 100 grams (80g resin, 20g hardener), and microballoons were added slowly and carefully. To avoid puffing them everywhere, a folding motion was used in the stirring process. The consistency that behaved the best was similar to toothpaste, although anything from a stiff cake batter to peanut butter would work. The surface of the mixture would transition from glossy and wet-looking to a drier satin finish at this point.



Figure 5.5: Application of resin and microballoons to groove in panel.

Once a good consistency was achieved, the mixture was applied to the cut groove in the panel, as seen in Figure 5.5. The microballoon mixture was applied primarily to the sides of the groove. Once the panel was folded the filler would be sufficiently pressed into the bottom. When the entire groove was lined with an excess of filler, the panel was bent and filler coverage checked. The entire cavity of the bend should be filled with the microballoon mixture with no hollows, and there should be filler squeezing out of the edges. This extra filler was very easy to scrape and wipe off before the wet layup was applied.

While most of the team was busy filling the bend, one or two people mixed the resin for the wet layup. This step used resin and hardener only, with no microballoons. In order to finish the entire layup within the resin's 1-hour pot life, the pseudo-prepreg carbon strips must be prepared while the bend is being filled.

The pseudo-prepreg process was carried out by placing the carbon tape on prepared strips of plastic. Drop cloth material worked perfectly. The plastic strips were a few inches longer than the carbon and wide enough to fold over the carbon strip with a few inches extra along the open edge. With the carbon laid out on the plastic, the resin was poured down the length of the carbon. A wooden popsicle stick was used to spread the resin thoroughly over the entire surface of the carbon tape, as in Figure 5.6. The plastic was then folded over the carbon and the excess resin was removed with a squeegee. This can also be done with another popsicle stick. Figure 5.7 shows one carbon strip with this process completed.

One or two firm passes of the squeegee down the length of the carbon removed enough resin. A diligent effort to remove all excess resin left the carbon too dry.



Figure 5.6: Resin being spread onto carbon tape to wet entire surface.



Figure 5.7: Completed pseudo-prepreg strip.

Once the bends were filled and the carbon tape was prepared, the panel was placed into its jig, with all tape markers aligned, as in Figure 5.8. Weights were placed on the panel to hold it into the jig, but in locations where they would not interfere with the layups. Aluminum and steel billets were used, since those happened to be plentiful. Angles and dimensions were checked again to verify that the part was still located correctly in the jig and that all the pieces would fit together well.



Figure 5.8: Locating panel in jig.

Once the panel was located correctly in the jig, the first layer of carbon was removed from its plastic wrapper. The carbon was placed carefully over the bend, with the seam in the panel running directly down the center of the tape. The tape was pressed lightly onto the panel with special care to get it well into the corner of the bend. All wrinkles were smoothed away as in Figure 5.9, and the process was repeated with the second layer.



Figure 5.9: Smoothing wrinkles out of carbon tape. Tape has been laid up onto bend.

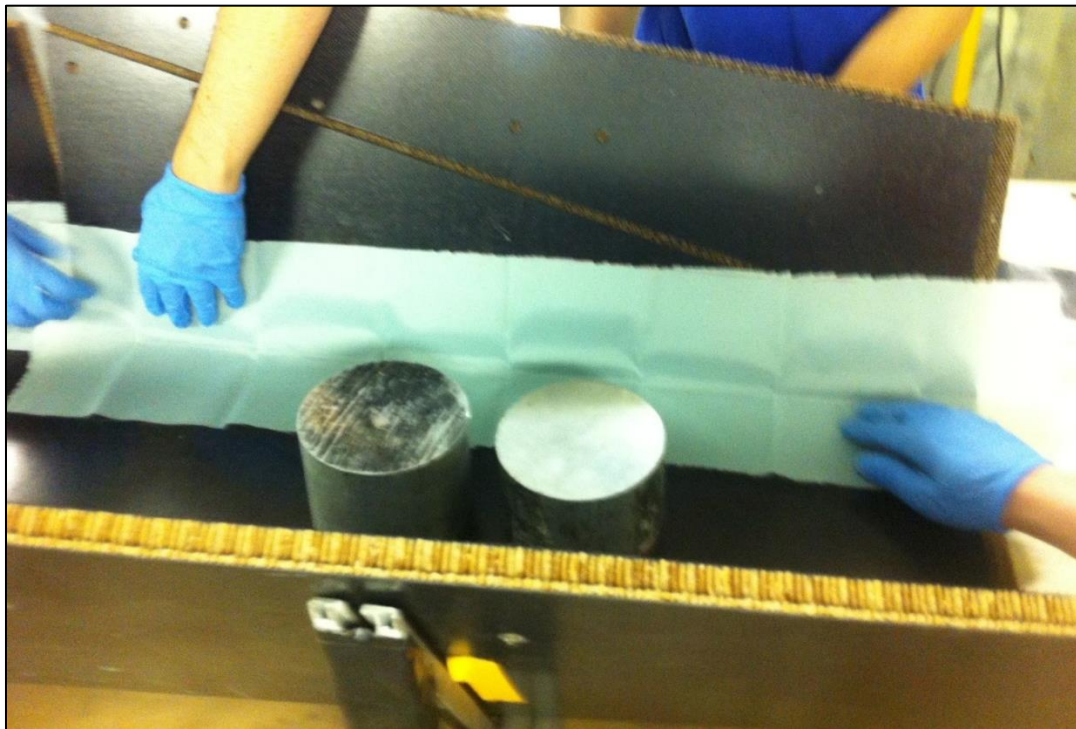


Figure 5.10: Peel ply completely covers wet carbon layup. Also visible is yellow masking tape marker for jig location.

The peel ply is placed on top of the carbon to allow for the resin to escape the carbon once the vacuum is applied. Care should be taken to cover all of the wet carbon with peel ply to keep the vacuum bag from getting resin on it.

After the peel ply is placed over the carbon, it may be necessary to hold the peel ply in place with masking tape. Then the breather is placed over the peel ply. The breather gives the excess resin a place to go when the vacuum is applied. The breather should cover the entire width of the carbon tape to ensure resin extraction. The breather may also need to be held in place by masking tape.

Peel ply was smoothed over the carbon layup, as seen in Figure 5.10, with care to cover all wet resin and remove as many wrinkles as possible. This was because without peel ply the resin would bond to anything it contacted. Since it was the layer in direct contact with the carbon, any wrinkles in the peel ply would show in the finished carbon surface. Once it was smoothed on, the peel ply was secured to the dry panel with masking tape. Breather was the next layer to go on, covering the entire area of the wet carbon to allow excess resin to be sucked out of the layup under vacuum. This can be seen in Figure 5.11. Breather was also secured with masking tape.

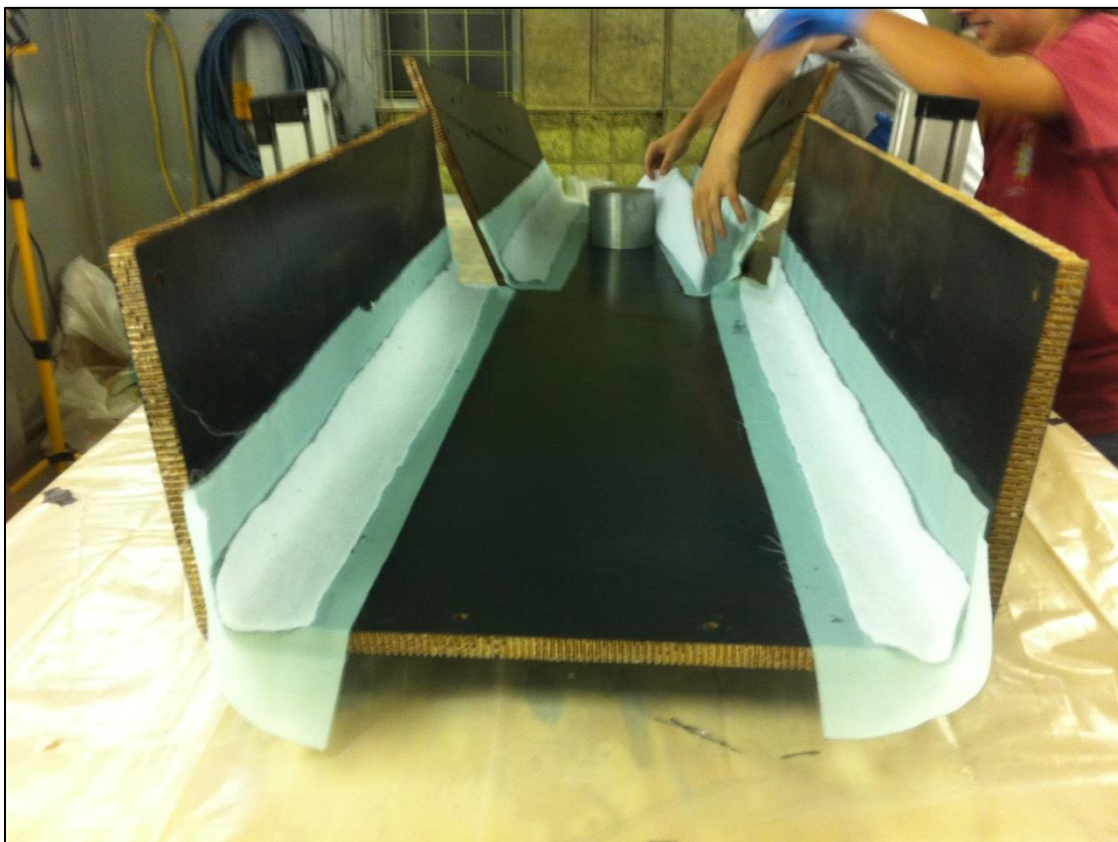


Figure 5.11: Bend layup with tape, peel ply and breather applied.

Before putting the panel in the vacuum bag, all sharp corners of the jig and the panel were found. These were padded with layers of tape, and sometimes breather, to avoid puncturing the bag under vacuum.

This padding can be seen in Figure 5.12. With all the corners padded, the panel was put into the bag. This was done very carefully, as any dragging or scooting the part or jig against the bag could still catch and tear it. Care was also taken to tuck excess bag into all possible voids around the jig to avoid the bag stretching too far and popping.



Figure 5.12: Vacuum bag sealed around panel.

Once the panel was in place inside the bag, but before beginning sealing the bag, the vacuum components were placed. If only a single layup was performed, the Venturi pump's pancake could be placed on the edge of the layup's breather. If there were more than one layup, a bridge made of several layers of breather was used to connect the two. The pancake was placed in the middle of this bridge, allowing the vacuum to access both layups equally. The breather bridge and Venturi pump components can be seen towards the front of the chassis in Figure 5.13.

After the pancake was placed, the final edge of the bag was sealed. It proved helpful to put a strip of tacky tape on this edge when the bag was being made. One side of the tape was sealed to the bag, and the paper backing was left on the other side, leaving it ready for sealing the bag closed during the layup process. After the bag was sealed, a small X-shaped hole was cut in the bag to allow the vacuum components to pass through. All edges of this hole were covered by the air fittings in the Venturi pump.

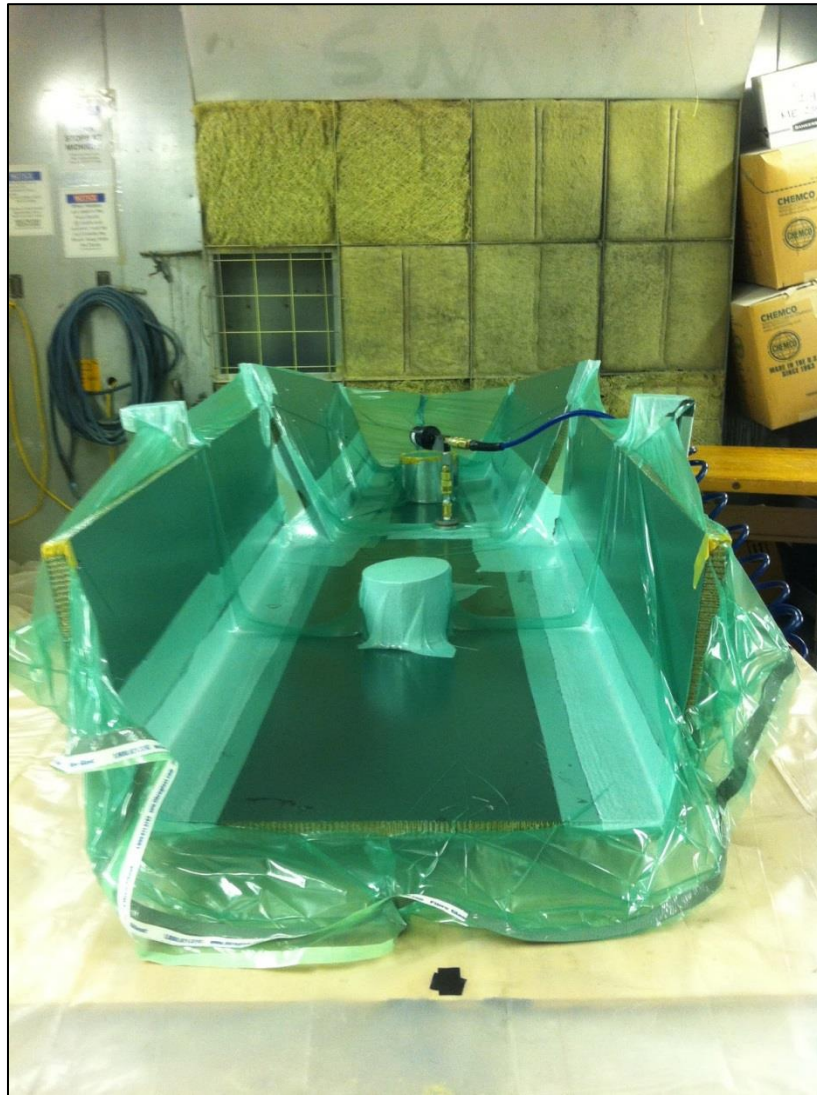


Figure 5.13: Bag under full vacuum for resin cure.

Depending on how much air was sealed inside the bag, it took anywhere from a few minute to a half hour to develop a good vacuum. Like the one shown in Figure 5.13, a vacuum was considered “good” when it was strong enough to firmly support the Venturi pump, even against the tension of an air hose pulling on it. The vacuum should suck the bag tightly into the panel bends and smash the breather as in Figure 5.14. Small wrinkles of bag could be pinched up from the surface of the panel with some difficulty. The layup was left under halogen work lights for mild heating to assist with maintaining cure temperature overnight.



Figure 5.14: Close-up of a good vacuum on bend reinforcement.

Lap Joint

The panels were joined together via a lap joint process. This is nearly the same as the bend reinforcement process, with a few minor differences. These layups needed no jigs. The Front Top panel simply sat on top of the main bottom one without any need for stabilization. The viscosity of the resin was enough to hold up the side panels until vacuum could be applied, however care had to be taken not to bump them out of position. The composite process for these layups was identical to the bend reinforcement layups. The finished lap joints can be seen in Figure 5.15.

Edge Closeout

Edge closeout on the chassis used only one layer of carbon tape instead of two. Microballoon filler was used to fill the edges of the core and give the outside layer of carbon a more smooth appearance. Where the tape needed to go around corners, cuts were made about $\frac{1}{4}$ " into the side of the tape. This allowed the outside of the bend to spread wider and the inside to overlap smoothly and not wrinkle. Only mild pressure was needed for this process. The closeouts where no vacuum was used turned out just as well as the ones made with a bag and Venturi pump.



Figure 5.15: Carbon chassis with completed bend reinforcements and lap joints.

After all layups were completed, bolt hole inserts were installed. Each hole was stuffed with microballoon filler and the insert was pushed in, with care to leave it flush with both the panel surfaces. The filler, unlike pure resin, was easy to drill out, so nothing had to be done to avoid getting filler inside the inserts. These required no vacuum at all.

Brackets and Backing Plates

Sheet metal brackets were made for attaching the roll hoops, suspension points, and drivetrain to the carbon chassis. Each bracket was designed with a tab on either side of a piece that would bolt flat to the carbon panel. These were designed in Solidworks, and flat patterns were generated as DXF files to be outsourced to a laser cutter. The laser cut pieces were then grouped in each of their mounting points.

Each flat piece was bolted to the car and its pair of tabs located with a jig. They were tack welded into position, then removed from the car. Full welding was completed on another table, to avoid damaging the carbon.

Chapter 6: Design Verification

Rules Required Tests: Descriptions and Results

Design verification relied largely on the tests required by the Formula SAE rules for monocoque panel testing and alternative frame rules loading.

3-Point Bend

As defined in Rule T3.31, the 3-point bend test compares the bending strength of the chosen composite material with the strength of two baseline steel tubes. The composite must be at least as strong as the tubes. A panel sample measuring 10.8" by 19.7" is used with the setup shown in Figure 6.1. This test setup was constructed by Cal Poly's Formula SAE team, along with all test fixtures required by rules unless otherwise noted. Results of this test were used to derive material properties, shown in Table 6.1, for use in finite element analysis and submittal to the Formula SAE rules committee.

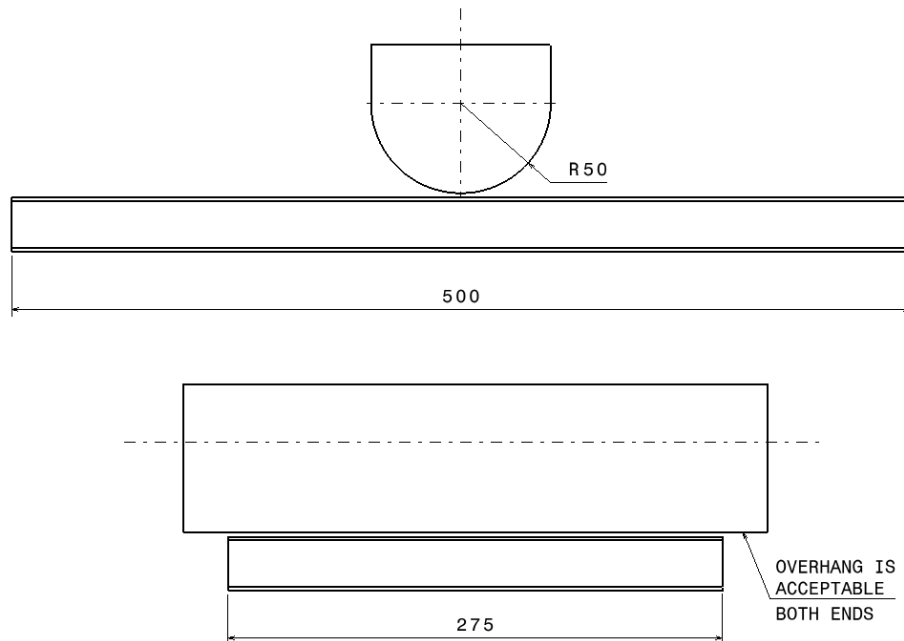


Figure 6.1: Testing rig diagram for 3 point bend.

Table 6.1: Composite material properties derived from 3 point bend test.

| Orthotropic Materials (units: [psi]) | E11 | E22 | G12 | G23 | G13 | v | T11 | T22 | C11 | C22 | Shear Limit |
|--------------------------------------|----------|----------|----------|----------|----------|------|----------|----------|----------|----------|-------------|
| Carbon | 5.77E+06 | 5.77E+06 | 1.21E+06 | 2.34E+03 | 2.34E+03 | 0.23 | 3.81E+04 | 3.81E+04 | 3.81E+04 | 3.81E+04 | 3.09E+04 |
| Glass | 3.26E+06 | 3.26E+06 | 1.73E+06 | 6.52E+03 | 6.52E+03 | 0.18 | 3.76E+04 | 3.76E+04 | 3.76E+04 | 3.76E+04 | 7.93E+03 |
| Core | 2.00E+01 | 2.00E+01 | 3.10E+03 | 1.85E+03 | 1.85E+03 | 0.05 | - | - | - | - | 90 |

Perimeter Shear

The perimeter shear test, also defined by T3.31, tests the perimeter strength of the panel. It is required for all structural composites. The panel sample rests on a flat plate with a 1” diameter hole through it, while a 1” diameter punch presses against the top of the panel. The composite must withstand 1240 pounds of force before failure. The flat plate for this test was provided by Cal Poly Formula SAE, but the punch was turned on a lathe, very carefully since any rough or slanted edges could skew the results. The data from the test is shown in Figure 6.2.

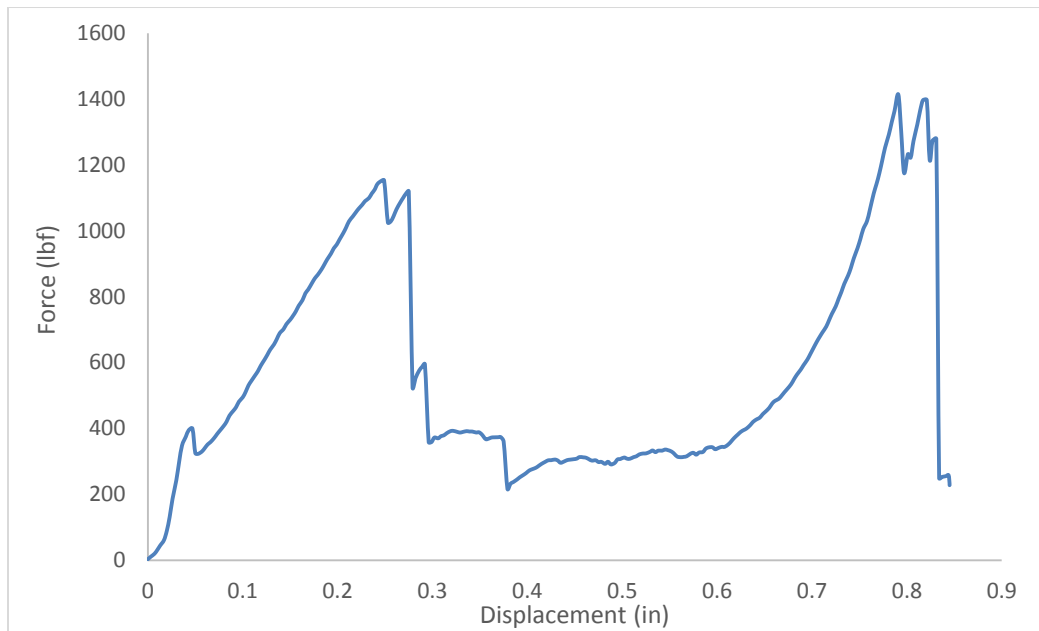


Figure 6.2: Perimeter shear test data.

Harness Attachment

The strength of the harness attachment to the tub was tested with the setup shown in Figure 6.2. The harness attachment was tested to a failure strength of at least 13kN as required by rules.

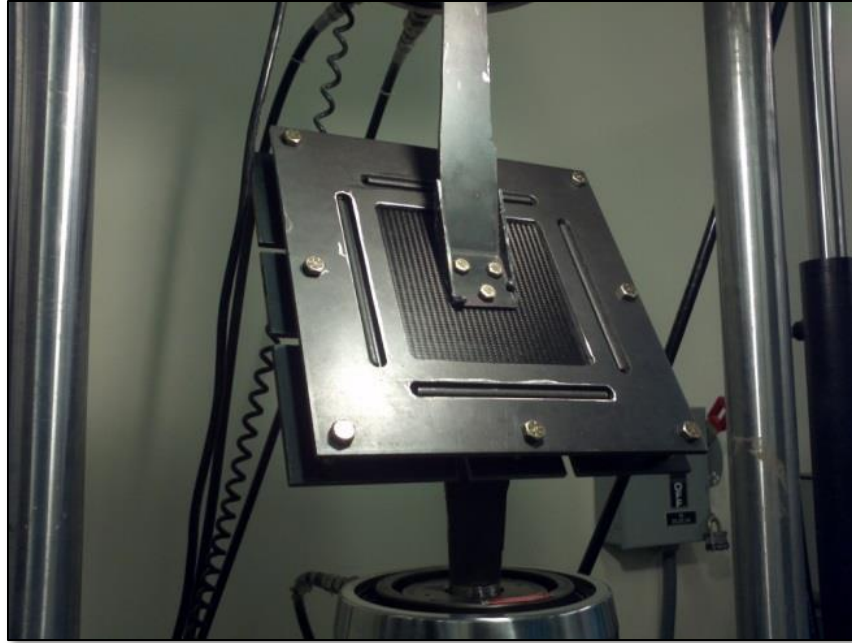


Figure 6.3: Cal Poly Formula harness testing rig.

Lap Joint

The lap joint test, a special test for the cut-and-fold construction method, was determined through communication with the Formula SAE rules committee. The rules clarification is included in the “Rules Clarifications” section of Chapter 3. This test verifies that the lap joint, as discussed in Chapter 5, maintains the integrity of the original panel. The test sample was made out of two pieces of panel. They were bonded together with a lap joint, with a bonded insert installed in either side. The sample was pulled to failure with a goal of breaking the panel before the joint. The inserts were used to bolt tabs to the panel. The sample was pulled by the tabs to avoid crushing the panel in the Instron’s jaws. This test showed that the cut-and-fold layups were stronger than the surrounding panel, satisfying the rules committee’s requirements.

Insert Pullout

Since joining the two halves of the chassis required bolting through the panel very near the edge, it was necessary to verify that the forces from driving the car would not rip the inserts out of the panel edge. To test this, a sample of panel was constructed with an edge closeout and bonded insert on either end. The insert was the same distance from the edge as designed at the bulkhead bolted joint. A bolt through each insert held tabs snugly on either side of the panel, in the same way as the tabs would fit to the panel at the bulkhead. A tab of the correct dimensions to fit in the Instron machine was then bolted loosely to the free ends of the panel tabs. The panel sample was pulled to failure in the Instron. The failure mode, as expected, was the insert ripping through the panel. This required roughly 1000lb of force, while the absolute worst case loading anticipated in the car was 750lb per insert.

Senior Project Requirement Results

Table 6.2: Chassis Initial Performance Goals and Results

| Category, with units | Target Value | Result Value | Tolerance | Risk | Compliance |
|---|--------------|--------------|-----------|------|------------|
| weight (lb) | 65 | 64.9 | Min | H | A,T |
| torsional stiffness (ft-lb/deg) | 1800 | 1825 | Min | M | A,T |
| time to get in (sec) | 5 | 2.5 | Max | H | T |
| time to get out (sec) | 5 | 3.2 | Min | M | T |
| number of steps to get in (n) | 5 | 4 | Max | H | T |
| number of steps to get out (n) | 5 | 4 | Med | M | T |
| total cost on cost report (\$) | 3000 | 2872 | Med | M | A,I |
| Total cost of entire project (\$) | 4000 | 3912 | Max | M | A,I |
| man hours to build frame (hours) | 200 | | Max | H | A,T |
| manufacturing processes (n) | 5 | 5 | Max | H | A |
| AF 4.1-4.7 (avg safety factor) | 1.25 | 1.82 | Min | H | A |
| places that can cut paper (n) | 0 | 0 | Med | M | I |
| time to assemble car (min) | 30 | 15-20 | Max | H | T |
| people that think it's comfortable (%) | 75 | 90 | Med | L | A,T |
| line of sight (deg) | 160 | 180 | Med | L | A,T |
| people that think it looks good (%) | 75 | 80 | Max | M | A,T |
| number of rocks in chassis after 10 min | 0 | 0 | Min | L | T |
| time to disassemble car (min) | 20 | 15-20 | Med | H | T |

Table 6.3: Weight Breakdown of Chassis Components

| | | | |
|-------------|---------------------------------------|--|--|
| 23.9 | Main Section Composites | | |
| 4.4 | Taco Composites | | |
| 11.1 | Main Hoop + Harness Bar + Welded Tabs | | |
| 5.8 | Front Hoop + Welded Tabs | | |
| 2.8 | Main Hoop Braces + Sleeves | | |
| 5.3 | Middle Bulkhead + Welded Tabs | | |
| 2.7 | Front Plates | | |
| 8.9 | All Other Chassis Tabs/Bolts | | |
| 64.9 | Total | | |

Table 6.2 shows the final chassis results for the goals set at the beginning of the project, shown in Table 1.1 in the *Senior Project* section of Chapter 1. The inspection and testing results were collected by the team during full car testing. To find the final weight of the chassis, the team disassembled the car and measured the chassis components individually. The results are shown in Table 6.3, with the final chassis

weight being 64.9 pounds, just under the project goal of 65. The composite sections include inserts and the metal tube sections include all welded tabs and other welded subsystem mounting, since they cannot be broken down further. The “all other chassis tabs/bolts” category includes only what is necessary to make the chassis structural according to the rules. This includes the shock mount plate and middle bulkhead attachment tabs and bolts, but not suspension or drivetrain attachment bolts and tabs. The chassis components were weighed after the car had passed a technical inspection and driven for testing for two main reasons. Weighing the final product gave the most accurate result, since small tabs and mounting are often forgotten until just before actually trying to drive the car. Also, it would have been very difficult to weigh resin, welding filler rod, and other materials used in manufacturing processes that add to the weight of the chassis.

The calculated torsional stiffness of 1825 ft-lb/deg was a result of an Abaqus FEA model, but was never physically tested. The FEA model included more detailed sub-models of all bolted joints to more accurately account for stiffness losses in the bolted chassis connections. Everyone that drove the car including a professional driver at Buttonwillow agreed that they felt no adverse handling caused by low chassis stiffness during extended testing. This implies that the minimum chassis stiffness is at least 1600 ft-lb/deg.

Ingress time did not include putting on the harness because the time to properly put on the harness is mostly unrelated to the ergonomics of getting into the chassis. Egress time was tested under competition conditions by Thomas Willson, after a few practice runs. The high side impact walls of the chassis were originally thought to make ingress and egress difficult, but with practice it was no more difficult than on an average SAE car, as reflected by ingress and egress times.

The original project budget was estimated to be \$10000 (as shown in Table 1.1), but was changed to \$4000 early on. The actual project spending of \$3912 includes around \$400 of equipment that can be used by the team in the future, including a vacuum pump and associated hardware and fixture materials. The composites part of the project also generated extra supplies such as spare carbon panels, resin, vacuum bag, and peel ply, which were used for other team projects.

The five manufacturing processes used were: flat panel machining, wet layups (including inserts), tube bending, tube and tab notching, and welding. Composite panel pressing and tab laser cutting were not included because those services were outsourced. Other small processes like random sanding and hole drilling were not included in the count. The original goal for total man hours to build the chassis was 200, but this proved to be very difficult to keep track of and count, which is why no result is listed.

The time to assemble and disassemble the car varied depended on what was being done. Removing the batteries for charging took no more than 5 minutes. Replacing the batteries took 5-10 minutes. Removing or replacing the suspension and drivetrain took 5-10 minutes each. These individual processes were timed for a group of 4 per subsystem. A full vehicle assembly wasn't completed all at once, but with enough people, should take 15-20 minutes with an upper limit of 30 for full driving preparation. The testing team noted that the car is very easy to assemble and work on because of the design and shape of the monocoque, the bonded inserts, and the overall simplicity of the chassis. They also noted

that the middle bulkhead was very easy to reassemble, which was a major point of concern in design reviews. The electrical team reported that the wide open battery and HV/LV box area made their work much easier than in previous years as well.

Rocks entering the chassis were a problem before the holes in the front shock mount plates were covered. After simple carbon covers were made and installed as designed, the only rocks to enter the chassis came in through the cockpit opening. The original intent of the 'rocks in chassis' metric was to avoid gaps in bodywork. Since none of the rocks came in through bodywork gaps or drivetrain clearance holes, that value is reported as zero.

Competition

Two elements of the Formula SAE competition serve as strong indicators of whether or not the chassis has fulfilled minimum design requirements. The Structural Requirements Certification Form (SRCF) was initially submitted on April 1, 2015, and certifies that the chassis design meets all requirements of the Alternative Frame rules. This form had undergone a few revisions and was on the point of being accepted when the team was informed that they would be unable to attend competition. The competition is restricted to 20 electric cars, and Cal Poly's Formula Electric team was the 25th team to register. Only four teams dropped out of the competition throughout the year, leaving Cal Poly still on the waitlist when it closed. This meant that Cal Poly Formula Electric's SRCF was now irrelevant to the FSAE judicial committee and would receive no further review.

A further consequence of the team's inability to attend competition is that the car as a whole, chassis included, has no opportunity for an official technical inspection. This means that the finished product cannot prove itself to the FSAE judges. However, Dr. Fabijanac (Cal Poly SAE's faculty advisor) has inspected the car using the rubric provided by the FSAE rules committee and has cleared the car to run. This is less compelling than a competition technical inspection, but is still validation to some degree.

Chapter 7: Conclusions and Recommendations

This project has been an enlightening process for all members of the senior project, from working with unfamiliar materials to exploring new uses for computer programs. More importantly to the future of Cal Poly SAE, the project explored a number of basic design concepts not normally even considered during the chassis design process. With seven distinct concepts initially, costs and benefits of a wide range of approaches were weighed.

The particular timing of this project helped greatly in allowing freedom to explore non-traditional ideas. The other subsystems of the car were already designed, instead of the normal timeline where all parts are being designed at the same time. This meant that constraints and requirements were clearly defined from the outset. The spring-start senior project allowed the timeline of the project to be not only shifted earlier by a quarter, but also extended since work could continue, albeit at a slower pace, over summer.

The new rulebook was published after the original chassis design was already completed. That was an annoying inconvenience but also a beneficial challenge. Had the thin-walled tubes not been disallowed, the depth and breadth of designs considered would have been far less. In the end, even the most unrealistic design concepts contributed to the finished product in some way. The steel bulkheads discussed with Jim Gerhardt in the course of aluminum monocoque evaluation led to the steel tube bulkhead in use behind the battery box, for example.

This project would be wasted without sharing the lessons learned with future teams. Maintain good contact with the FSAE officials on rules clarifications. At this point the alternative frame rules are still rather underdeveloped and need much clarification, especially when a monocoque chassis is involved. The rules committee can very helpful throughout the design, construction and testing of the car.

Testing early and often will help the design phase to a surprising degree. The results of the material testing heavily influenced choices made for the final design. Testing is not something to be done only once the car runs and people are getting to drive. It is a data collection process that is necessary to make data-driven decisions in all areas of the design.

The final design of the chassis could have been more efficient had all subsystems been developed in parallel. While the fixed constraints were helpful to the design process, there are things that could have been designed together to interface better. The battery box area was purposely designed slightly larger than necessary because the battery box itself was not designed yet, and it was critical that the finished box fit into the finished chassis. The narrow rear suspension points are another place where concurrent design could have made the two systems fit together with fewer large sacrifices from either.

Ordering components as early as possible can help manufacturing immensely. This way there is a safety factor for when outsourced parts are not correct, when a part is backordered, or when a team of students seeking donations suddenly becomes the very last on a manufacturer's long list of priorities.

The panel vendors were very helpful, but it would have been better to make contact with a few more manufacturers early on. The car could have been made from a single 8'x8' panel, simplifying manufacturing greatly. ACP, though wonderfully helpful, does not have the capability to press a panel that large, but some panel suppliers do.

The driver position could have been better. There is too much focus on driver comfort and ergonomics, allowing the driver to take up more space in the car than necessary and raising the center of gravity. With greater attention to detail the cockpit mockup could be fine-tuned to better determine what level of comfort is reasonable for drivers and what approaches a luxury sedan seating position.

A good extension of the cut and fold concept from the current design would be to make custom panels in-house. This would allow for different layup schedules in different areas of the chassis and allow for balsa core to be added near suspension points to improve point-load stiffness. A custom layup schedule would take weight out of areas that need less reinforcement and provide much stiffer joints. Depending on in-house capabilities, the chassis could possibly be made from a single large panel instead of many smaller ones. However, this method would require the team to be extremely confident in the quality of skin-to-core bonds in their panels.

The chassis came out well. It met its weight goal and supports a running car. Those who have driven it have no complaints. This is good, but what is better is that it has introduced several new and useful concepts to the Formula Electric team and to Cal Poly SAE as a whole. Future teams can take this chassis, the work done on it, and the lessons learned from it, and improve this design into better and better iterations. They may not choose to do this, and that is their choice to make. Even if this chassis concept never sees competition, the cut-and-fold concept is already being incorporated into other SAE applications such as battery boxes and firewalls. Whether or not this design is continued, the project that developed it left the club with useful tools.

Appendix A: QFD

Formula Electric Chassis QFD


| | driver | maintenance | manufacturing | Rules committee | marketing | weight (lb) | torsional stiffness (ft-lb/deg) | time to get in (sec) | time to get out (sec) | number of steps to get in (n) | number of steps to get out (n) | total cost on cost report (\$) | man hours to build frame (hours) | manufacturing processes (n) | AF 4.1-4.7 (avg safety factor) | places that can cut paper (n) | time to assemble car (min) | people that think it's comfortable (%) | line of sight (deg) | people that think it looks good (%) | number of rocks in chassis after 10 mins of driving | time to disassemble car (min) | Cal Poly Electric 13-14 | Cal Poly Hybrid 11-12 | Cal Poly Formula 13-14 |
|--------------------------|--------|-------------|---------------|-----------------|-----------|-------------|---------------------------------|----------------------|-----------------------|-------------------------------|--------------------------------|--------------------------------|----------------------------------|-----------------------------|--------------------------------|-------------------------------|----------------------------|--|---------------------|-------------------------------------|---|-------------------------------|-------------------------|-----------------------|------------------------|
| light weight | 16 | 9 | 11 | | 17 | ● | | | | | | Δ | | | | | | | | | | | | | 4 |
| stiff | 17 | | | 7 | 16 | ● | | | | | | | | Δ | | | | | | | | | | | 1 |
| quick to get in | 8 | | | | 1 | | ● | | | Δ | | | | | | | | | | | | | | | 16 |
| quick to get out | 13 | | | 16 | 2 | | | ● | | | Δ | | | | | | | | | | | | | | 5 |
| easy to get in | 11 | 6 | | | 3 | | ○ | | ● | | | | | | | | | | | | | | | | 15 |
| easy to get out | 14 | 7 | | | 4 | | | ○ | | | ● | | | | | | | | | | | | | | 14 |
| material cost | | | 15 | | 15 | | | | | | ● | | | | | | | | | | | | | | 12 |
| manufacturing time | | | 17 | | 9 | | | | | | Δ | | ● | ○ | | | | | | | | | | | 9 |
| ease of manufacturing | | | 16 | | 8 | | | | | | | | ○ | ● | | | | | | | | | | | 13 |
| Driver Safety | 10 | | | 17 | 14 | | | | | | | | | | ● | | | | | | | | | | 11 |
| Working safety | 9 | | 14 | 14 | 10 | | | | | | | | Δ | | ● | | | | | | | | | | 7 |
| ease of assembly | | 16 | 13 | | 13 | | | | | | | | | | | | ● | | | | | | | | 3 |
| driver comfort | 12 | | | | 11 | | | | | | | | | | | | | ● | | | | | | | 2 |
| driver visibility | 15 | | | 13 | 6 | | | | | | | | | | Δ | | | | ● | | | | | | 8 |
| visual appeal | 8 | | | | 7 | | | | | | | | | | | | | | | ● | | | | | 6 |
| environmental resistance | 7 | | | 15 | 5 | | | | | | | | | | | | | | | | ● | | | | 10 |
| ease of disassembly | | 17 | 12 | | 12 | | | | | | | | | | | | | | | | | ● | | | 9 |
| Units | | | | | | | | | | | | | | | | | | | | | | | | | |
| Targets | | | | | | 65 | ### | 5 | 5 | 5 | 5 | ### | 200 | 5 | 1.3 | 0 | 30 | 75 | 160 | 75 | 0 | 20 | | | |
| Cal Poly Electric 13-14 | | | | | | 82 | ### | 6 | 4 | 6 | 4 | ### | N/A | 6 | 0.3 | 5 | N/A | 75 | 150 | 50 | N/A | N/A | | | |
| Cal Poly Hybrid 11-12 | | | | | | 76 | 500 | | | | | ### | | | | | | | | | | | | | |
| Cal Poly Formula 13-14 | | | | | | 70 | ### | | | | | ### | | | | | | | | | | | | | |

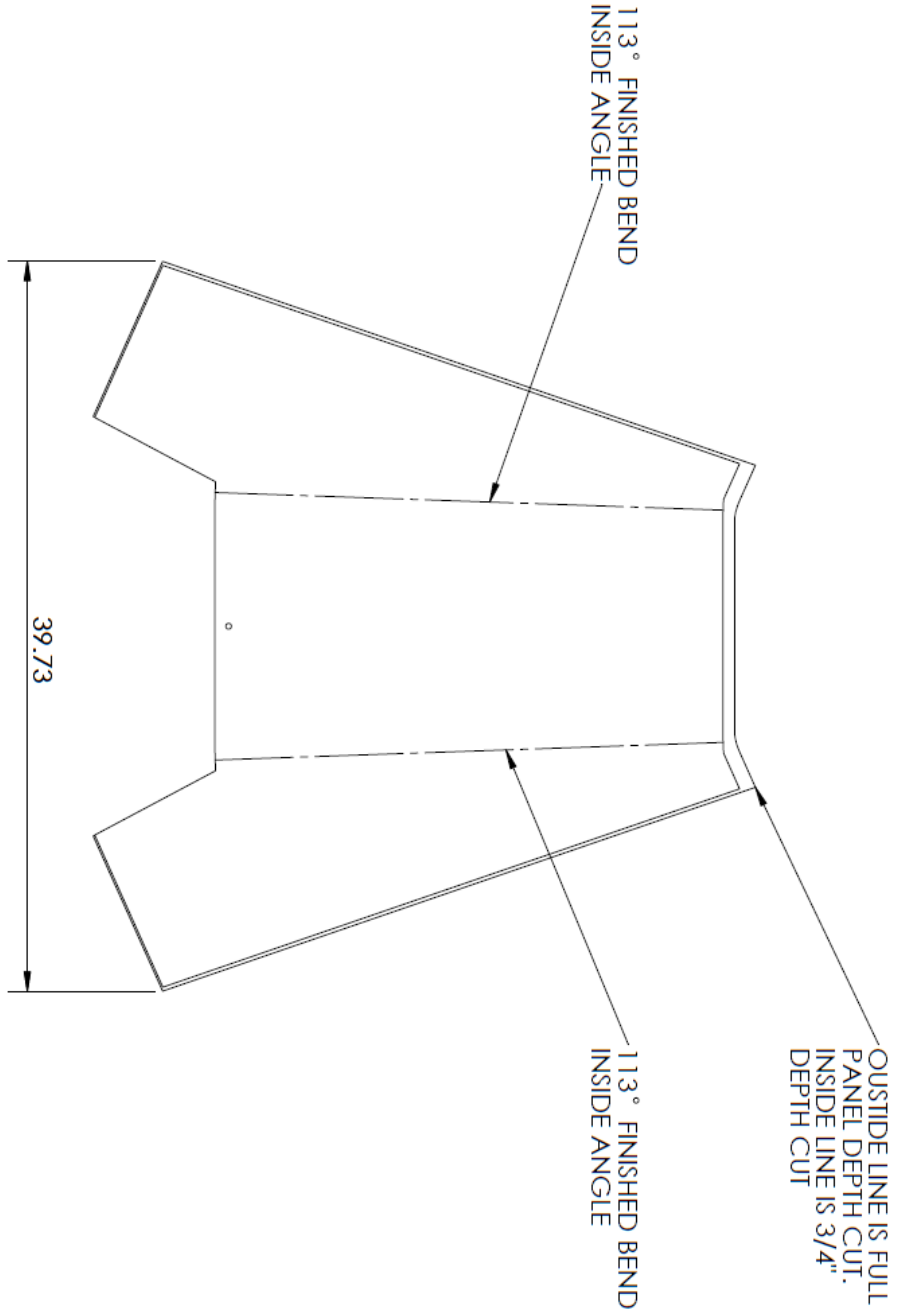
- = 9 Strong Correlation
- = 3 Medium Correlation
- Δ = 1 Small Correlation
- Blank No Correlation

Appendix B: Drawing Packet

The drawing shows a mechanical chassis base with a width of 32.24. It features several bends: a 95° finished bend on the top edge, 157.5° finished bends on the side edges, and 112° finished bends on the bottom edge. A note specifies that the outside line is a full panel depth cut, while the inside line is a 3/4" depth cut.

| | | | | | | | | |
|------------------------|------------|----------|---|------------|------------------|---------------------|-------------------|----------------|
| COMPANY | SIGN OFF | | DESCRIPTION | | PART # | | MAIN BOTTOM PANEL | |
| | DRAFTER | ENGINEER | MAIN CHASSIS BASE | VENDOR # | XXXX | ENGINEER | ENGINEER | |
| CUSTOMER | OPERATIONS | | BILLING INFO | | DATE | | PHONE | |
| | NA | CUSTOMER | 1 Grand Ave Mustang 60 San Luis Obispo, CA 93407 | 01-18-2015 | CHRISTOPHER PELL | BRANDON STITT | (805) 878-1115 | (702) 501-0872 |
| Mechanical Engineering | | | | E-MAIL | | bjstitt@calpoly.edu | | |

| | | | | | | | | | |
|---|----|-------------|--|---------------------------|--|----------|---------------------|-----------|------------------|
| COMPANY | | SIGN OFF | | DESCRIPTION | | PART # | | TOP PANEL | |
|  | | DRATER | | TOP PANEL FOR FRONT OF | | VENDOR # | XXXX | | |
| | | ENGINEER | | CAR | | DATE | 01-18-2015 | ENGINEER | CHRISTOPHER PELL |
| | | OPERATIONS | | BILLING INFO | | PHONE | (805) 878-1115 | ENGINEER | BRANDON STITT |
| | | MANUFACTURE | | 1 Grand Ave Mustang 60 | | E-MAIL | bjstitt@calpoly.edu | | |
| CUSTOMER | NA | CUSTOMER | | San Luis Obispo, CA 93407 | | | | | |

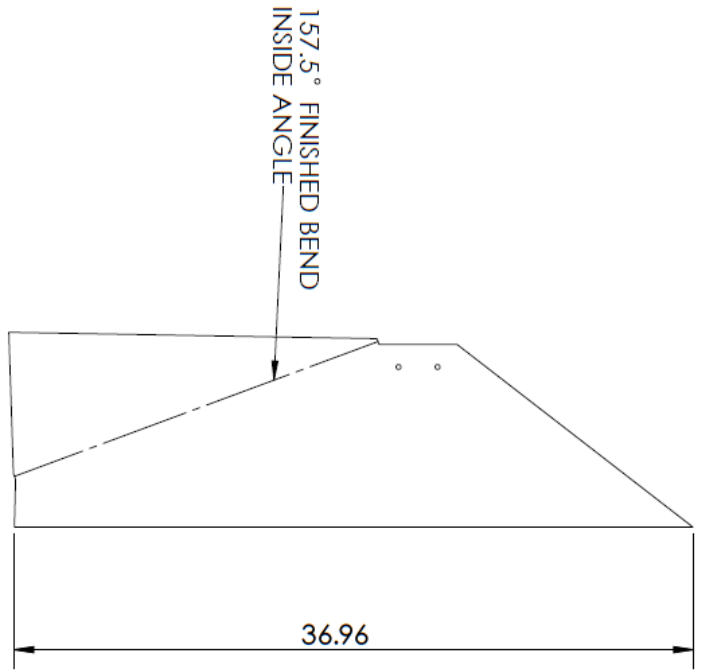


| | | | | | | | | |
|----------|---------------------------|----------|---|------------------|---------------------|----------------|---------------|---------------|
| COMPANY | SIGN OFF | | DESCRIPTION | | PART # | | BACK TACO | |
| | DRATER ENGINEER | | REAR PORTION OF CARBON PANEL FOR DRIVERAIN | VENDOR # XXXX | ENGINEER | ENGINEER | ENGINEER | ENGINEER |
| CUSTOMER | OPERATIONS MANUFACTURE | | BILLING INFO | DATE | ENGINEER | ENGINEER | ENGINEER | ENGINEER |
| | NA | CUSTOMER | 1 Grand Ave Mustang 60 San Luis Obispo, CA 93407 | 01-18-2015 | CHRISTOPHER PELL | BRANDON STITT | BRANDON STITT | BRANDON STITT |
| | | | | PHONE | (805) 878-1115 | (702) 501-0872 | | |
| | | | | E-MAIL | bjstitt@calpoly.edu | | | |

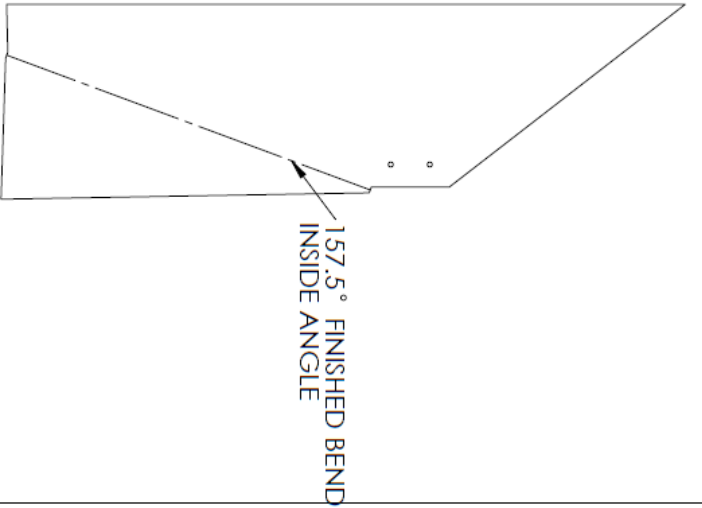
106.5° FINISHED BEND
INSIDE ANGLE

36.01


106.5° FINISHED BEND
INSIDE ANGLE



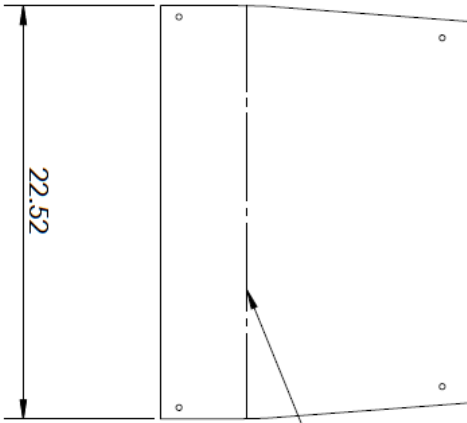
RIGHT PANEL




LEFT PANEL

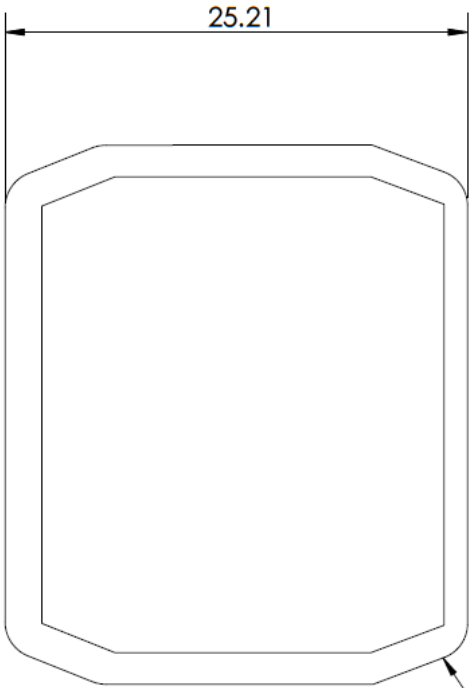
| | | | | | | | | | |
|---|----|-------------|----------|---------------------------------------|--|--------------|---|----------------------|---------------|
| COMPANY | | SIGN OFF | | DESCRIPTION | | PART # | | LEFT AND RIGHT SIDES | |
|  | | DRATER | | UPPER PANEL PORTIONS FOR MAIN BODY | | VENDOR # | XXXX | ENGINEER | ENGINEER |
| | | ENGINEER | | | | DATE | 01-18-2015 | CHRISTOPHER PELL | BRANDON STITT |
| | | OPERATIONS | | | | BILLING INFO | 1 Grand Ave Mustang, 60 San Luis Obispo, CA 93407 | | |
| CUSTOMER | NA | MANUFACTURE | CUSTOMER | | | E-MAIL | bjstitt@calpoly.edu | | |
| | | | | | | PHONE | (805) 878-1115 | (702) 501-0872 | |

| | | | | | | | | |
|----------|------------------------|--|--|----------|---------------------|------------------|---------------|--|
| COMPANY | SIGN OFF | | DESCRIPTION | | PART # | | FIREWALL | |
| | DRFTER ENGINEER | | FIREWALL FOR DRIVER/BATTERY SEPERATION | VENDOR # | XXXX | ENGINEER | ENGINEER | |
| CUSTOMER | OPERATIONS MANUFACTURE | | BILLING INFO | DATE | 01-18-2015 | CHRISTOPHER PELL | BRANDON STITT | |
| | CUSTOMER | | 1 Grand Ave Mustang 60 San Luis Obispo, CA 93407 | PHONE | (805) 878-1115 | (702) 501-0872 | | |
| | | | | E-MAIL | bjstitt@calpoly.edu | | | |

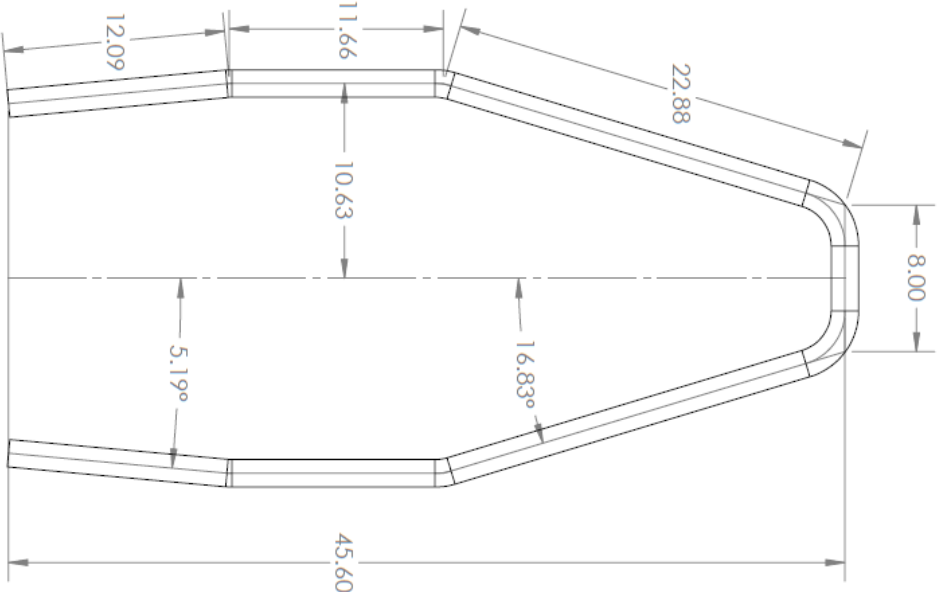


124° FINISHED BEND
INSIDE ANGLE

| | | | | | | | | | |
|---|--|-------------|--|---------------------------|--|----------|---------------------|------------------|----------------|
| COMPANY | | SIGN OFF | | DESCRIPTION | | PART # | | AL PANEL | |
|  | | DRFTER | | ANIT INTRUSION PANEL | | VENDOR # | XXXX | ENGINEER | ENGINEER |
| CUSTOMER | | ENGINEER | | BILLING INFO | | DATE | 01-18-2015 | CHRISTOPHER PELL | BRANDON STITT |
| NA | | OPERATIONS | | 1 Grand Ave Mustang, 60 | | PHONE | (805) 878-1115 | | (702) 501-0872 |
| | | MANUFACTURE | | San Luis Obispo, CA 93407 | | E-MAIL | bjstitt@calpoly.edu | | |

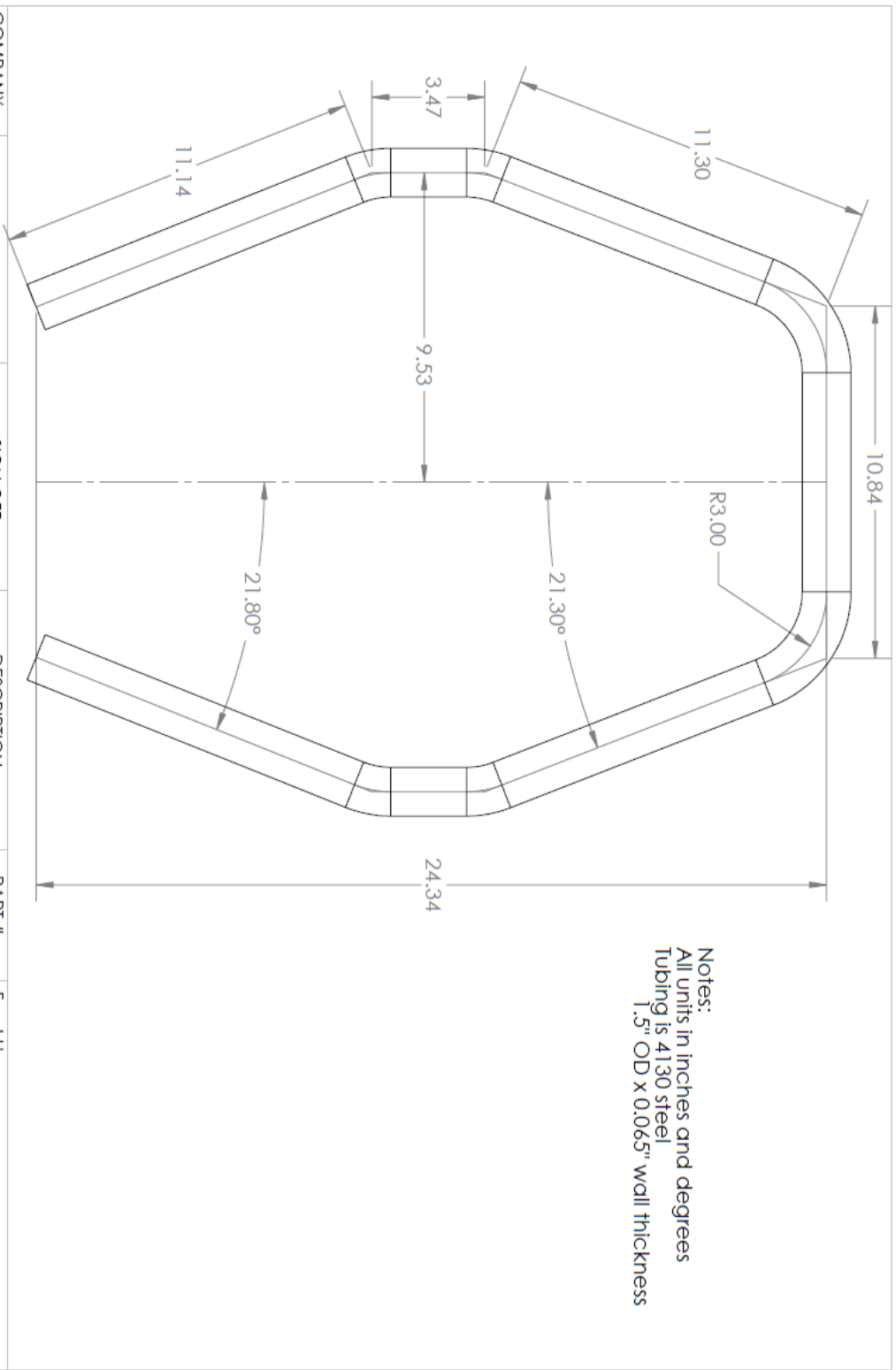


OUTSIDE LINE IS FULL
 PANEL DEPTH CUT.
 INSIDE LINE IS 3/4"
 DEPTH CUT

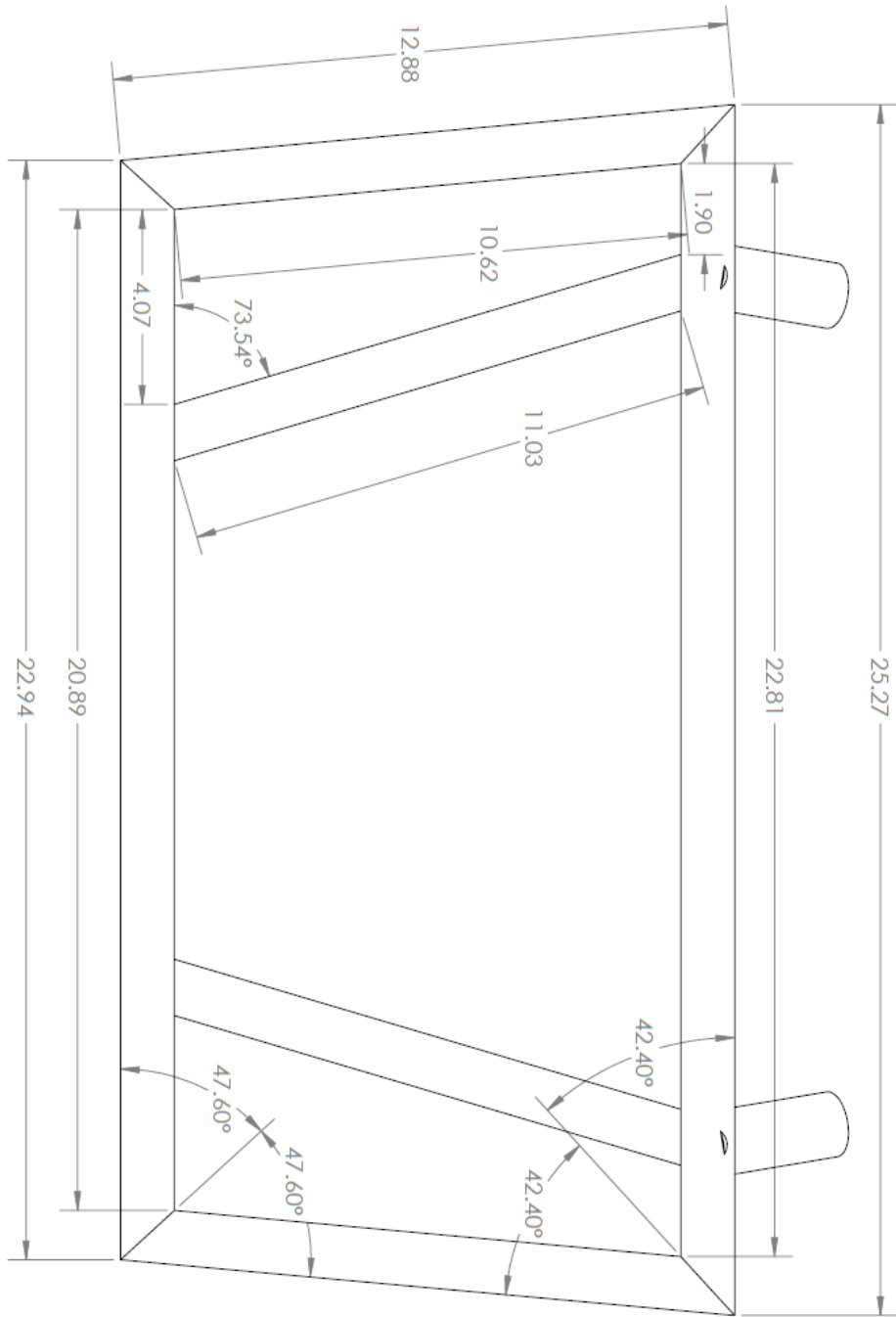


Notes:
 All units in inches and degrees
 Tubing is 4130 steel - 1.5" OD x 0.065" wall thickness

| | | | | | | | | | |
|---|--|-------------|--|---------------------------|--|------------|--|---------------------|--|
| COMPANY | | SIGN OFF | | DESCRIPTION | | PART # | | Main Hoop | |
|  | | DRAFTER | | BILLING INFO | | VENDOR # | | XXXX | |
| | | ENGINEER | | | | DATE | | ENGINEER | |
| CUSTOMER | | OPERATIONS | | 1 Grand Ave Mustang 60 | | 11/13/2014 | | CHRISTOPHER PELL | |
| NA | | MANUFACTURE | | San Luis Obispo, CA 93407 | | PHONE | | (805) 878-1115 | |
| | | CUSTOMER | | | | E-MAIL | | bjstitt@calpoly.edu | |
| | | | | | | | | BRANDON STITT | |
| | | | | | | | | (702) 501-0872 | |



| | | | | | | | | | |
|---|----|------------|-------------|---|--|----------|---------------------|----------------|------------------|
| COMPANY | | SIGN OFF | | DESCRIPTION | | PART # | | Front Hoop | |
|  | | DRAFTER | | BILLING INFO | | VENDOR # | XXXX | ENGINEER | ENGINEER |
| | | ENGINEER | | | | DATE | 11/13/2014 | ENGINEER | CHRISTOPHER PELL |
| CUSTOMER | NA | OPERATIONS | MANUFACTURE | 1 Grand Ave Mustang 60 San Luis Obispo, CA 93407 | | PHONE | (805) 878-1115 | (702) 501-0872 | |
| | | CUSTOMER | | | | E-MAIL | bjstitt@calpoly.edu | | |



Appendix C: Vendor List

| Vendors | Supplying | Contact |
|--------------------|----------------------|--------------------------|
| ACP | Composite Panels | Justin 925-443-5900 x 12 |
| Maxium Motorsports | Tube Bending Service | Karlos 619-726-9299 |
| Discount Steel | Square Steel Tube | discountsteel.com |
| McMaster-Carr | Billet Aluminum | mcmaster.com |
| 80/20 | Jigging | 8020.net |
| Online Metals | Round Steel Tube | onlinemetals.com |
| Fibreglast | Bonding Supplies | Fibreglast.com |
| FSAE | Impact Attenuator | FSAE.com |

| Part | Dimensions | Cost | Supplier |
|-----------------------|-------------------------------------|----------------|----------------|
| Carbon Panels | one 48"x96", one 48"x72" | \$2,500 | ACP Composites |
| Roll Hoops | 16ft - 1.5"x0.065" round 4130 | \$320 | Online Metals |
| Main Hoop Braces | 8ft - 1.375"x0.049" round 4130 | \$50 | Online Metals |
| Middle Bulkhead Tubes | 10ft - 1.125"x0.049" square 4130 | \$64 | Discount Steel |
| Impact Attenuator | one standard item | \$150 | SAE |
| Front Machined Plates | one 12"x12"x1" thick 7075-T6 | \$150 | McMaster |
| Carbon Tape | one 30yd roll x 4" wide | \$199 | Fibreglast |
| Series 2000 Resin | one gallon | \$69 | Fibreglast |
| 2020 Resin Hardener | one quart | \$49 | Fibreglast |
| Glass Microspheres | one carton (6 gallons) | \$69 | Fibreglast |
| Sheet Metal for Tabs | one 24"x48"x0.125" thick 6061-T6 | \$93 | McMaster |
| Sheet Metal for Tabs | one 24"x24"x0.080" thick mild steel | \$44 | McMaster |
| Sheet Metal for Tabs | one 24"x24"x0.060" thick mild steel | \$42 | McMaster |
| Total | | \$3,799 | |

Appendix D: Supporting Analysis

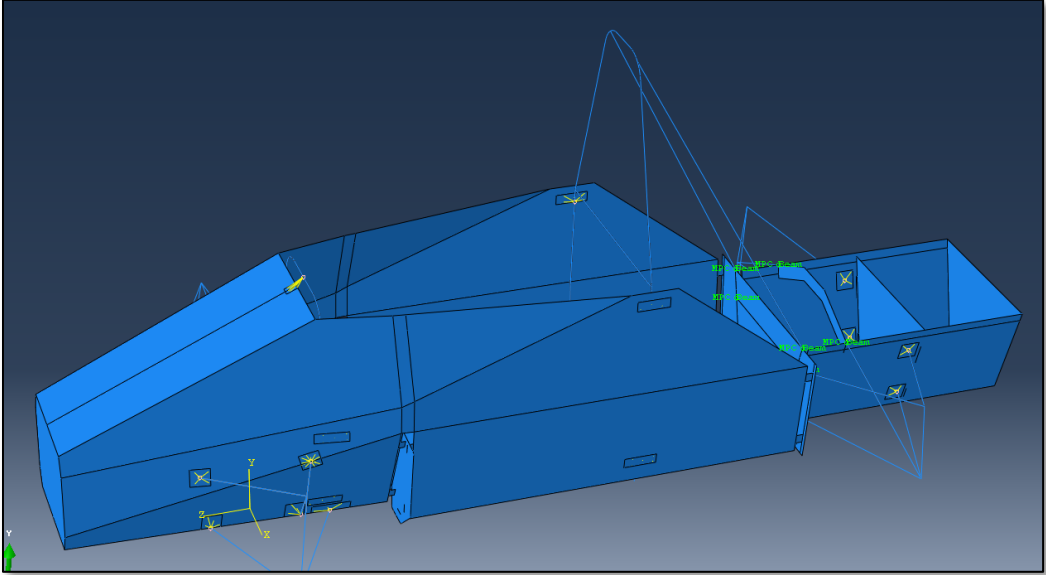


Figure D.1: Abaqus model.

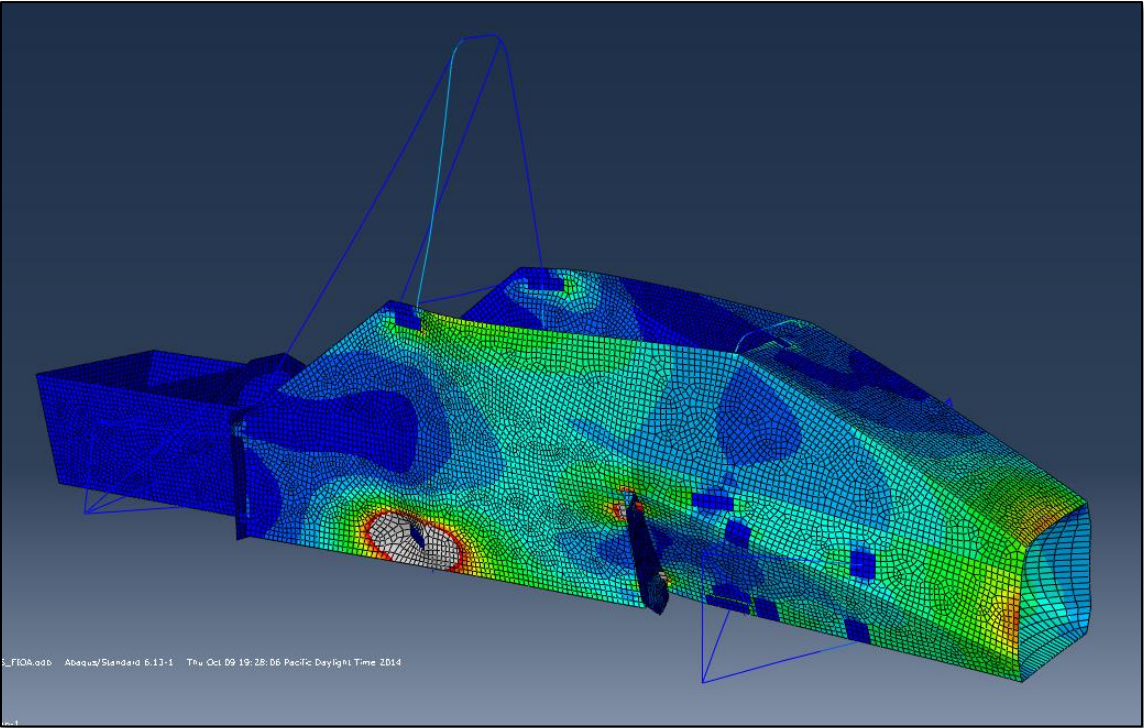


Figure D.2: Front impact off axis deflection results.

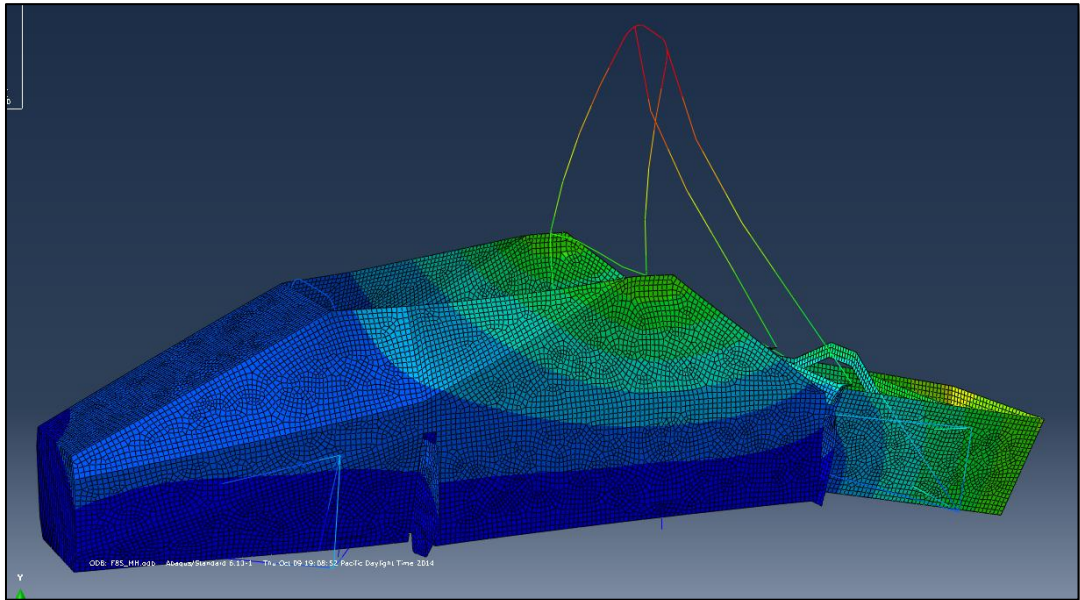


Figure D.3: Main hoop deflection results

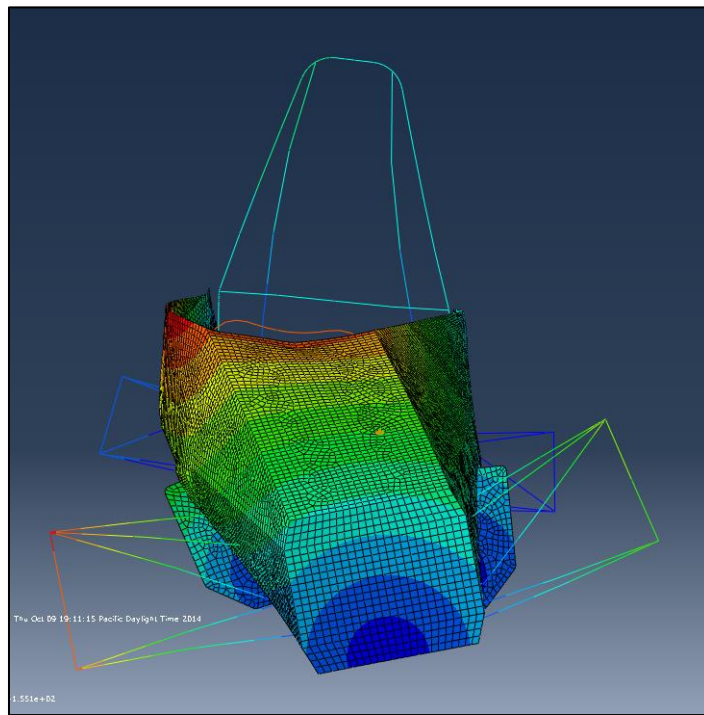


Figure D.4: Front Hoop deflection result.

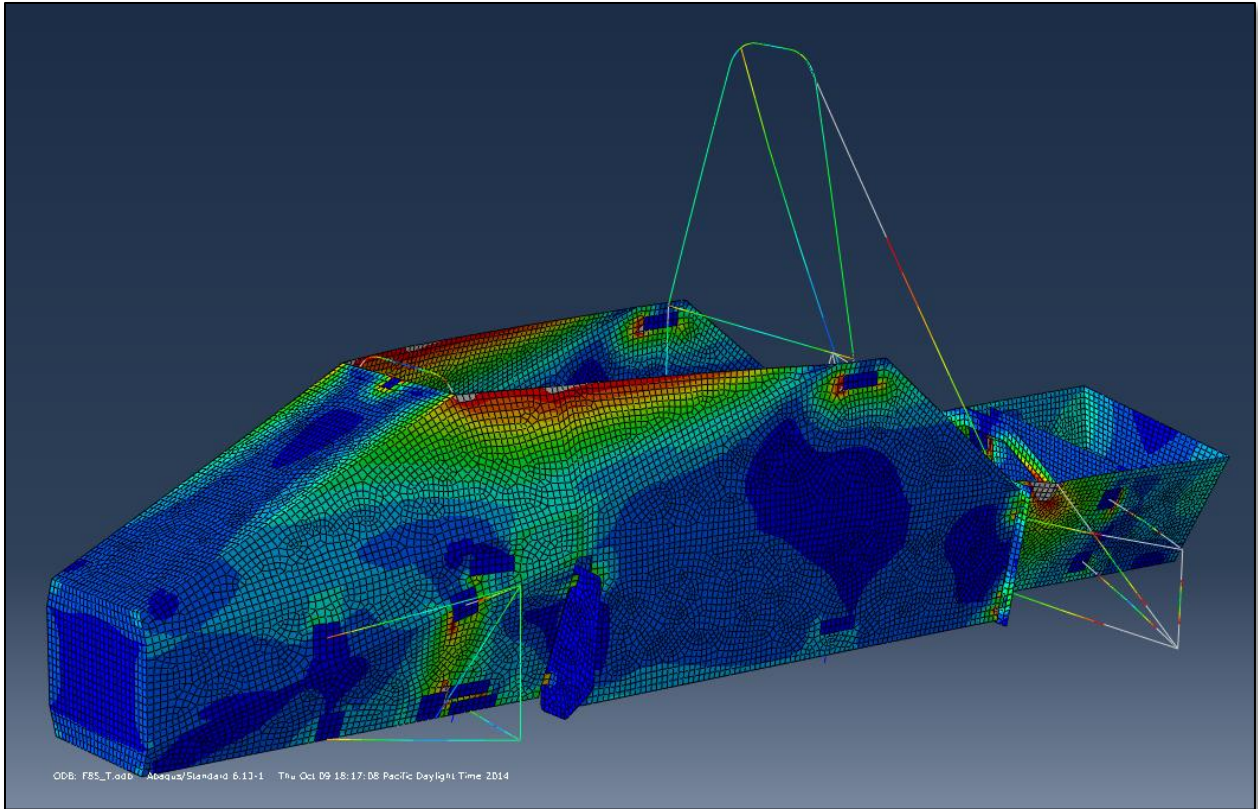
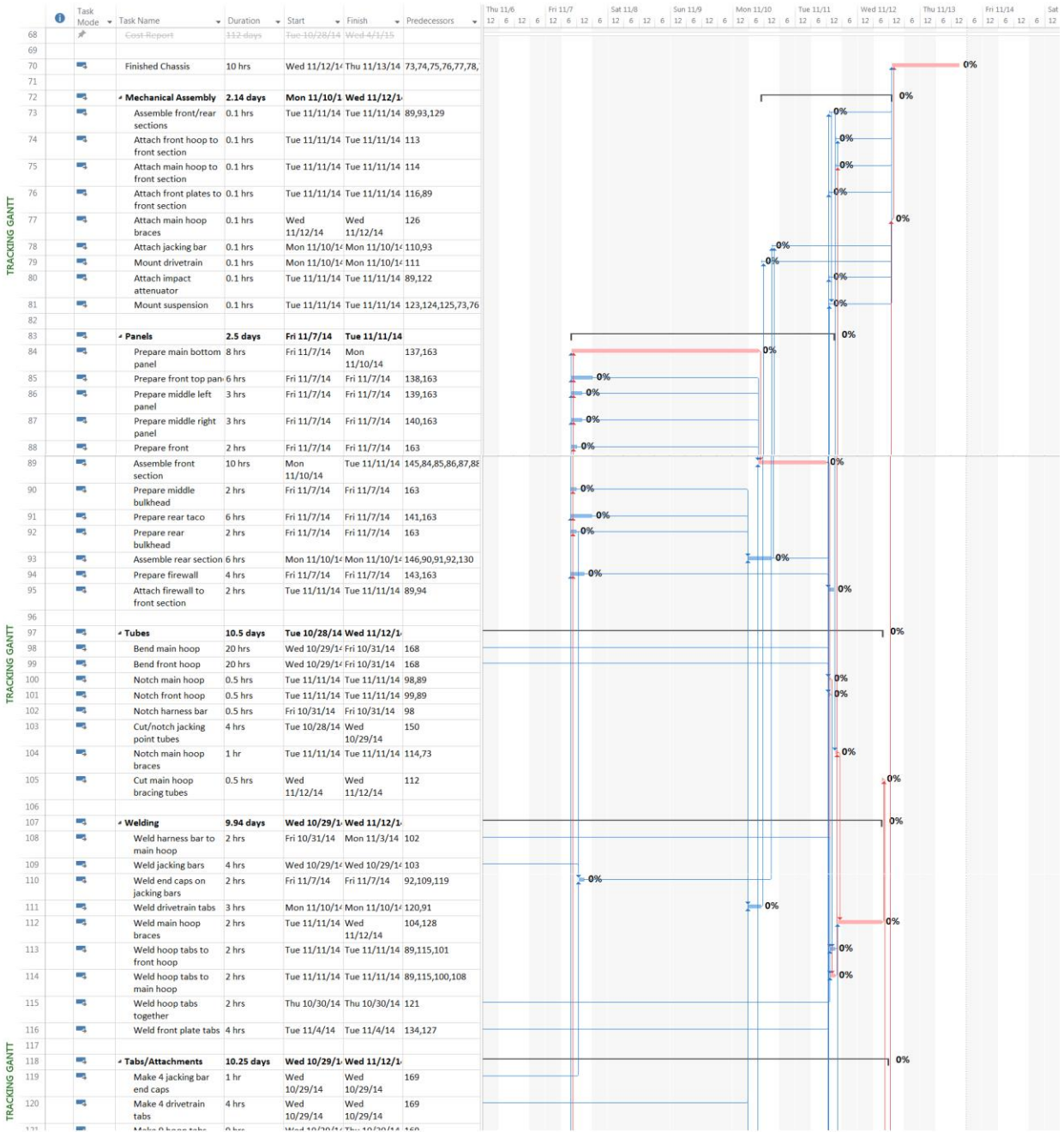
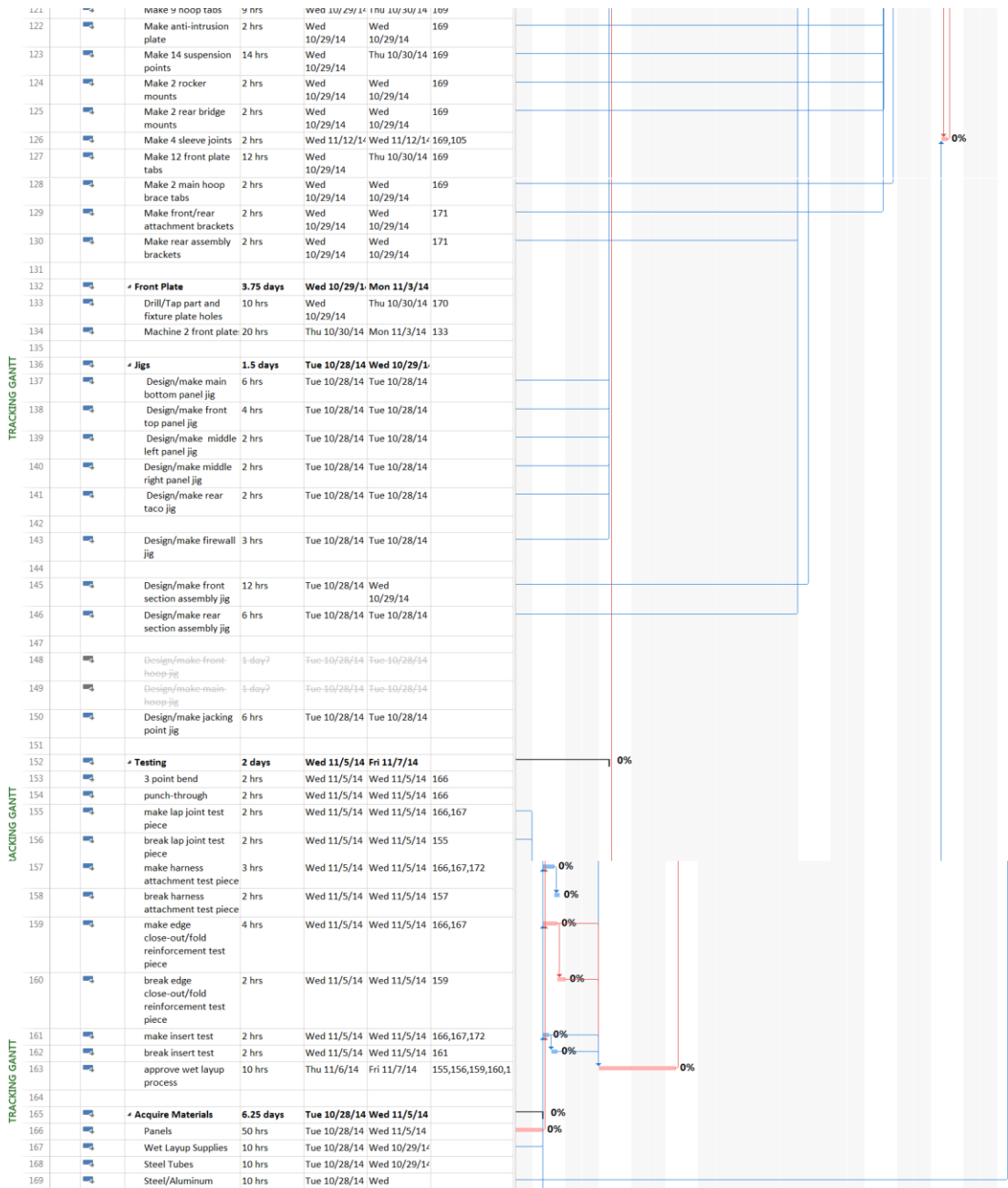


Figure D.5: Torsion deflection results

Appendix E: Gantt Chart





Appendix F: FMEA

| FMEA Formula Electric Chassis | | | | | | | |
|-------------------------------|---------------------------|--|---|--------|----------|-------------|---|
| Item/ Functional Identity | Failure Mode | Failure Cause | Failure Effect | Target | Severity | Probability | Actions |
| Harness | Broken Strap | Poor Manufacture/ Defective | Loss of safety in crash, difficulty egress | | 4 | 1 | Buy high quality strap |
| | Harness attachment breaks | Broken Welds/heated bolt | Crash safety decreases | | 4 | 2 | Test harness attachment points |
| Tires | Flat Tire | Road Debris, rolled bead over | Loss of car control | | 3 | 1 | Check pressures regularly |
| Battery Box | Battery Fire | Confined space, defective battery, short | Uncontrollable Fire | | 5 | 1 | Design enough space and ventilation for battery box |
| Battery Mount | Broken Mount | Hard Impact to car | Loss of Power and control | | 5 | 1 | Overbuild mounts and test them |
| Tie Rod | Broken Tie rod | Hard cornering, poor manufacture | Loss of control | | 4 | 3 | Brake kill switch |
| Brakes | Brake failure | Fluid leak, Broken Line | Diminished stopping ability | | 3 | 2 | check lines |
| | Brake failure | Overheating (fading) | Diminished stopping ability | | 3 | 4 | Don't brake too hard!! Use sparingly |
| Steering Wheel | Detachment from column | Improper reattachment | Loss of steering control | | 4 | 1 | take care when attaching wheel |
| Motor | Electrical Failure | Short | Loss of power | | 1 | 1 | |
| Differential | Rear end lock up | Broken Gears | Rear tires cease moving | | 4 | 1 | |
| Wheels | Cracked/Broken Rim | Hard Impact to car | Flat Tire, loss of steering | | 3 | 2 | Give proper clearance and travel for suspension |
| Steel tube chassis | Weld failure | Defective weld, large impact | Chassis stiffness and safety compromised | | 1 | 3 | Practice welding several times and test pieces to find strength |
| Stress Skin | Panel panel failure | Bad rivet, defective adhesive bond | Chassis stiffness and safety compromised | | 1 | 3 | Practice adhering panels and test strength |
| Composite Floor | Cracked panel | Bad rivet, defective adhesive bond | Chassis stiffness and safety compromised | | 2 | 4 | Practice adhering panels and test strength |
| | Cracked panel | Large impact, road debris | Driver safety/chassis stiffness compromised | | 3 | 3 | Design panel to take impacts (test different panel materials) |
| Chain | Panel-chassis disconnect | Large impact, poor bonding | Driver safety/chassis stiffness compromised | | 4 | 2 | Test bonding methods for composite methods |
| | Broken Chainlink | Impact, defective chain | Loss of powertrain | | 2 | 1 | Use quality chain and build to be protected from road debris |
| | Broken Chain Guard | Improper design, impact | Driver injury due to flying chain | | 5 | 1 | Test chain guard against varying impacts |
| Motor Mount | Broken motor mount | Impact, bad weld | Damage to car from spinning motor | | 4 | 2 | Test motor mount strength |